MOLECULAR CHARACTERIZATION OF MICROBIAL COMMUNITIES FOULING CONCRETE INFRASTRUCTURES

A Thesis
Presented to
The Academic Faculty

by

David John Giannantonio

In Partial Fulfillment
of the Requirements for the Degree
Master of Science in the
School of Biology

Georgia Institute of Technology
August 2008

MOLECULAR CHARACTERIZATION OF MICROBIAL COMMUNITIES FOULING CONCRETE INFRASTRUCTURES

Approved by:

Dr. Patricia Sobecky, Advisor
School of Biology
Georgia Institute of Technology

Dr. Kimberly Kurtis
School of Civil and Environmental Engineering
Georgia Institute of Technology

Dr. Jim Spain
School of Biology
School of Civil and Environmental Engineering
Georgia Institute of Technology

Date Approved: June 27, 2008

ACKNOWLEDGEMENTS

This work would not have been possible without the support of many people who deserve recognition. First and foremost, I must thank my advisor Dr. Patricia Sobecky for the opportunity to perform my graduate studies. Her infinite encouragement, patience, and understanding have truly made this work a fulfilling experience. I would also like to thank Dr. Kimberly Kurtis for all of her collaborative help and optimism, which made this biology student's introduction into the world of concrete science not only possible, but enjoyable. I also thank my partner in research, Jonah Kurth, for his ingenuity in the lab and friendship outside of it. Credit must be given to him for photography of the sample sites, as well as concrete property measurements taken both in the field and in the lab. I would also like to thank Dr. Robert Martinez for his unrivaled patience and willingness to both teach me the ropes of lab research and take the time to help me with any questions and setbacks I had. I thank Wayne Hawkins and Dr. Ben Mohr at Tennessee Technological University for their help in performing ESEM imaging. Finally, I thank the Georgia Department of Transportation for their financial support of this research (project no. 06-15).

TABLE OF CONTENTS

LIST OF TABLES

LIST OF FIGURES

LIST OF SYMBOLS

Al	aluminum
Ba	barium
C	carbon
Ca	calcium
Fe	iron
H	hydrogen
K	potassium
Mg	magnesium
Mn	manganese
Na	sodium
O	oxygen
P	phosphorous
S	sulfur
Si	silicon
Sr	strontium
Ti	titanium

LIST OF ABBREVIATIONS

C-S-H	calcium silicate hydrate
C_2S	$2CaO \cdot SiO_2$
C_3A	$3CaO \cdot Al_2O_3$
C_3S	$3CaO \cdot SiO_2$
C_4AF	$4CaO \cdot Al_2O_3 \cdot Fe_2O_3$
C_4ASH_{18}	$4CaO \cdot Al_2O_3 \cdot SO_3 \cdot 18H_2O$
$C_6AS_3H_{32}$	$6CaO \cdot Al_2O_3 \cdot 3SO_3 \cdot 32H_2O$
DNA	deoxyribonucleic acid
ESEM	environmental scanning electron microscopy
GU	general use
hv	photon energy
ITS	internal transcribed spacer
LOI	loss on ignition
PCR	polymerase chain reaction
RFLP	restriction fragment length polymorphism
RNA	ribonucleic acid
SCM	supplemental cementitious material
sp	species
UV	ultraviolet
w/cm	water to cement ratio

SUMMARY

The objective of this study was to identify and characterize naturally-occurring communities of *Bacteria* and *Fungi* fouling the surfaces of concrete structures in Georgia, USA, through the use of culture-independent and culture-dependent approaches. Genomic DNA was extracted and ribosomal RNA genes were PCR amplified from 4 biofouled sites located in or around the cities of Atlanta, Gainesville, LaGrange, and Savannah. Bacterial and fungal community composition was determined by phylogenetic analysis. Molecular analysis revealed five bacterial phyla, and representatives of the phylum *Cyanobacteria* and the classes *Betaproteobacteria* and *Gammaproteobacteria* dominated the bacterial clone libraries. Fungal clone libraries showed the dominant phylotypes to be most closely related to *Alternaria*, *Cladosporium*, *Epicoccum* and *Udeniomyces*. Phylogenetically distinct microbial populations were present at each of the biofouled sites. In addition, cultured isolates were obtained from sites and tested for their ability to foul concrete of varied compositions under laboratory-controlled conditions. Biofouling tests revealed that fungal isolates obtained from the field were able to colonize concrete surfaces when supplied with moisture (95-100% relative humidity) and a nutrient source, and that fouling was affected by concrete water/cement ratio, surface roughness, and the presence of photocatalytically-activated cement added to inhibit microbial growth.

CHAPTER 1

INTRODUCTION

Statement of the Problem

The biofouling (i.e. colonization and discoloration) of concrete and stone surfaces can have deleterious effects on structural integrity and aesthetic appeal (Gaylarde and Morton, 1999; Dubosc et al., 2001). The deteriogenic biofilms inhabiting these surfaces can expedite the destruction of historic structures, which can result in the loss of symbols of cultural heritage (Warscheid and Braams, 2000). Similarly, biologically-mediated corrosion of infrastructure, including buildings, highways, and sewers, represents a large economic loss in the form of maintenance and repair costs (Gu et al., 1998). Furthermore, exposure to biofilms colonizing buildings may be of concern for public health (Gaylarde and Morton, 1999; Shirakawa, 2003). For these reasons, it is important to understand the nature of these microbial communities, and begin developing strategies to mitigate colonization.

A phylogenetically diverse group of organisms has been reported to colonize concrete and stone surfaces, including algae, *Bacteria*, and *Fungi* (Warscheid et al., 1991; Gaylarde and Morton, 1999; Bartosch et al., 2003). For example, *Chlorophyceae* and *Cyanophyceae* have been observed to colonize the exterior concrete surfaces of buildings in the south of France (Dubosc et al., 2001), while numerous species of other algae have been detected on the outer walls of cathedrals and other structures throughout both Europe and Latin America (Gaylarde and Gaylarde, 2005). Diverse groups of *Bacteria* have been discovered on concrete, including *Cyanobacteria* isolated from historic

buildings in Latin America (Gaylarde et al., 2007), as well as *Pseudomonas*, *Bacillu*s, and *Xanthomonas* spp. that have been found to co-inhabit limestone surfaces (Mitchell and Gu, 2000). Sulfur oxidizers (e.g. *Thiobacillus* spp.) and nitrifiers (e.g. *Nitrosomonas* and *Nitrobacter* spp.) have been found to colonize the interior of concrete sewer pipes (Milde et al., 1983; Sand, 1997; Nica et al., 2000), as well as concrete structures in hydraulic facilities (Zherebyateva, 1991). The numerous *Fungi* found to foul concrete include *Cladosporium* spp. on the interior mortars of buildings (Shirakawa, 2003), as well as the fungal genera *Alternaria*, *Aspergillus*, *Epicoccum*, *Mucor*, *Penicillium*, and *Trichoderma* reported to foul other concrete and stone surfaces (Gaylarde and Morton, 1997; Mitchell and Gu, 2000; Shirakawa et al., 2002).

The biofouling of concrete and stone often appears as a dark to black-pigmented crust that covers the surface of a structure (Warscheid and Braams, 2000; Gaylarde and Gaylarde, 2005; Perry, 2005; Gaylarde et al., 2007). The appearance and severity of this biofouling are depicted on several structures in Figure 1.1. The dark hue of this fouling may be attributed to the pigmentation (e.g. melanins) found in the organisms that compose these biofilms (Sterflinger, 2000; Warscheid and Braams, 2000). The morphological similarity of these organisms, particularly fungi, can often disguise the diversity of fouling communities (Chertov, 2004).

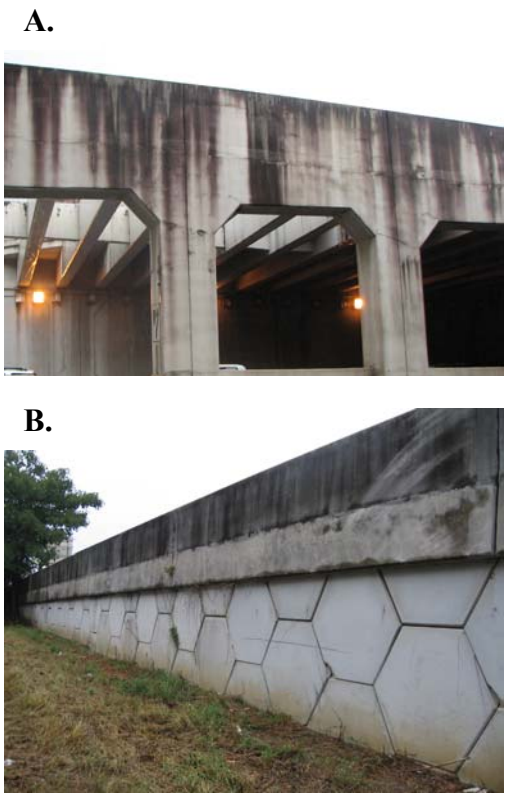

Figure 1.1. Examples of concrete biofouling. Fouling of a bridge parapet (A) and a concrete cap on a retaining wall (B) in Atlanta, Georgia.

Structure and Sustainability of Fouling Communities

The biofouling of concrete and stone structures can result from a number of different types of colonization and succession paths (Gaylarde and Morton, 1999; Warscheid and Braams, 2000). As a result, a variety of metabolic reactions may be present in fouling communities, which are summarized in Table 1.1. The initial colonizers of these surfaces are often autotrophs (Gaylarde and Morton, 1999; Warscheid and Braams, 2000). Chemolithotrophs, such as sulfur-oxidizers and nitrifiers, can initially colonize surfaces utilizing sulfur and nitrogen-containing compounds found in the surrounding environs (e.g. sewage in concrete pipes, outdoor urban air pollution) and fixing CO_2 (Sand and Bock, 1991; Warscheid and Braams, 2000; Perry, 2005).

Phototrophs capable of carbon fixation and harvesting energy from sunlight, such as algae and *Cyanobacteria*, are often initial colonizers of outdoor concrete and stone surfaces (Gaylarde and Morton, 1999; Warscheid and Braams, 2000; Shirakawa et al., 2002). Initial colonization by autotrophs can provide a carbon and energy source as well as ameliorate an inhospitable surface for heterotrophic populations (Sand, 1997; Gaylarde and Morton, 1999; Warscheid and Braams, 2000).

Colonization by heterotrophic microorganisms, however, can also occur without the initial presence of other primary colonizers (Warscheid and Braams, 2000). Primary heterotrophic colonizers can establish themselves using carbon derived from air pollutants, dust, and rain (Warscheid and Braams, 2000). Carbon introduced in this way often originates from industrial and vehicular fuel combustion (Warscheid et al., 1991; Warscheid and Braams, 2000). In addition, microorganisms may utilize carbon derived from surface coatings, including paint (Shirakawa et al., 2002; Gaylarde and Gaylarde, 2005). In particular, *Fungi* (e.g. *Alternaria*, *Aspergillus*, *Cladosporium*) have been found to readily colonize newly painted surfaces (Shirakawa et al., 2002).

Table 1.1. Some metabolic processes of concrete and stone colonizers.

Metabolism	Reaction
Phototrophy	$CO_2 + H_2O \xrightarrow{hv} C(H_2O) + O_2$
Chemolithotrophy	
Nitrification	$NH_4^+ + 1.5O_2 \rightarrow NO_2^- + 2H^+ + H_2O$
	$NO_2^- + 0.5O_2 \rightarrow NO_3^-$
Sulfur oxidation	$HS^- + H^+ + 0.5O_2 \rightarrow S^0 + H_2O$
	$S^0 + 1.5O_2 + H_2O \rightarrow SO_4^{2-} + 2H^+$
Heterotrophy	$C(H_2O) + O_2 \rightarrow CO_2 + H_2O$

Composition of Concrete

The composition and characteristics of a concrete structure can directly influence its susceptibility to biofouling (Guillitte, 1995; Dubosc et al., 2001); thus knowledge of the building material is needed to fully understand the microbial communities colonizing it. Concrete is defined by the American Society for Testing and Materials (ASTM) as a complex of binding material in which larger particulates are embedded (ASTM C 125, 2007). An estimated 11 billion metric tonnes of concrete are used each year worldwide (Mehta, 2006). The construction material's widespread use is largely due to its resistance to water, ability to be shaped into a variety of structures, and economic availability (Mehta, 2006). Concrete is typically composed of a hydrated cement binder mixed with coarse (i.e. particles larger that 4.75 mm, such as gravel) and fine aggregate (i.e. particles between 75 μm and 4.75 mm, such as sand) (ASTM C 125, 2007). A concrete mix composed only of hydrated cement and fine aggregate is defined as mortar (ASTM C 125, 2007).

Cement is defined as a dry material that incurs binding properties subsequent to undergoing hydration or reaction with water. Worldwide, the most common binder used in construction is Portland cement, which consists principally of grains ranging in size from 1 to 50 μm composed of calcium silicates, calcium aluminates, and calcium sulfates, among other phases (ASTM C 150, 2007). ASTM provides a classification system for Portland cements based upon variations in the proportions of different reactants, as shown in Table 1.2.

Table 1.2. Composition (%) of various Portland cements. Adapted from Mehta (2006).

Cement Type	C_2S	C_3S	C_3A	C_4AF
I	15-20	50-55	5-12	6-10
II	15-20	50-55	5-7	6-12
III	10-15	50-60	8-12	6-10
IV	25-35	40-50	0-4	10-15

Upon hydration, Portland cement reacts to form four major products: calcium silicate hydrates, calcium hydroxide, calcium sulfoaluminate hydrates, and unhydrated cement particles (Mehta, 2006). The solid compounds that compose hydrated Portland cement are listed in Table 1.3. Calcium silicate hydrate, abbreviated C-S-H, composes 50-60% of the solid volume in cement paste, and is described as a high surface-area nanostructure of calcium-silicate compounds of varying compositions (Mehta, 2006). Calcium hydroxide ($Ca(OH)_2$) composes 20-25% of cement paste solid volume, forming relatively large crystals within the matrix (Mehta, 2006). Calcium sulfoaluminate hydrates compose about 15-20% of the solid volume of cement paste. These hydrates are generally ettringite, with chemical formula $6CaO{\cdot}Al_2O_3{\cdot}3SO_3{\cdot}32H_2O$ (abbreviated $C_6AS_3H_{32}$), and monosulfate hydrate, $4CaO{\cdot}Al_2O_3{\cdot}SO_3{\cdot}18H_2O$ (abbreviated C_4ASH_{18}). Aluminum ions are sometimes replaced by iron in these crystals (Mehta, 2006).

Table 1.3. Solid compounds generally present in hydrated Portland cement.

Compound	Abbreviation	Formula
Calcium silicate hydrates	C-S-H	
Calcium hydroxide		$Ca(OH)_2$
Calcium sulfoaluminates		
Ettringite	$C_6A\bar{S}_3H_{32}$	$6CaO{\cdot}\ Al_2O_3{\cdot}3SO_3{\cdot}32H_2O$
	$C_4A\bar{S}H_{18}$	$4CaO{\cdot}Al_2O_3{\cdot}SO_3{\cdot}18H_2O$

In addition to hydrated cement and aggregate, supplementary cementing materials (SCMs) are often added to concrete mixes in order to enhance workability, increase strength, improve durability, and reduce cost (Mehta, 2006). Many of these SCMs are by-products of other industrial processes, such as the burning of coal or production of ore smelting (Mehta, 2006). One commonly used SCM is fly ash, which is produced from coal impurities (e.g. clays, quartz) that melt during combustion and solidify into spherical glass particles upon cooling (Mehta, 2006). Another common SCM is blast-furnace slag, which consists of the impurities (e.g. aluminosilicates) that separate from molten metal during the smelting process (Mehta, 2006). The production of silicon and ferrosilicon from the heating of quartz produces SiO vapors that eventually cool to produce spherical particles of silica fume, another SCM (Mehta, 2006). One other example of an SCM is metakaolin, which is not an industrial by-product, but is produced through heat treatments of the clay kaolin (Lagier, 2007). These SCMs consist mostly of reactive (i.e. amorphous) silicates and aluminosilicates, but will also contain some calcium, magnesium, iron or other impurities. For example, fly ash may also contain small amounts of sulfates and carbon (Mehta, 2006).

Characteristics of Concrete

There are a number of properties that can be utilized as measures of the overall quality of concrete (Mindness, 2003). These characteristics, including compressive strength, permeability, moisture content, porosity, and surface roughness are both interrelated and affected by other concrete composition properties, such as cement Type, SCM additions, and water/cement ratio, as well as age and environmental exposure

(Mehta, 2006). The bioreceptivity of concrete is thought to be influenced by a combination of these characteristics (Guillitte, 1995; Dubosc et al., 2001; Shirakawa, 2003; Pinheiro, 2004).

Of the properties used to evaluate the quality of concrete, strength is considered by many to be one of the most highly valued indicators (Mehta, 2006). In general, this is measured as compressive strength, which is the ability of a material to withstand an axial force (Mehta, 2006). The compressive strength of concrete can reflect other various concrete characteristics, such as porosity, permeability, cement type, water/cement ratio, and SCM addition, age, and exposure (Mehta, 2006).

Permeability, which is defined as the flow rate of liquid through a porous solid (i.e. the concrete matrix), is related to the interconnectivity of intrinsic porosity and cracking (Mehta, 2006). Porosity has been observed to increase the bioreceptivity of concrete (Guillitte, 1995; Dubosc et al., 2001). Higher permeability may allow for greater flow of moisture through interconnected pores, which in turn could affect microbial colonization of concrete surfaces (Dubosc et al., 2001).

The water/cement ratio by weight (w/cm) of concrete is an important characteristic that has a combination of effects on a structure's properties. A high w/cm can result in excess water in the hydration reaction, which will eventually leave the structure upon hardening, resulting in both a decrease in strength and increases in permeability and porosity (Mehta, 2006). The w/cm of concrete has been found to be positively related to a structure's susceptibility to biofouling (Dubosc et al., 2001).

The surface roughness of concrete has also been previously suggested to influence biofouling susceptibility; specifically, smoother surfaces have been observed to harbor

less growth (Pinheiro, 2004). Surface roughness can be described as a ratio of surface area to projected area, which can be quantified through the calculation of a roughness number (Kurtis, 2003). Surface roughness can be an indicator of porosity, as well as aggregate size and texture (Mehta, 2006).

In addition, the degree of surface carbonation of concrete can be an indicator of a structure's receptivity to colonization as well as its exposure to atmospheric carbon dioxide or biogenic acids (Zherebyateva, 1991; Sand, 1997; Papadakis, 2000). New concrete has a surface pH of 12-13, which inhibits microbial colonization (Sand, 1997; Shirakawa, 2003). However, exposure to atmospheric carbon dioxide can drive the production of calcium carbonate from calcium hydroxide (Figure 1.2), resulting in a lower surface pH (Zherebyateva, 1991; Sand, 1997). The carbonation depth of concrete due to atmospheric CO_2 exposure can be estimated using the model developed by Papadakis (2000) with a structure's age. While this process occurs naturally, the resulting lower surface pH facilitates microbial colonization, which can then in turn expedite carbonation via acid-producing metabolic processes (Sand, 1997; Shirakawa, 2003).

$$Ca(OH)_2 + CO_2 \longrightarrow CaCO_3 + H_2O$$

Figure 1.2. The carbonation of concrete by exposure to carbon dioxide, which results in loss of surface alkalinity.

Properties of Photocatalytic Cement

The addition of photocatalytic substances such as nano-crystalline titanium dioxide (TiO_2) to cements has been used to incur self-cleaning properties to outdoor structures (Cassar, 2007). Photocatalytic oxidation can be described as the adsorption of a

photon by a semiconductor material, which results in the catalytic generation of hydroxyl and perihydroxide radicals from nearby water molecules (Goswami, 2003; Blob, 2007). These radicals can then oxidatively mineralize organic compounds, essentially cleaning the area surrounding the photocatalytic agent (Goswami, 2003; Blob, 2007; Tanizaki, 2007). This generation of free radicals and subsequent oxidation of organics by anatase or rutile forms of TiO_2, which are commonly used as photocatalysts, is described in Figure 1.3. Specifically, titanium dioxide is activated via exposure to near UV wavelengths (~400 nm or less) and, to a smaller degree, visible light (Goswami, 2003; Hashimoto, 2007).

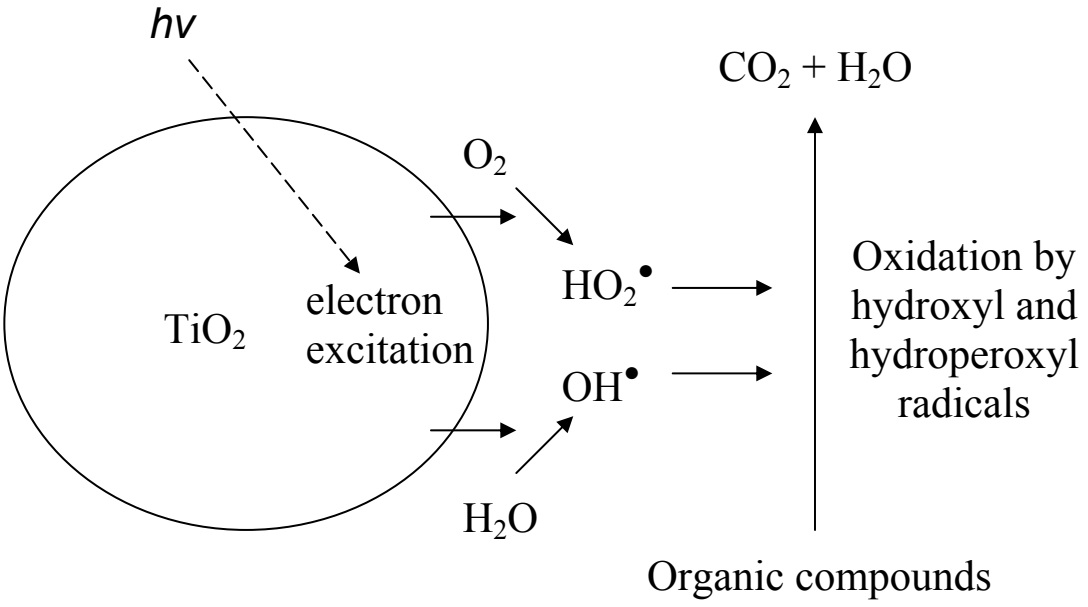

Figure 1.3. Photocatalytic oxidation by TiO2. Adapted from Blob & Elfenthal (2007).

TiO_2 has been tested for its ability to incur self-cleaning properties in a variety of materials, including cements, glass mirrors, and medical devices (Cassar, 2007; Hashimoto, 2007; Tsuang, 2008). In addition, photocatalytically-active TiO_2 has been

shown to have antimicrobial activity against *Escherichia coli*, *Pseudomonas aeruginosa*, and *Staphylococcus aureus*, as well as inactivate humam rotavirus and human astrovirus strains (Sang, 2007; Tsuang, 2008). The potential benefits of TiO_2 have sparked its testing and use in concrete and other cementitious construction materials (Cassar, 2007).

Microbial Deterioration of Concrete

Biologically-mediated deterioration of concrete and stone structures can occur by a number of different mechanisms, both chemical and physical (Gaylarde and Morton, 1999; Warscheid and Braams, 2000). The most well-known and characterized process, however, is corrosion via the microbial production of acids (Warscheid and Braams, 2000). This is of particular importance in concrete sewer pipes, where the resulting deterioration can cause leakage and failure in infrastructure (Sand and Bock, 1991). In these systems, sulfur-oxidizing bacteria such as *Thiobacillus thiooxidans* have been shown to deteriorate concrete sewer pipes through the generation of sulfuric acid (Parker, 1945; Milde et al., 1983; Sand and Bock, 1991; Nica et al., 2000). Specifically, sulfides originating from sewage volatilize into unfilled portions of the pipe and precipitate as sulfur compounds on the inner wall (Figure 1.4). This sulfur is then oxidized by bacteria to produce sulfuric acid, which corrodes concrete, producing gypsum ($CaSO_4$) among other products (Sand and Bock, 1991). Loss of concrete strength, cracking, and eventual failure can result (Sand and Bock, 1991; Mehta, 2006).

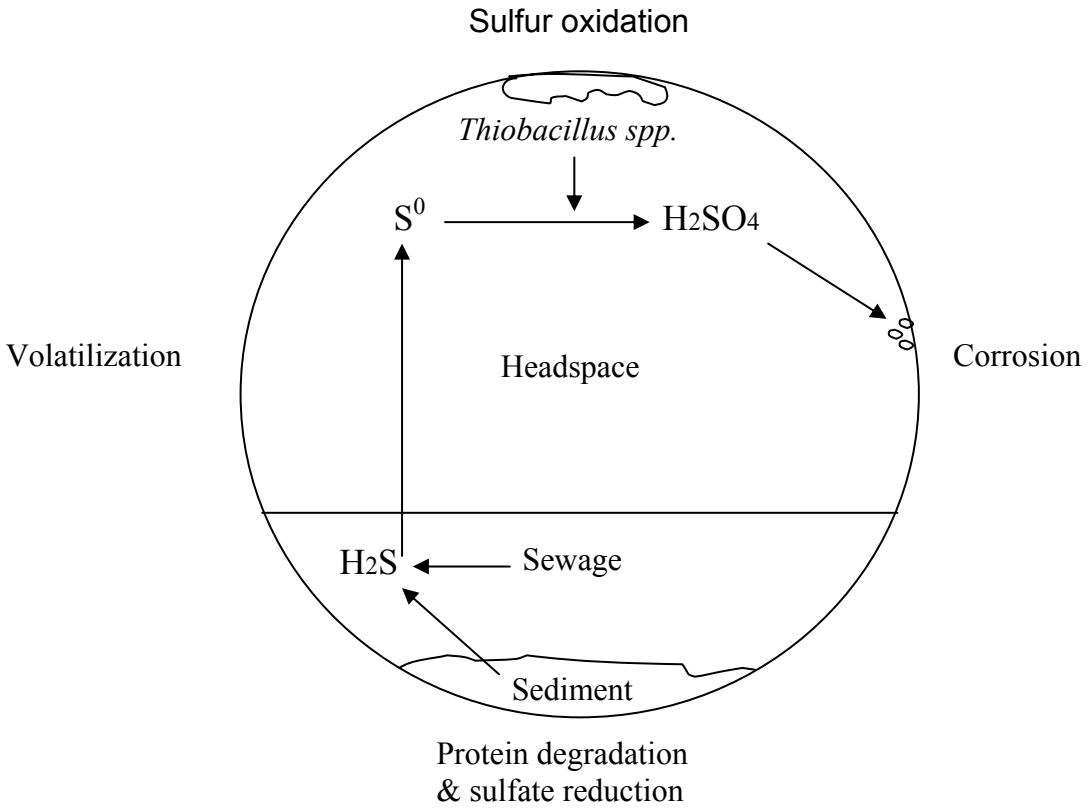

Figure 1.4. Corrosion of a concrete sewer pipe by biogenic sulfuric acid. Adapted from Sand & Bock (1991).

Acid attack on concrete can also be performed by nitrifiers such as *Nitrosomonas* and *Nirobacter* spp., which produce nitrous and nitric acid, respectively, corroding buildings and other structures (Zherebyateva, 1991; Sand, 1997; Gu et al., 1998). The carbonation of concrete surfaces can be expedited by the microbial production of CO_2, leading to surface acidification and facilitating the colonization of additional organisms (Sand, 1997).

The excretion of organic acids, particularly by fungi also contributes to concrete deterioration (Gu et al., 1998; Gaylarde and Morton, 1999). A multitude of fungal genera (e.g. *Alternaria*, *Fusarium*, *Penicillium*, *Trichoderma*) have been observed to produce organic acids (Sterflinger, 2000). Biogenic organic acids (e.g. acetic, glucuronic, oxalic)

can damage concrete through the formation of insoluble calcium complexes, which precipitate from the structure, resulting in weight loss and increased permeability and porosity (Gu et al., 1998). The fungi *Fusarium* sp. and *Penicillium frequentans* are reported to deteriorate concrete and stone, respectively, through the production of organic acids (De La Torre et al., 1993; Gu et al., 1998).

The microbial deterioration of concrete and stone can also occur by physical means (Gaylarde and Morton, 1997; Warscheid and Braams, 2000). *Cyanobacteria* are able to colonize within small fissures of a structure's surface and expand via the uptake of water, which exerts pressure that can further open the cracks (Gaylarde and Morton, 1997). The production of extracellular polymeric substances by microbial biofilms can also induce stress by swelling (Warscheid and Braams, 2000). Hyphae produced by a *Fusarium* sp. have been found to penetrate concrete surfaces (Gaylarde and Morton, 1997; Gu et al., 1998). The penetration of hyphae can increase permeability and help to accelerate deterioration resulting from abiotic processes, such as freeze-thaw cycles (Warscheid and Braams, 2000).

Molecular Detection of Microbial Communities

While the microorganisms fouling many concrete and stone surfaces have been identified based on morphological attributes and their mechanisms of deterioration characterized, studies in this particular field have relied primarily on microscopy-based determination and culture-based techniques for microbial characterizations. Although this approach is valuable for obtaining isolates that are able to be characterized in the lab, it can only identify a small fraction of a given microbial community, as most microorganisms are resistant to cultivation (Staley and Konopka, 1985). To date, few

studies have conducted molecular-based characterizations of the microbial communities on concrete and stone surfaces (Crispim et al., 2006). Recently, however, the molecular diversity of endolithic microbial communities inhabiting the pore space in rocks has been described (McNamara et al., 2006; Norris and Castenholz, 2006; Walker and Pace, 2007).

Molecular phylogenetic methods, such as polymerase chain reaction and restriction fragment length polymorphism (PCR-RFLP) (Figure 1.5), are well-established and have been used to characterize microbial communities from a variety of environments by culture-independent means (Horton and Bruns, 2001; Anderson et al., 2003; Mills et al., 2003; Pang and Mitchell, 2005; Martinez et al., 2006; Michaelsen et al., 2006).

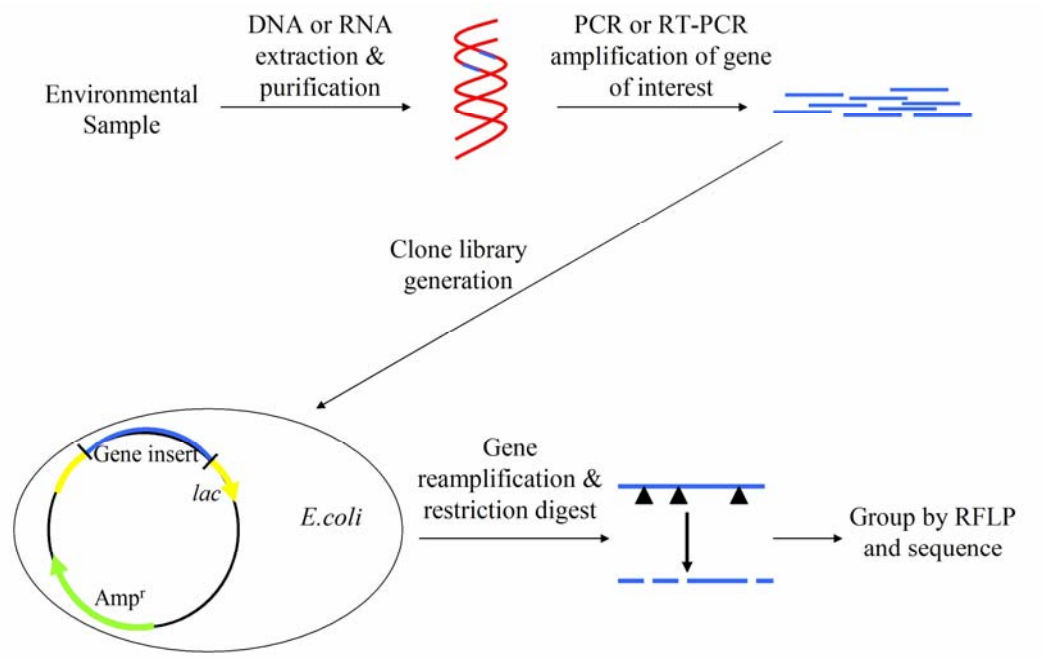

Figure 1.5. Overview of clone library analysis of environmental DNA and RNA.

While 16S ribosomal RNA (rRNA) gene sequence analysis has been integral in characterizing the environmental diversity of *Bacteria*, the use of rRNA genes to determine fungal diversity is relatively nascent, due largely in part to the difficulty of designing unbiased PCR primers that exclusively amplify fungal sequences (Anderson et al., 2003). 18S rRNA gene analysis has been successfully used to evaluate fungal community composition in a number of environments, such as crop rhizospheres and aquatic sediments (Smit et al., 1999; Tun, 2002; Takano et al., 2006). While the 18S rRNA gene is well-suited for comparison of distantly-related organisms and assessment of total fungal diversity, its sequence conservation can lead to low resolution analysis (Horton and Bruns, 2001; Hunt et al., 2004; Takano et al., 2006). The internal transcribed spacer (ITS) region (i.e. ITS1, 5.8S and ITS2) of fungal rRNA genes is an increasingly used sequence region for fungal molecular taxonomy studies (Torzilli et al., 2006; Midgley et al., 2007). While this more variable region yields higher resolution than the 18S rRNA gene, ITS primers can amplify plant DNA that may be present in samples, and sequences may be too disparate for alignment (Hunt et al., 2004). Fungal diversity and phylogeny is thus often determined using the analysis of multiple genes, including 18S and ITS rRNA genes, as well as 28S rRNA genes, α-tubulin, β-tubulin, and others (Takano et al., 2006; Hibbett et al., 2007).

Lab-based Simulations of Concrete Biofouling

While the identification of the microorganisms present on concrete in the field is the first step toward understanding biofouling, laboratory-controlled biofouling tests can be performed to evaluate surface colonization, biological or chemical degradation, and material bioreceptivity (Ehrich, 1999; Dubosc et al., 2001; Shirakawa, 2002). There have

been a number of variations that simulate the *in vitro* biofouling of concrete surfaces. To understand the colonization and corrosion of concrete sewers, Gu et al. (1998) constructed a miniaturized concrete pipe from which a concrete specimen was hung and sprayed from below with culture medium inoculated with *Thiobacillus intermedius* or a *Fusarium* sp. Similarly, Ehrich et al. (1999) designed a humidity chamber in which *Thiobacillu*s-inoculated mortar specimens were sprayed with a mineral salt solution and exposed to circulated air containing H_2S in order to simulate biogenic sulfuric acid corrosion. The susceptibility of phosphogypsum has been tested by initially spraying tiles with a fungal inoculum and incubating within a controlled humidity chamber (Shirakawa, 2002). Shirakawa et al. (2003) similarly tested the bioreceptivity of mortar by drying media onto a mortar cube, inoculating with *Cladosporium sphaerospermum,* and suspending the specimen in a chamber at 100% relative humidity. The susceptibility of concrete of different water/cement ratios to algal colonization has also been tested, using a spray system that recycles inoculum onto specimens (Dubosc et al., 2001).

CHAPTER 2

STATEMENT OF OBJECTIVES

Though the fouling of outdoor concrete is a frequent occurrence that may have an impact on the integrity of many historic and functional structures, little research has been done regarding the specific community compositions of these biofouling agents aside from general culture-dependent methods. Furthermore, few tests have been performed that examine the susceptibility of a wide range of concrete composition variables to fouling by isolates cultured directly from structures in the field. In this study, both molecular-based and culture-dependent approaches were used to examine the microbial communities fouling concrete, specifically looking at the fouling of selected outdoor concrete structures throughout the state of Georgia, USA. Specifically, we wished to accomplish the following objectives:

- Characterize the microbial community composition of biofouled concrete structures in order to test the hypothesis that distinct microbial populations exist on different fouled surfaces.
- Test isolates cultured from fouled concrete surfaces for the ability to foul concrete under controlled laboratory conditions, both in nutrient-rich environs and settings that more closely resemble *in situ* field conditions.
- Test the hypothesis that variations in concrete composition and construction practices can affect susceptibility to biofouling by both examining the properties of concrete sample sites and testing the ability of cultured isolates to foul concrete of various characteristics.

CHAPTER 3

MATERIALS AND METHODS

Site Description and Sampling

Four outdoor concrete sites located throughout the state of Georgia, USA, (Atlanta, 33º48'N, 84º22'W; Gainesville, 34º15'N, 83º57'W; LaGrange, 33º03'N, 84º57'W; Savannah, 32º13'N, 81º37'W) and a control site north of Atlanta (33º52'N, 84º27'W) that lacked any visible fouling were chosen for study. A coating of acrylic paint was present at two of the sites, LaGrange and Savannah. All of the sites (excluding the control site) had visibly fouled surface characteristics, i.e. black crusts on the concrete appearing as either vertical striations or covering the entire surface. To collect samples for DNA extraction, 5-10 strips (5 cm x 1 cm) of heterotrophic plate count agar (Difco, USA) and potato dextrose agar (EMD, USA) were aseptically pressed against the concrete surfaces. Samples were stored at 4ºC until DNA extraction (1-3 days). Additional agar strips of the same media type were used to culture isolates, which were collected from concrete surfaces as described above. These agar strips, however, were placed directly onto solid media, incubated at 25ºC for 7 days and re-streaked multiple times to ensure purity. Purity was verified microscopically and by molecular analysis of the ITS region. Concrete was also chipped directly off the surfaces for environmental scanning electron microscopy (ESEM), photo-pigment extractions, and thermogravimetric/differential thermal analysis (TG/DTA).

Molecular Analysis of Sample Sites

DNA Extraction and PCR Amplification

DNA was extracted and purified from agar strip samples taken from concrete surfaces using an UltraClean™ Soil DNA Isolation Kit (Mo Bio Laboratories, Inc.) according to manufacturer's instructions. Three separate DNA extractions per sampling site were performed and pooled by site. Bacterial 16S rRNA genes were amplified using primers 27F and 1522R (Mills et al., 2003; Martinez et al., 2006). Fungal 18S rRNA genes were amplified using primers NS1 (White, 1990) and FR1 (Zhou et al., 2000). The ITS region of fungal rRNA genes (i.e. ITS1, 5.8S and ITS2; Figure 3.1) were amplified using primers ITS1 and ITS4 (White, 1990). Sequences of PCR primers used in this study for amplification of extracted DNA are listed in Table 3.1.

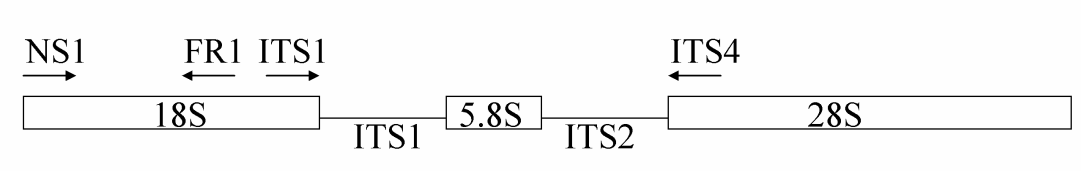

Figure 3.1. Positions of primers along fungal rRNA genes. 18S rRNA genes were amplified using primers NS1 (White, 1990) and FR1 (Zhou, 1990). The ITS region of fungal rRNA genes was amplified using primers ITS1 and ITS4 (White, 1990). Figure adapted from Takano et al. (2006).

Table 3.1. Oligonucleotide primers used in PCR amplification and sequencing.

Primer	Specificity	Annealing temp (ºC)	Sequence (5'-3')	Reference
27F	*Bacteria* 16S rRNA	52	AGAGTTTGATCCTGGCTCAG	Mills et al. (2003)
1522R			AAGGAGGTGATCCARCCGCA	Mills et al. (2003)
NS1	*Fungi* 18S rRNA	52	GTAGTCATATGCTTGTCTC	White (1990)
FR1			CTCTCAATCTGTCAATCCTTATT	Zhou et al. (2000)
ITS1	*Fungi* ITS rRNA	60	TCCGTAGGTGAACCTGCGG	White (1990)
ITS4			TCCTCCGCTTATTGATATGC	White (1990)
M13F	Cloning vector	55	GTAAAACGACGGCCAG	
M13R			CAGGAAACACGTATGAC	

PCR reactions were performed using GoTaq^{R} Green Master Mix (Promega), 2.5 μM of each primer, and 50 ng extracted DNA. Amplification of 16S rRNA genes and ITS region of rRNA genes were performed as previously described (Mills et al., 2003; Michaelsen et al., 2006). Thermocycling parameters for 18S rRNA gene amplification were as follows: 95ºC for 3 minutes, followed by 25 cycles of 95ºC for 1 minute, 52ºC for 1 minute, and 72ºC for 2 minutes, and a final elongation temperature of 72ºC for 10 minutes. Amplified PCR products were separated on 1.0% agarose gels and purified using a QIAquick gel extraction kit (Qiagen) according to manufacturer's instructions.

Clone Library Construction and RFLP Analysis

Clone library construction and RFLP analysis was performed as previously described (Mills, 2005; Martinez et al., 2006). Purified amplicons were cloned into the TOPO cloning vector pCR2.1 and transformed into TOP10 electrocompetent cells according to the manufacturer's instructions (Invitrogen). Three clone libraries (16S,

18S, and ITS) per sample site were constructed. Inserts were subsequently PCR amplified from lysed colonies with vector-specific primers M13F and M13R (Invitrogen), which were used in order to prevent amplification of the host *E.coli* 16S rRNA gene. PCR products from bacterial and fungal rRNA gene libraries were double digested with *Hha*I/*Msp*I and *Hae*III/*Rsa*I (Promega), respectively. Clones were grouped according to RFLP banding patterns, and representative clones were sequenced from RFLP groups containing three or more members. Clones containing 16S rRNA genes were sequenced as previously described (Mills et al., 2003), using vector-specific primers M13F, M13R, as well as internal primers 907R (5'-CCGTCAATTCMTTTRAGTTT-3') and 1392R (5'-ACGGGCGGTGTGTRC-3'). Clones containing the ITS region of rRNA genes were sequenced using primers M13F and M13R, and clones containing 18S rRNA genes were sequenced using primers M13F, M13R, as well as internal primer NS3 (5'-GCAAGTCTGGTGCCAGCAGCC-3') (White, 1990). Sequencing was performed at the Georgia Tech Genome Center using a BigDye Terminataor v3.1 Cycle sequencing kit on an automated capillary sequencer (model 3100 Gene Analyzer, Applied Biosystems).

Phylogenetic Analysis

Phylogenetic and rarefaction analysis was performed as previously described (Martinez et al., 2006). Sequences obtained for individual clones were aligned and assembled using the program BioEdit v7.0.9.0 (Hall, 1999). Sequences were checked for chimeras using Chimera Check from the Ribosomal Database Project II (Maidak, 1999). Sequences from this study, as well as reference sequences obtained from the GenBank database provided by the National Center for Biotechnology Information (http://www.ncbi.nlm.nih.gov/), were aligned and neighbor-joining trees were

constructed in MEGA 4 (Tamura et al., 2007) using the Jukes-Cantor model (Jukes and Cantor, 1969). An average of 1,500 nt for 16S sequences, 1,220 nt for 18S sequences, and 600 nt for ITS sequences were used for analysis. Bootstrap data represent a percentage of 1000 samplings. Rarefaction analysis was performed using equations as previously described (Heck, 1975). Sequences have been deposited in the GenBank database under accession numbers EU409843-EU409893.

Detection of Photo-Pigments on Concrete Surfaces

To determine if fouled concrete samples contained photosynthetic pigments, which would indicate the presence of active photoautotrophs, chlorophyll and carotenoid extraction procedures were conducted essentially as described in Parsons (Parsons, 1984) with minor modifications. Triplicate powdered concrete samples (5 g) obtained from each site were suspended in 15 ml sterile saline and filtered onto 0.22μm membrane filters (Millipore). Filters were suspended in 90% acetone and incubated at 4ºC in the dark for 12h. The resulting solution was centrifuged for 5 min at 5000 rpm and photometrically quantified as previously described (Parsons, 1984). Controls were conducted that included using known dilutions of chlorophyll a standard (Turner Designs), extractions of clean (non-fouled) concrete samples, and extractions of clean concrete samples mixed with known concentrations of chlorophyll a standard. These controls were performed in order to validate the procedure and to ensure that any quenching or inhibition of photo-pigment measurements by the concrete suspension was included in calculations.

Analysis of Concrete Properties

Study sites were subjected to a number of physical and chemical tests to assess overall concrete quality (Mindness, 2003). Field compressive strength was assessed by a Schmidt HM75 rebound hammer (Gilson Company), field permeability with a P-6050 Poroscope Plus (James Instruments), and moisture content of the concrete surfaces was measured with an M-70 Aquameter (James Instruments). All readings were taken according to manufacturer's instructions. To determine the pH of the concrete, a mixture of 1% phenolphthalein, 80% ethanol, and 19% water (v/v) was sprayed onto the surface of the sites and the underlying concrete (McPolin et al., 2007); a color change (pink) indicated a pH > 9, while no color change indicated a more acidic surface. The degree of carbonation at the sample sites was determined from concrete powder samples collected at depths of 0-1 cm from the surface and analyzed by thermogravimetric differential thermal analysis (TG/DTA), which measured mass loss and the amounts of calcium hydroxide and calcium carbonate of samples over a temperature range of 25-900º C; this was performed using a Seiko 320U analyzer as described previously (Bhatty et al., 1988).

Field measurements of compressive strength, permeability, and moisture content, as well as carbonation depth measurements, were compared to the amount of biofouling observed, which was measured as a percentage of the $2m^2$ sample site area. Field measurements were also compared to microbial diversity, which was determined by calculating a Shannon-Weaver index using both the bacterial and fungal phylotypes detected at each site (Figure 3.2). Measurements were standardized for comparison by subtracting the mean value from each measurement and dividing by the standard deviation, which generated a z-score for each characteristic. Measurements were fit to

linear equations, and R^2 values were calculated. A standard t-test was used determine correlative strength by generating p-values representing statistical significance. In addition to these comparisons, the degree of surface carbonation at each site was compared to expected carbonation depths, which were calculated using the actual ages of the structures based on Georgia Department of Transportation (GDOT) records (Patterson, 2005; Simmons, 2005; Cribb, 2006; Matthews, 2006) and the Papadakis model (2000) (Kurth, 2008).

$$H = -\sum_{i=1}^{S}(p_i)\ln(p_i)$$

Figure 3.2. Computation of the Shannon-Weaver index. The terms are defined as follows: H, Shannon-Weaver index; S, total number of phylotypes; pi, the relative abundance of a phylotype i.

Biofouling Tests

Incubation Chamber Description

In order to investigate the biofouling of concrete surfaces under controlled laboratory conditions, incubation chambers capable of spraying liquid media onto concrete tiles and recycling runoff were constructed (Figures 3.3 & 3.4). Prior to biofouling experiments, incubation chambers were sterilized by flushing with 10% (v/v) bleach solution for 24 hours, followed by flushing with sterile water for 24 hours. Cultured isolates suspended in 0.85% saline were inoculated in 100 µl aliquots onto the surfaces of sterile mortar tiles placed within the incubation chambers. Incubations were

run at 25ºC, which consisted of 300 ml of liquid media being sprayed onto tile surfaces and recycled. This spraying was cycled on and off over six-hour time intervals; relative humidity of incubation chambers was 100% during spray cycles and 95% during non-spray cycles. Following incubation, tiles were stored in sterile Petri dishes at 25ºC until further analysis.

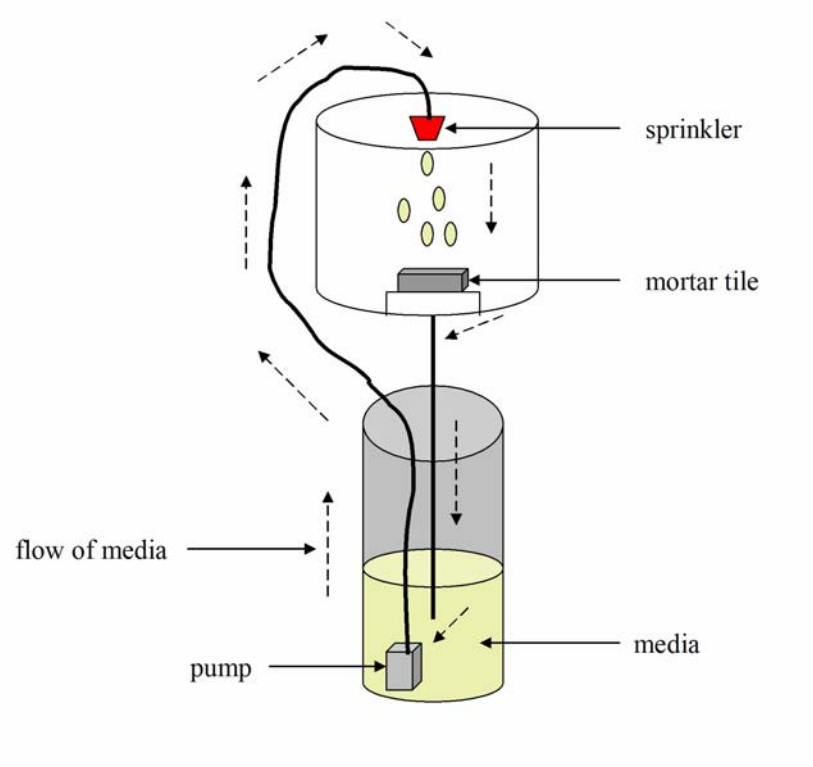

Figure 3.3. Diagram of the biofouling incubation chamber. Media was sprayed onto an inoculated mortar tile and then recycled through a pump-driven sprinkler system. Spraying was cycled over six-hour on/off intervals.

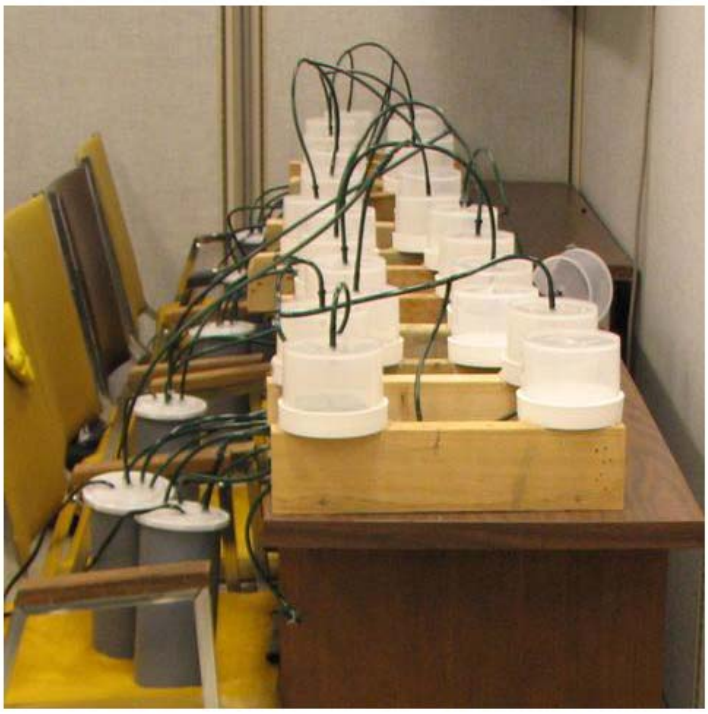

Figure 3.4. Incubation chambers constructed for biofouling tests.

Mortar Compositions Tested

In order to determine the effects that different concrete properties had on susceptibility to biofilm formation, mortar tiles (6 x 6 x 0.4 cm) of varying compositions were constructed (mixes with only sand fine aggregate (i.e. mortar mixes) were more conducive to the small tiles cast for this study). Cement paste was mixed with a sand fine aggregate and cast into tiles against flat, galvanized steel using a plastic framework. Tiles were then cured in limewater at 25ºC for 28 days, during which time varying finishes (i.e. brushing, polishing, or paint coating) were applied. Following curing, tiles were carbonated in a chamber (Nuaire US Autoflow NU-4850) at 20% CO_2, 40ºC, and

55% relative humidity for 30 days to reduce their surface pH to that seen in the field; this was confirmed by spraying the phenolphthalein indicator solution described earlier on the mortar tile surfaces. Tiles were sterilized by autoclaving (121ºC and 24 psi) prior to inoculation.

Using these tiles, we wished to test the effects of varying cement composition, supplementary cementing material addition, water/cement ratio, compressive strength, and surface roughness on biofouling. The specific compositions of each tile type tested are listed in Table 3.2.

Table 3.2. Compositions of mortar mixes used in fouling tests. Standard mix is in bold.

Mix ID	Cement	w/cm	SCM addition	Surface Finish
A	**Holcim GU I/II**	**0.5**	**none**	**brushed**
B	Holcim GU + 5% limestone	0.5	none	brushed
C	Essroc I/II	0.5	none	brushed
D	Essroc Tx Aria	0.5	none	brushed
E	Holcim GU I/II	0.3	none	brushed
F	Holcim GU I/II	0.4	none	brushed
G	Holcim GU I/II	0.6	none	brushed
H	Holcim GU I/II	0.5	fly ash (10%)	brushed
I	Holcim GU I/II	0.5	fly ash (18%)	brushed
J	Holcim GU I/II	0.5	fly ash (25%)	brushed
K	Holcim GU I/II	0.5	slag (10%)	brushed
L	Holcim GU I/II	0.5	slag (25%)	brushed
M	Holcim GU I/II	0.5	slag (50%)	brushed
N	Holcim GU I/II	0.5	silica fume (5%)	brushed
O	Holcim GU I/II	0.5	silica fume (10%)	brushed
P	Holcim GU I/II	0.5	silica fume (15%)	brushed
Q	Holcim GU I/II	0.5	metakaolin (8%)	brushed
R	Holcim GU I/II	0.5	none	acrylic paint
S	Holcim GU I/II	0.5	none	polished (600 grit)
T	Holcim GU I/II	0.5	none	polished (120 grit)

Several different Portland cement mixes were tested in this study. First, a General Use (GU) Type I/II cement provided by Holcim (www.holcim.com) commonly used in Georgia (GDOT, 2001) was chosen for analysis; this was the default cement type used when testing other tile composition variables. We also tested a GU Type I/II cement (Holcim) interground with 5% limestone. A Type I/II cement provided by Essroc Co. (www.essroc.com) was also analyzed. In addition, an Essroc Tx Aria cement was tested; this is an Essroc Type I/II cement that contains TiO_2, designed to impart photocatalytic properties to the UV-exposed surfaces of cement-based materials. Mortar tile mixes A, B, C, and D (Table 3.2) represent tile types varying only in cement composition.

Mortar tiles with water/cement ratios of 0.30, 0.40, 0.50, and 0.60 were chosen for analysis; these values vary around the typical GDOT construction water/cement ratio of 0.44 (GDOT, 2001). As mentioned previously, this property may be a significant factor in the susceptibility of concrete to biofouling (Dubosc et al., 2001). A default water/cement ratio of 0.50 was used when testing other tile mix variables. Mortar mixes A, E, F, and G (Table 3.2) represent tile types that vary only in water/cement ratio.

A number of SCMs typically used in Georgia concrete construction projects (GDOT, 2001) were examined. These include Class C fly ash (Holcim), blast furnace slag (Holcim), silica fume (W.R. Grace Force 10000D), and metakaolin (MK 349) added to cement mixes at different replacement percentages by weight (Table 3.2). Oxide analysis, loss on ignition (LOI - an estimate of carbon-based impurities), and Bogue potential compositions (i.e., prediction of the compounds formed when a cement is hydrated) were performed for the cements and SCMs used in this study (Kurth, 2008), and are summarized in Table 3.3. Briefly, the cements in this study are primarily

composed of CaO and SiO_2, predominately forming the calcium silicates C_3S and C_2S (Table 3.3). The SCMs, while largely containing SiO_2, also contained relatively large proportions of Al_2O_3 (in the case of the fly ash, metakaolin, and slag), MgO (fly ash and slag), Fe_2O_3 (fly ash), as well as CaO (fly ash and slag) (Table 3.3). Mortar tile mixes A, and H-Q (Table 3.2) represent tile types varying only in SCM addition.

Table 3.3. Oxide analysis and Bogue potential compositions of cements and SCMs.

	Holcim GU I/II	Holcim GU I/II + 5% limestone	Essroc Tx Aria	Essroc I/II	Fly ash	Slag	Silica fume	Metakaolin
Oxide analysis								
SiO_2	19.82	18.69	19.18	20.09	35.47	38.21	97.12	52.10
Al_2O_3	5.01	4.76	4.71	5.65	18.38	8.47	0.01	44.03
Fe_2O_3	4.06	3.39	2.07	2.95	6.92	0.35	0.05	0.92
CaO	63.84	64.29	60.10	61.67	25.01	36.39	0.37	0.47
MgO	1.32	1.13	2.84	3.20	5.71	13.16	0.28	0.13
SO_3	2.87	3.09	2.82	3.40	1.89	1.70	0.04	0
Na_2O	0.14	0.18	0.27	0.32	1.95	0.27	0.04	0.02
K_2O	0.43	0.32	0.50	0.73	0.50	0.35	0.58	0.14
TiO_2	0.27	0.21	4.19	0.25	1.41	0.35	0.02	1.42
P_2O_5	0.18	0.14	0.13	0.10	1.27	0	0.08	0.17
Mn_2O_3	0.03	0	0.05	0.04	0.03	0.63	0.04	0.01
SrO	0.09	0.08	0.12	0.14	0.39	0.05	0.01	0.01
BaO	0.01	0.05	0	0.05	0.71	0.05	0	0.02
LOI	1.97	3.62	3.04	1.4	0.36	0.03	1.36	0.56
Bogue potential composition								
C_3S	61.54	73.97	56.19	46.44				
C_2S	10.73	0	12.90	22.83				
C_3A	6.42	6.88	8.98	9.99				
C_4AF	12.34	10.31	6.29	8.97				

We also examined the effect that compressive strength had on biofouling of tile surfaces. Since every mortar composition had a different compressive strength, all the mortar mixes used in this study were analyzed. To accomplish this, mortar cubes (5 x 5 x

5 cm) were cast using the same mixes from which the tiles were made. Following casting and curing, these cubes were crushed at 28 days to determine the compressive strength of each mortar mix, according to ASTM specifications (ASTM C 109, 2007).

The effect of surface roughness on biofouling was also analyzed. This was tested by varying the surface finishes on tiles, which directly affect roughness. A total of four different surface finishes were performed. In the first finish, mortar tiles were floated with a steel trowel and brushed with a paintbrush (mix A; Table 3.2). This was the default surface finish used when testing other tile composition variables. A second finish was performed by polishing tiles cured for 24 hours with 120 grit polishing paper (mix T; Table 3.2). The third surface finish was accomplished by polishing tiles cured for 24 hours using 120 grit polishing paper, then coating tiles with cement paste at a w/cm of 0.50, and finally polishing again with 600 grit polishing paper (mix S; Table 3.2). These latter two finishes generated significantly smoother surfaces, and thus lower roughness numbers. The final finish included dipping tiles cured for 28 days into water-based acrylic paint (mix R; Table 3.2); this finish was performed primarily to examine the effect of a paint coating on biofouling. The finishes used in this study were similar to those typically used in GDOT construction projects (GDOT, 2001).

To quantify surface roughness, a roughness number (RN) for each of the tile compositions was calculated. Data for roughness number determination was obtained by imaging tiles using a Leica SP-1 Confocal Microscope and aggregating images into using Leica LCS Lite version 2.6.1. A roughness number for each map was then calculated using ImageJ software (http://rsb.info.nih.gov/ij/), which has been previously described (Chinga, 2007).

Cultured Isolates Tested

In addition to the mortar tile variations tested, biofouling tests were performed using several combinations of the cultured isolates obtained via agar strips from the fouled sample sites. Table 3.4 summarizes all the permutations performed for biofouling tests.

Table 3.4. Parameters used in concrete biofouling tests.

Test	Cultured isolates	Tile mixes	Media	Time
Individual isolate tests	All (separated)	Standard mix A	20% potato dextrose broth	One week
Concrete composition tests	All (pooled by sample site) *T. viride* ATCC 52438	All tile mixes	20% potato dextrose broth	One week
Nutrient-limiting tests	All (pooled)	All tile mixes	Sterile deionized water Sterilized rainwater Sterilized rainwater with tiles coated in form-release oil Sterilized rainwater exposed to air pollution	One month
Photocatalytic cement tests	All (pooled)	Tile mixes C & D	20% potato dextrose broth artificial sunlight exposure	One week

Isolates obtained from the four fouled sample sites were cultured to purity using potato dextrose agar (EMD, USA) and identified by analysis of the ITS region of rRNA genes as described earlier. All cultured isolates were individually tested for their ability to foul standard mortar tiles (mix A; Table 3.2). Also, isolates pooled by sample site origin (i.e. Atlanta, Gainesville, LaGrange, or Savannah) as well as *Trichoderma viride* ATCC 52438 (a type strain related to an isolate predominately cultured from the sample sites) were used to examine the effects of mortar tile variations on biofouling. Individual isolate and site-pooled incubations, as well as uninoculated negative control tiles, were run for one week in the dark using 20% (v/v) potato dextrose broth as the liquid media.

In addition, cultured isolates from all sites were pooled together to test their ability to foul tiles using parameters that more closely simulated conditions in the field. Specifically, incubations using several low-nutrient media were examined. Tiles inoculated with a mix of all cultured isolates were run under sterile de-ionized water and sterilized rainwater collected in the city of Atlanta. Incubations using sterilized rainwater were also run in which tiles were coated with a DuoGuard form-release agent composed of #2 Fuel Oil (diesel-based) and petroleum oil-base stock (W.R. Meadows, Inc.). In addition, an incubation using sterilized rainwater exposed to vehicular exhaust and air pollution was also run. This media was created by submerging a used (5 years old) air filter from a diesel truck driven in the city of Atlanta into rainwater, shaking for 24 hours at 200 rpm, removing the filter, and finally sterilizing the rainwater by autoclaving. All the above incubations, as well as corresponding negative controls, were run in the dark for one month, utilizing all mortar tile types cast for this study.

The ability of cultured isolates to foul photocatalytically active cement was also examined. A mix of all cultured isolates was inoculated onto mortar tiles composed of either Essroc Type I/II cement (mix C; Table 3.2) or photocatalytically active Essroc Tx Aria (mix D; Table 3.2), with no other varying mortar properties. These incubations were run for one week using 20% (v/v) potato dextrose broth. However, in addition to six hour media spray cycles, inoculated tiles as well as uninoculated control tiles were also exposed to artificial sunlight generated by Ultravitalux Daylight lamps (Osram), as shown in Figure 3.5. Tiles exposed to artificial sunlight received approximately $10W/m^2$ near-UV irradiation (close to outdoor levels) over six-hour on/off cycles. Artificial sunlight and media spray cycles overlapped by three hours so that incubations experienced equal time under light/dark and media rain/non-rain conditions.

Figure 3.5. Biofouling incubations exposed to artificial sunlight. Tile surfaces received approximately 10 W/m^2.

Analysis of Biofouling Tests

A number of analyses were performed in an attempt to both quantify the biofouling coverage observed on mortar tiles and correlate that coverage to the variables tested. To quantify the fouling observed, a flatbed scanner with 1200 dpi resolution was used to image tiles 48 hours following incubation (storage of tiles in separate, sterile Petri dishes at room temperature allowed for drying so that color differences were accurately observed). Images obtained were then visually partitioned into 16 smaller fragments, essentially creating a 4 x 4 grid of images for each tile. Each image fragment was then

analyzed, which consisted of confirming the presence of growth (if any) by its color. Three separate observers performed this analysis for all tiles, identifying any combination of red, yellow/beige, green, black/dark, or no growth. Biofilm coverage on each tile was then calculated using the equation shown in Figure 3.6. The colors yellow and red appeared much more frequently than observed in the field; to counteract this bias seen in our incubations, growth colors were given weighted coefficients to more closely match field observations of predominately dark biofouling.

$$\frac{\text{Coverage of biofouling (\%)}}{\text{Tile}} = \frac{[(1.00 \times \text{yellow}) + (1.33 \times \text{red}) + (1.67 \times \text{green}) + (2.00 \times \text{black})]}{[(16 \text{ fragments/tile}) \times (1.00 + 1.33 + 1.67 + 2.00)]}$$

Figure 3.6. Equation used to quantify coverage of biofouling on tiles. Colors observed were given weighted coefficients to better correlate to the darker fouling observed in the field.

Multiple linear regression using Limdep 7.0 was performed to determine any relationships between the amount of biofouling observed on the tiles and the variables tested by the incubations. Measurements were fit to linear models, and R^2 values describing closeness of fit were obtained. In the case of categorical variables (i.e. cement type and surface finish), p-values were obtained using a standard t-test to determine significant differences in biofouling.

ESEM Imaging

Surface samples from each field site as well as selected mortar tiles from biofouling experiments were imaged on a FEI Quanta 200 environmental scanning electron microscope at the Tennessee Technological University (Cookeville, TN). Samples were examined in an 85% relative humidity atmosphere at stage temperature 5ºC and 733.3 Pa. Samples from concrete biofouling experiments were gold-sputtered and viewed in high vacuum mode to maintain adherence of the abundant growth for high resolution imaging.

CHAPTER 4

RESULTS

Sample Site Characteristics

Visual observations during sampling at each of the sites indicated that fouling appeared apparently exclusively on the surface (Figure 4.1 A-D), and that the underlying concrete (i.e., Figure 4.1 D) as well as the surface of the non-fouled control site (Figure 4.1 E) was devoid of any apparent discoloration. At the LaGrange and Savannah sites, fouling occurred mainly on surface coatings composed of paint, which could easily be peeled from the structure (Figure 4.1 C, D). The amount of fouling appeared greatest at these sites with surface coatings.

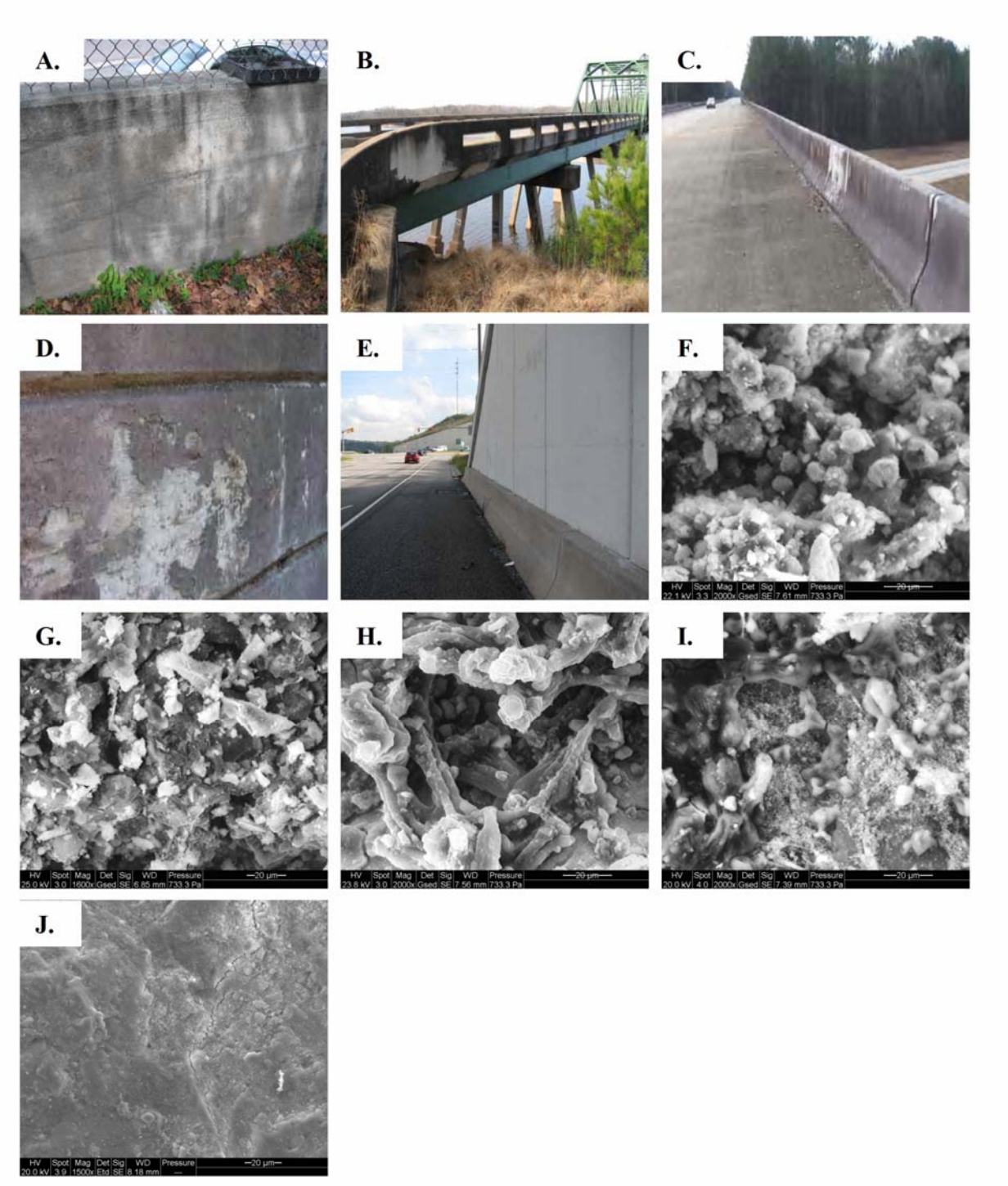

Figure 4.1. Examples of fouled concrete surfaces (A-D): (A) Atlanta site with black biofilm on unpainted surface. (B) Gainesville site with black crust on unpainted surface. Note removal of the crust by power washing as seen in the lighter areas. (C) LaGrange site with black crust on painted concrete surface. Lighter areas denote spots that have been cleaned. (D) Savannah

site with black crust on painted surface. Note areas of peeling showing underlying concrete with no visible biofilms. (E) Example of a non-fouled surface. Examples of ESEM images from samples collected at: (F) Atlanta; (G) Gainesville; (H) LaGrange; (I) Savannah; (J) non-fouled surface.

The pH of all the concrete surfaces was less than 9, while underlying concrete was more alkaline (> 9), as expected. Attempts to correlate field assessments of concrete compressive strength ($R^2 = 0.04$), permeability ($R^2 = 0.43$), and moisture content ($R^2 = 0.01$) to the amount of fouling over a given surface area at each site did not reveal any significant trends (Figure 4.2 A-C). Also, TG/DTA data did not reveal any trends ($R^2 = 0.25$) relating the amount of biofouling at the sites to the degree of surface carbonation (Figure 4.2 D). Specifically, the unfouled control site exhibited carbonation depths comparable to depths examined at sites exhibiting the greatest amount of biofouling (LaGrange and Savannah). In addition, the degree of surface carbonation measured was generally less than expected based on the structures' ages (Figure 4.2 D).

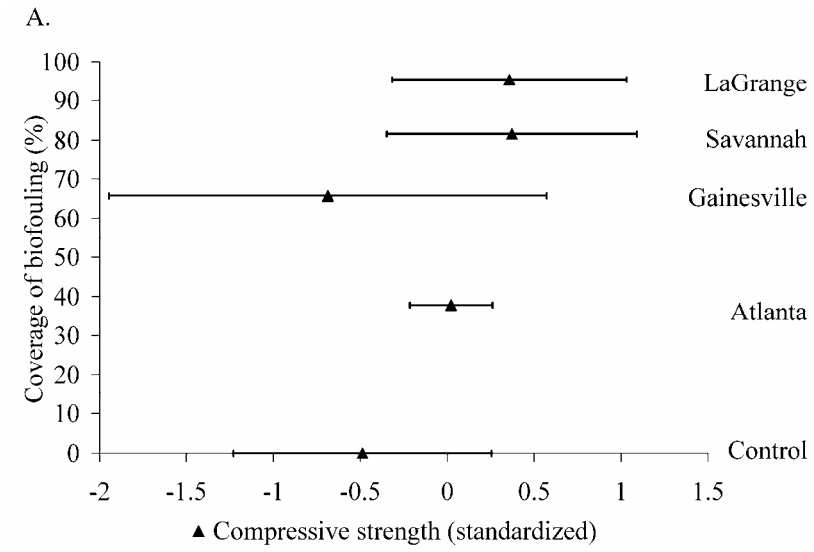

Figure 4.2.A. Comparison of compressive strength to the amount of biofouling observed at each sample site. No trend ($R^2 = 0.036$) was observed through these measurements.

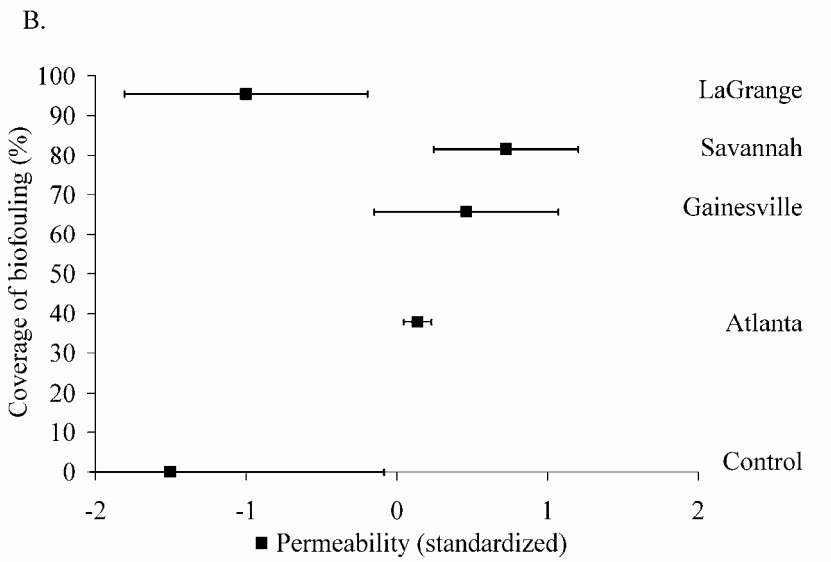

Figure 4.2.B. Comparison of permeability to the amount of biofouling observed at each sample site. No trend ($R^2 = 0.433$) was observed through these measurements.

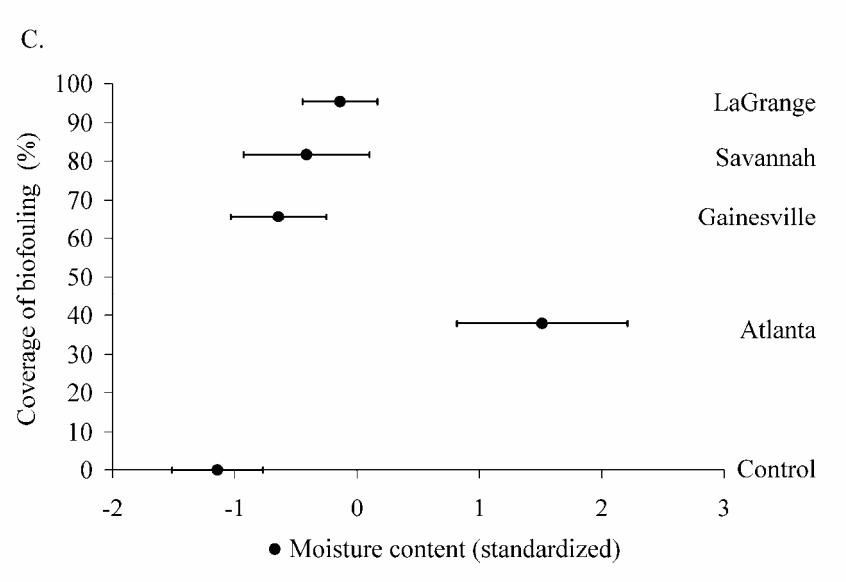

Figure 4.2.C. Comparison of moisture content to the amount of biofouling observed at each sample site. No trend ($R^2 = 0.012$) was observed through these measurements.

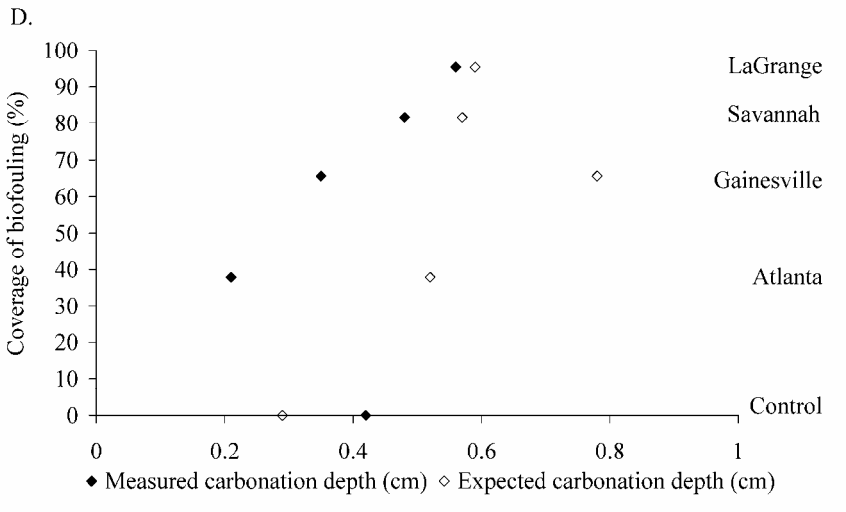

Figure 4.2.D. Comparison of measured and expected carbonation depths to the amount of biofouling observed at each sample site. No trend ($R^2 = 0.253$) was observed between biofouling and measured surface carbonation depth. Surface carbonation depth at the fouled sites was less than what was expected by modelling.

A comparison of compressive strength ($R^2 = 0.05$), moisture content ($R^2 = 0.20$), and surface carbonation depth to microbial diversity determined for each also did not reveal any strong trends (Figures 4.3 A, C, & D). Concrete permeability, however, did show a positive relationship to community diversity at the sample sites ($R^2 = 0.94$; Figure 4.3 B).

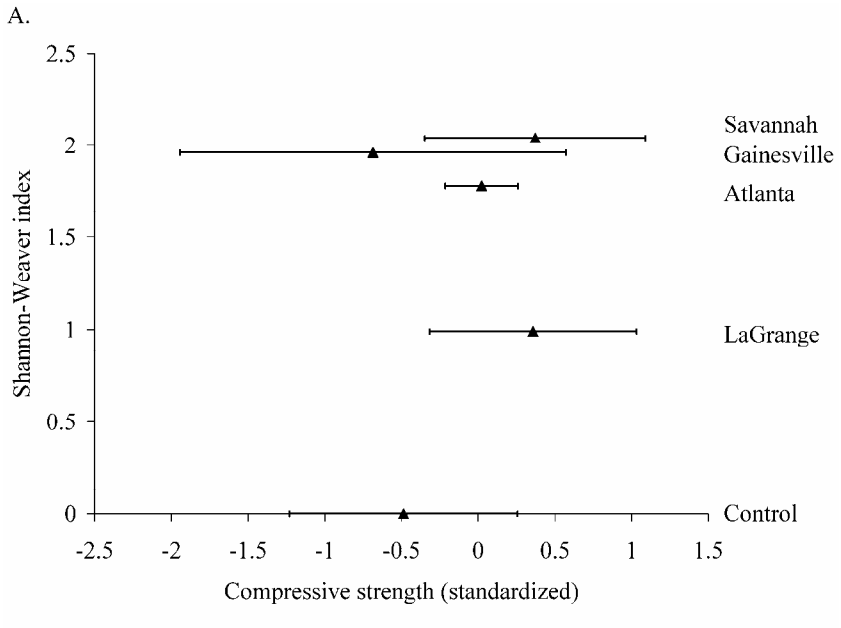

Figure 4.3.A. Comparison of compressive strength to the microbial diversity observed at each sample site. No trend ($R^2 = 0.05$) was observed through these measurements.

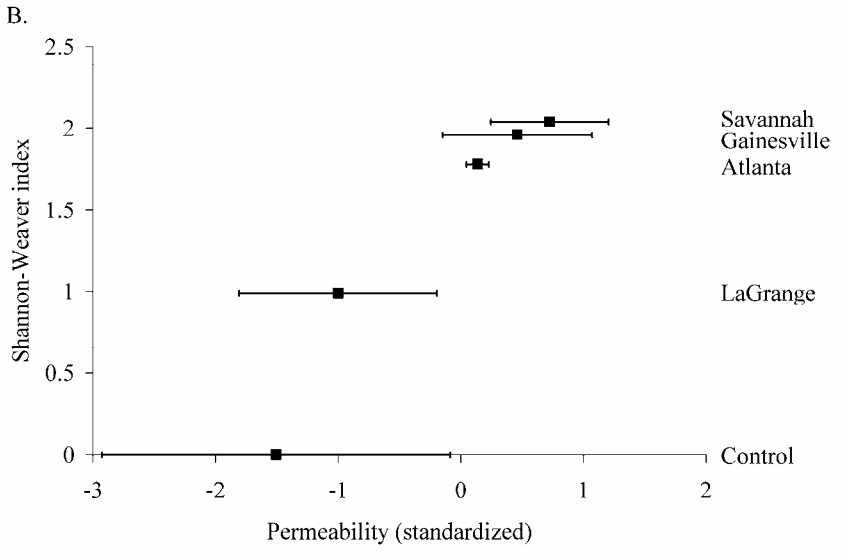

Figure 4.3.B. Comparison of permeability to the microbial diversity observed at each sample site. A strong positive trend ($R^2 = 0.94$) was observed through these measurements.

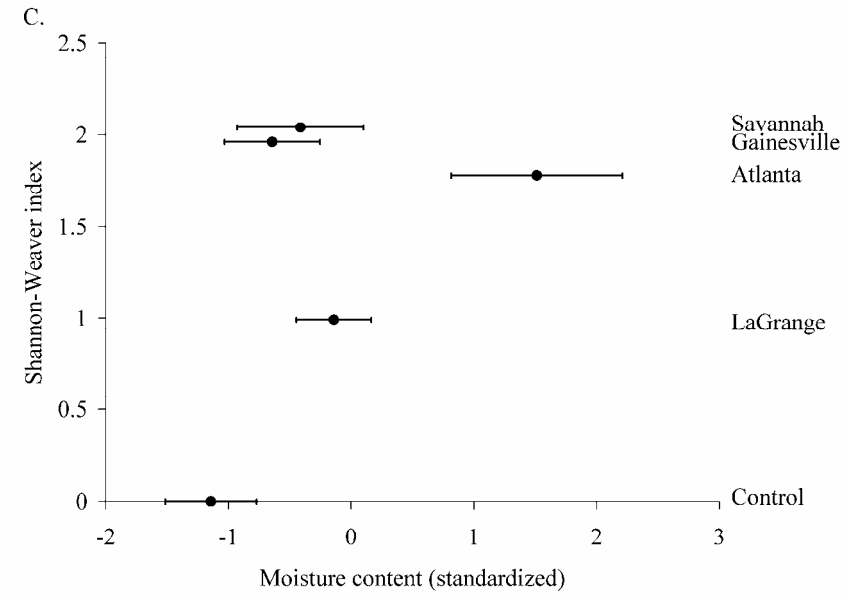

Figure 4.3.C. Comparison of moisture content to the microbial diversity observed at each sample site. No trend ($R^2 = 0.20$) was observed through these measurements.

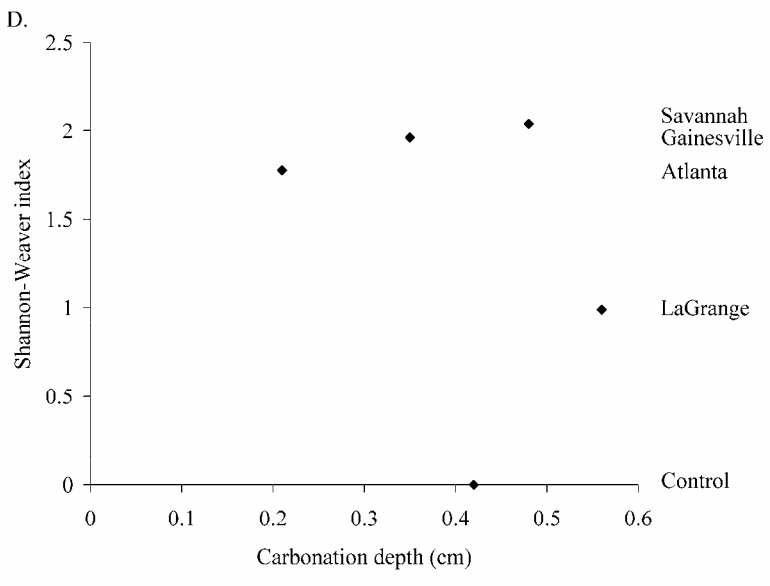

Figure 4.3.D. Comparison of surface carbonation depth to the microbial diversity observed at each sample site. No trend ($R^2 = 0.09$) was observed through these measurements.

Phylogenetic Diversity of Bacterial Communities

The composition of the bacterial communities was determined by 16S rRNA gene phylogenetic analysis. PCR amplifiable DNA was recovered from all four of the sampled sites. DNA was not recovered from samples collected from the control site with no visible fouling (Figure 4.1 E). A total of 180 clones representing the 4 sites were grouped into 40 RFLP patterns. Rarefaction analysis was applied to determine if a sufficient number of clones were screened to estimate diversity within each of the clone libraries sampled (Figure 4.4 A). For those bacterial clones obtained from the Atlanta site, the curve indicated saturation (Figure 4.4 A). Thus, a sufficient number of clones were sampled representative of the diversity of the bacteria in this library. Numerically

dominant RFLP groups, ranging from 8% to 23% of all clones were obtained for each of the four libraries (Table 4.1). In contrast, rarefaction curves generated for rRNA gene clones obtained from Gainesville, LaGrange and Savannah did not indicate saturation (Figure 4.4 A). Although additional sampling of clones would be needed to reveal the full extent of the diversity, numerically dominant RFLP groups were obtained (Table 4.1). Specifically, one dominant group of clones from each of the libraries (Gainesville, LaGrange and Savannah, represented by RFLP groups 1, 18, and 30, respectively) comprised 12%, 17% and 8% of all clones, respectively (Figure 4.5 A).

Analysis of 156 *Bacteria* clones from RFLP groups with three or more members revealed a greater diversity relative to the fungal clone library (Table 4.1) and included predominately uncultured bacterial lineages (Figure 4.6). A considerable majority of the clone sequences (102 of 156) were representative of the phylum *Proteobacteria*, (Table 4.1). Of these, 75% were related to the *Gammaproteobacteria*, including the most numerically dominant phylotype represented by the clone 16A1 (23% of the total clone library; Table 4.1). This phylotype, present at the Atlanta, Gainesville, and Savannah sites, was most closely related (99% similar) to a non-cultured organism [uncultured clone ctg_CGOF104; (Penn et al., 2006)] obtained from deep-sea coral on a Gulf of Alaska seamount (Figure 4.6). The second most dominant phylotype (17% of all clones; Table 4.1), belonging to the *Cyanobacteria*, was most closely related (93% similar) to a non-cultured organism obtained from a spacecraft assembly clean room [uncultured clone JSC2-A6; (Moissl et al., 2007)] (Figure 4.6). This phylotype, represented by clone 16L3, was only found at the LaGrange site (Table 4.1). The third most dominant phylotype (8% of all clones; Table 4.1), found in Savannah, was most closely related (99% similar)

to *Pantoea ananatis* BD 561 (Figure 4.6), a gammaproteobacterium found to be the causal agent of brown stalk rot in maize grown in South Africa (Goszczynska et al., 2007).

Comparisons of bacterial community diversity between concrete sites without (Figure 4.7 A-B) and with (Figure 4.7 C-D) acrylic paint coating were also conducted. Although there were differences in the diversity patterns between unpainted and painted sites there were also different patterns amongst all four sites (Figure 4.7 A-D). For example, clone 16A1 (Table 4.1), the most frequently detected phylotype, was recovered from painted and unpainted sites (Fig 4.7 A, B, & D), while the second most frequently detected phylotype, 16L3, was only detected at one of the two sites with paint coating (Figure 4.7 C). However, additional bacterial lineages were also found to occur on one or both surfaces, and/or at one of the four sites (Table 4.1 and Figure 4.7 A-D).

Table 4.1 Summary of representative sequences from 16S and ITS rRNA gene clone libraries

	Representative Sequence	No. related clones	Site acquired	Nearest relative	Phylogenetic group	Similarity (%)
16S	16A1	41	A, G, S	ASC clone ctg_CGOF104 [DQ395781]	*γ-Proteobacteria*	99
	16A12	4	A	ID clone BF0002D02 [AM697512]	*β-Proteobacteria*	92
	16A18	7	A	RS bacterium m5 [DQ453814]	*γ-Proteobacteria*	96
	16G1	14	G	OCS clone OCS7 [AF001645]	*β-Proteobacteria*	93
	16G10	6	A, G, S	GW clone 005C-B03 [AY661994]	*γ-Proteobacteria*	93
	16G48	5	G, L, S	*Janthinobacterium lividum* GA01 [DQ473538]	*β-Proteobacteria*	93
	16L2	4	A, L	ARV clone AYRV1-102 [DQ990927]	*Cyanobacteria*	98
	16L3	30	L	SAC clone JSC2-A6 [DQ532167]	*Cyanobacteria*	93
	16L4	3	L	SAC clone KSC6-17 [DQ532358]	*Acidobacteria*	95
	16L13	3	L	ID clone BF0001B010 [AM696984]	*β-Proteobacteria*	97
	16L33	2	L	clone ODP1230B22.23 [AB177177]	*Cyanobacteria*	98
	16S2	11	S	*Pedobacter steynii* WB2.3-45T [AM491372]	*Bacteroidetes*	99
	16S3	7	A, S	*Pseudomonas lutea* OK2 [AY364537]	*γ-Proteobacteria*	98
	16S5	15	S	*Pantoea ananatis* BD 561 [DQ133546]	*γ-Proteobacteria*	99
	16S32	2	S	*Rhodococcus erythropolis* EPWF [AY822047]	*Actinobacteria*	99
	16S46	2	S	SAC clone JSC9-A3 [DQ532271]	*Cyanobacteria*	87
ITS	IA1	27	A, G	*Alternaria* sp. CID62 [EF589849]	*Pleosporales*	100
	IA3	17	A	*Hypocrea lixii* [AJ608956]	*Hypocreales*	99
	IA5	5	A	*Aspergillus niger* 16888 [AY373852]	*Eurotiales*	99
	IG2	6	G	*Trichosporon pullulans* CBS 2541 [AF444418]	*Cystofilobasidiales*	100
	IG3	3	G	soil fungus clone 164-21 [DQ420945]	*Pleosporales*	100
	IG6	3	G	*Mucor racemosus* UWFP 1053 [AY213661]	*Mucorales*	99
	IG22	3	G	*Udeniomyces megalosporus* CBS 7236 [AF444408]	*Cystofilobasidiales*	100
	IG24	3	G	*Davidiella tassiana* cla063 [EF589965]	*Capnodiales*	99
	IL2	33	L	*Udeniomyces pseudopyricola* [AY841862]	*Cystofilobasidiales*	98
	IL40	20	L, S	*Epicoccum* sp. G7A [EF432273]	*Pleosporales*	99
	IS1	13	S	*Cladosporium cladosporioides* [DQ810182]	*Capnodiales*	100
	IS8	35	G, S	*Cladosporium* sp. B5B [EF432298]	*Capnodiales*	100

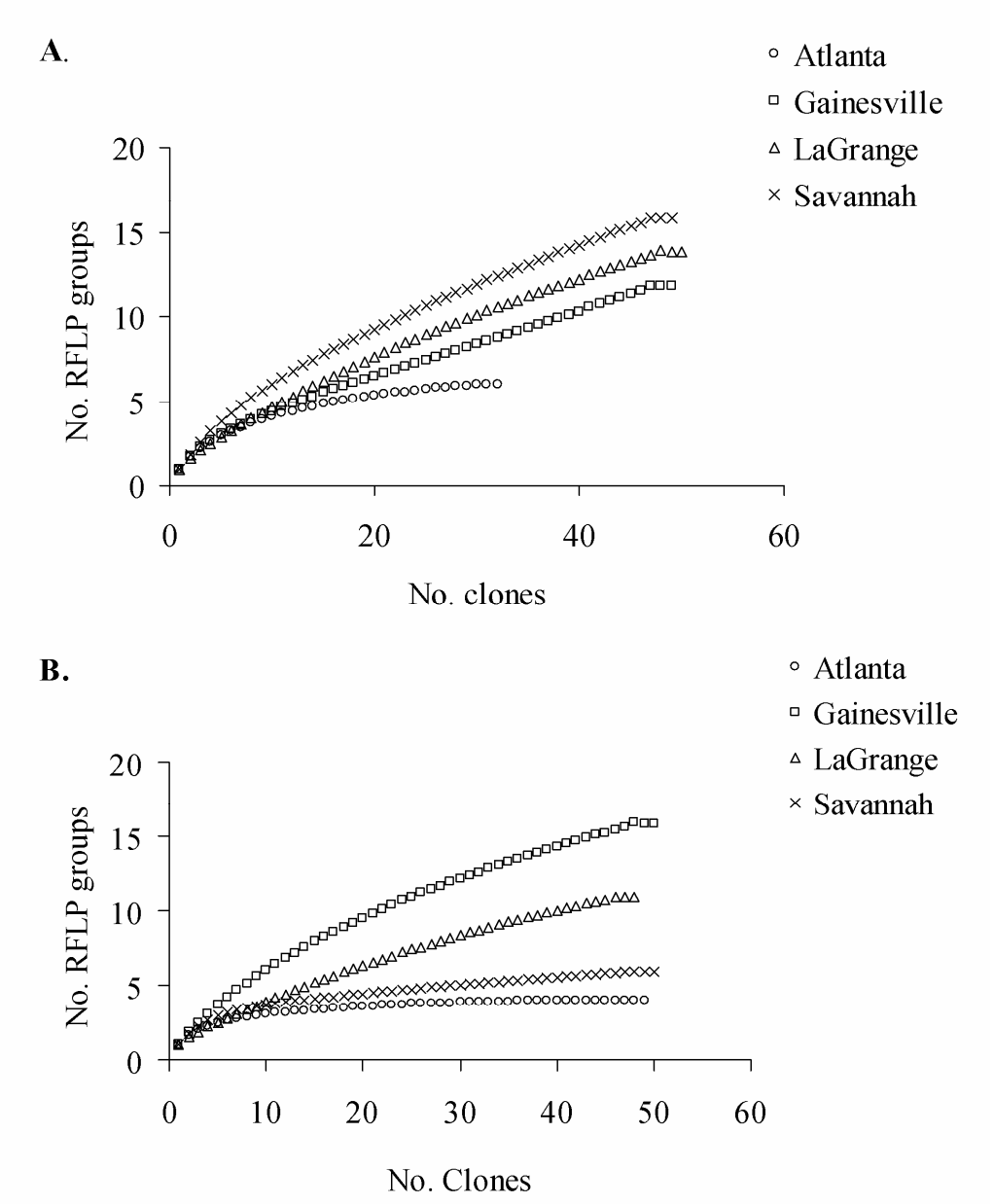

Figure 4.4. Rarefaction curves determined for the different RFLP patterns of (A) bacterial 16S rRNA gene clones and (B) ITS region of fungal rRNA gene clones obtained from each study site.

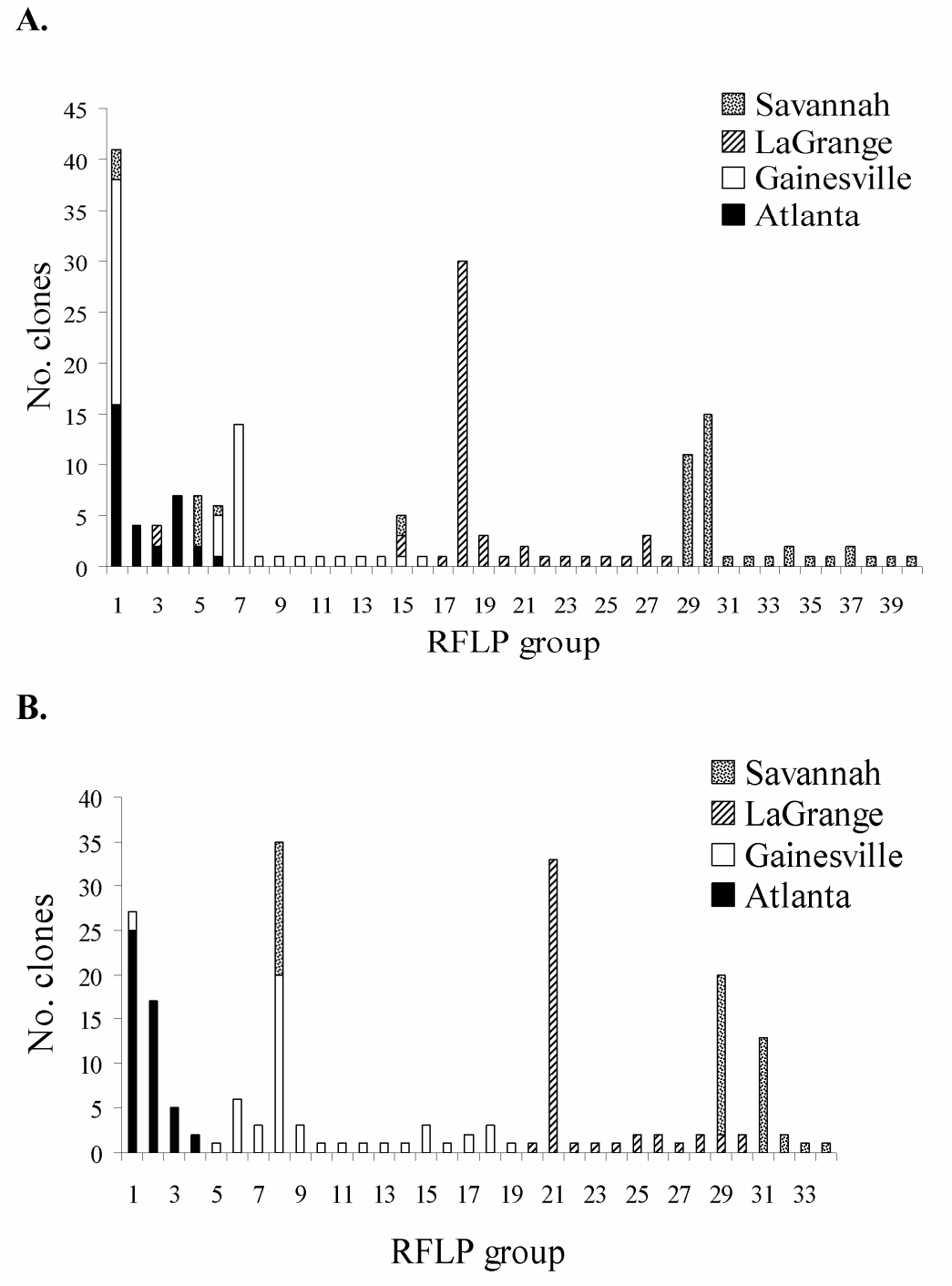

Figure 4.5. Frequency of (A) bacterial 16S and (B) fungal ITS RFLP groups obtained from each study site.

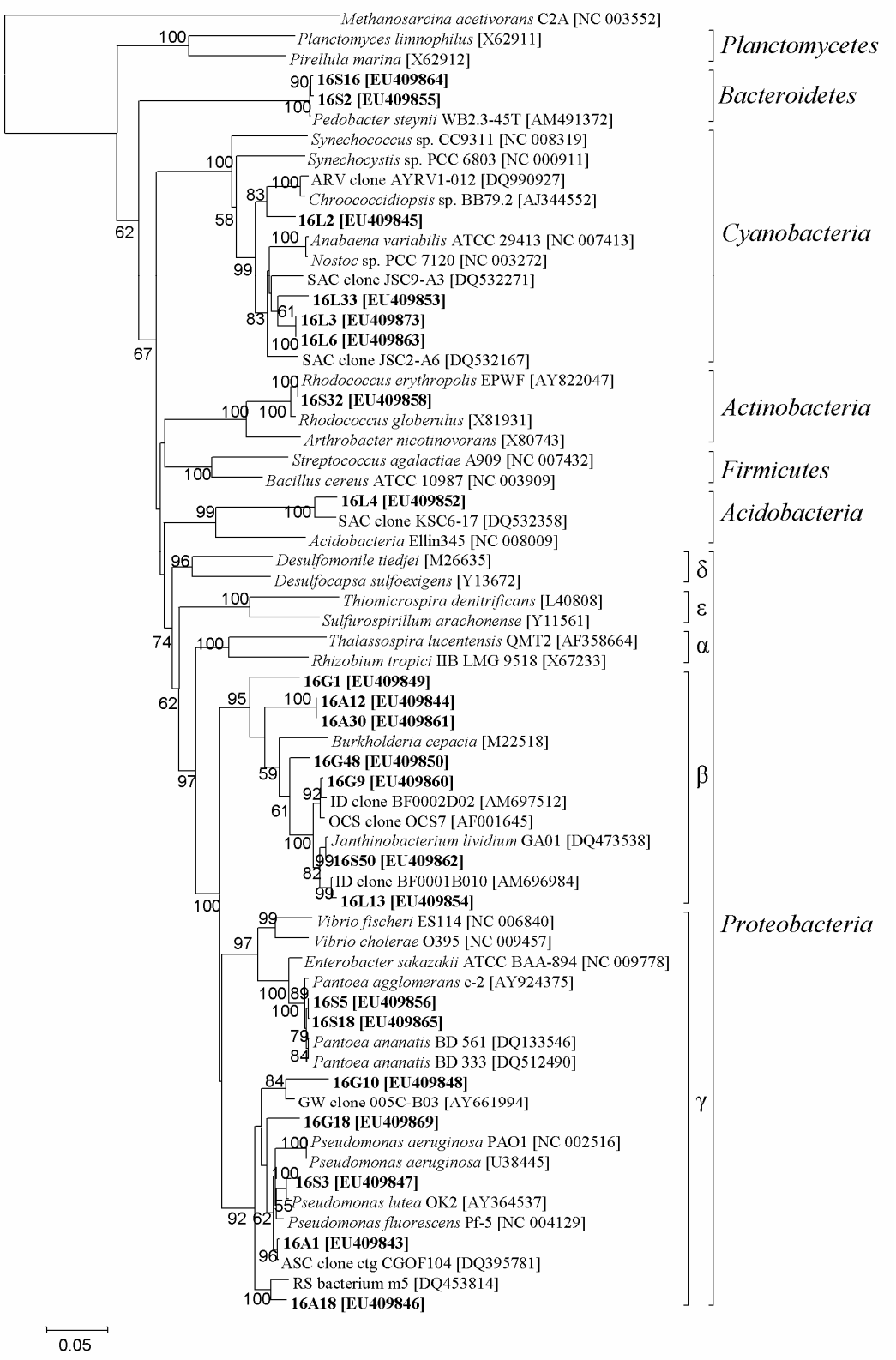

Figure 4.6. Phylogenetic analysis of bacterial 16S rRNA gene clone sequences, as determined by distance Jukes-Cantor analysis, from concrete surfaces in Georgia, USA

(in boldface), to selected cultured isolates and uncultured clones. Sequences derived from 16S rRNA gene templates are denoted by 16, and study site is denoted by A, Atlanta; G, Gainesville; L, LaGrange; S, Savannah. Designations of environmental clone sequences are ARV, Atacama Desert rock varnish; ASC, Alaskan seamount coral; GW, groundwater; ID, indoor dust; OCS, Oregon continental shelf; RS, red soil; SAC, spacecraft assembly cleanroom. Genbank accession numbers are in brackets. Bootstrap values represent 1000 replicates and only values greater than 50% are reported. The scale bar represents 0.05 substitutions per nucleotide position.

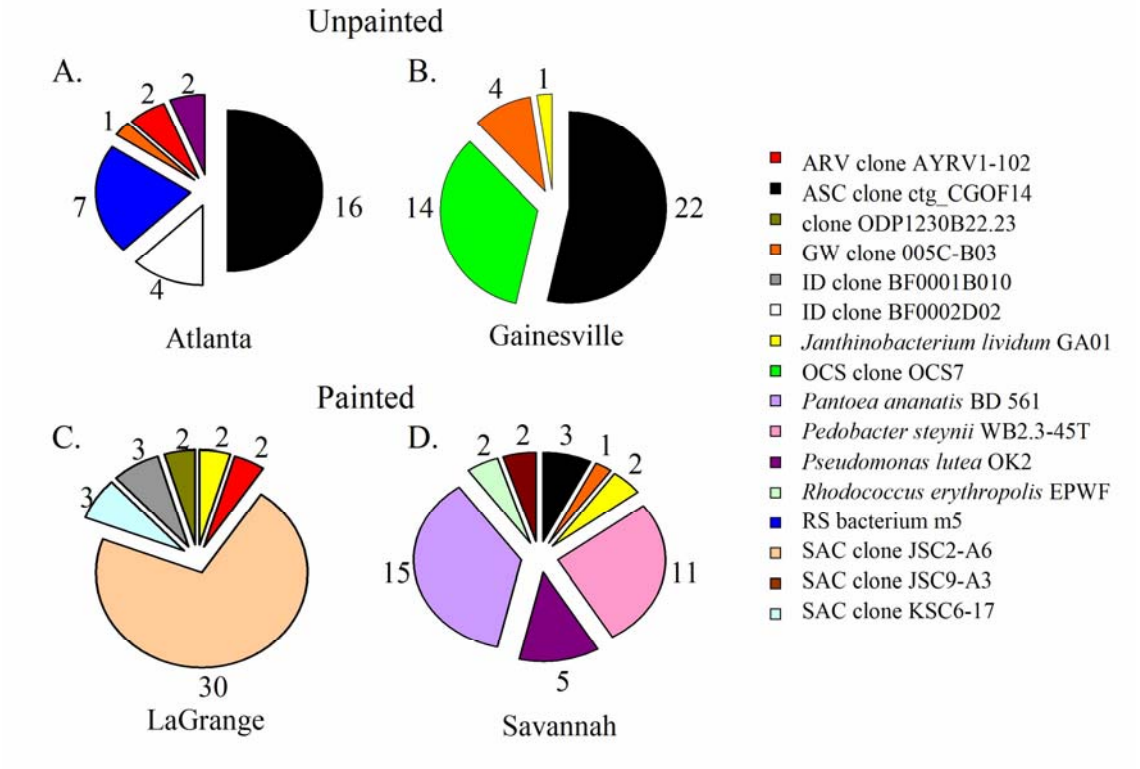

Figure 4.7. Phylotypes detected in 16S gene clone libraries derived from (A) Atlanta (B) Gainesville (C) LaGrange and (D) Savannah sites. Numbers of clones associated with each phylotype from which a representative clone had been sequenced are shown.

Phylogenetic Diversity of Fungal Communities

The composition of fungal communities was determined by examining a total of 197 clones containing the ITS region of rRNA genes, which grouped into 34 RFLP patterns. Rarefaction analysis was applied to determine if a sufficient number of clones

were screened to estimate diversity within each of the fungal clone libraries sampled (Figure 4.4 B). For those clones obtained from the Atlanta and Savannah sites, the curves indicated saturation (Figure 4.4 B). Thus, a sufficient number of clones were sampled representative of the diversity of the fungi in each respective library. Numerically dominant RFLP groups, ranging from 10 to 18% of all clones were obtained for each of the four libraries (Table 4.1). In contrast, curves generated for clones obtained from Gainesville and LaGrange did not indicate saturation (Figure 4.4 B). Additional sampling of clones would be needed to reveal the full extent of the diversity. However, as observed with the bacterial libraries, numerically dominant RFLP groups were obtained (Table 4.1, Figure 4.5 B). Specifically, one dominant group of clones from each of the libraries (Gainesville, represented by RFLP group 8 and LaGrange, represented by RFLP group 21; Figure 4.5 B) comprised 10 and 17% of all clones, respectively (Table 4.1).

Analysis of the 168 fungal clones from RFLP groups with three or more members revealed the greatest similarity to previously cultured organisms (Figure 4.8). A large number of clones (51 of 168) were representative of the order *Capnodiales* (Table 4.1). Of these, 90% were related to the genus *Cladosporium*, including the most numerically dominant phylotype, represented by clone IS8 (18% of total clones; Table 4.1). This phylotype, present in Gainesville and Savannah, was most closely related (100% identity) to *Cladosporium* sp. B5B (Figure 4.8). The second most dominant phylotype, represented by clone IL2 (17% of total clones; Table 4.1), only found at the LaGrange site, was most closely related (98% similar) to *Udeniomyces pseudopyricola* (Figure 4.8). The order *Pleosporales* was also highly represented (47 of 168; Table 4.1). This lineage

included the third most dominant phylotype (14% of total clones; Table 4.1), which was found at Atlanta and Gainesville and was most closely related (100% identity) to *Alternaria* sp. CID62 (Figure 4.8), as well as the phylotype most closely related (99% similarity) to *Epicoccum* sp. G7A, which was found at LaGrange and Savannah (10% of total clones; Table 4.1, Figure 4.8).

As observed with bacterial community diversity, fungal diversity between concrete sites without (Figure 4.9 A-B) and with (Figure 4.9 C-D) acrylic paint coating indicated that fungal phylotypes were not distributed solely according to surfaces coatings. Similar results were obtained for fungal biodiversity patterns, i.e., different phylotypes were detected at each of the four sites with some phylotypes occurring on both painted and unpainted surfaces. For example, clone type IS8 (Table 4.1) was recovered from painted and unpainted sites (Figure 4.9 B & D), while the second most frequently detected phylotype, IL2, was only detected at one of the two sites with paint coating (Figure 4.9 C). In contrast, IA1 was detected on unpainted surfaces only (Figure 4.8 A-B).

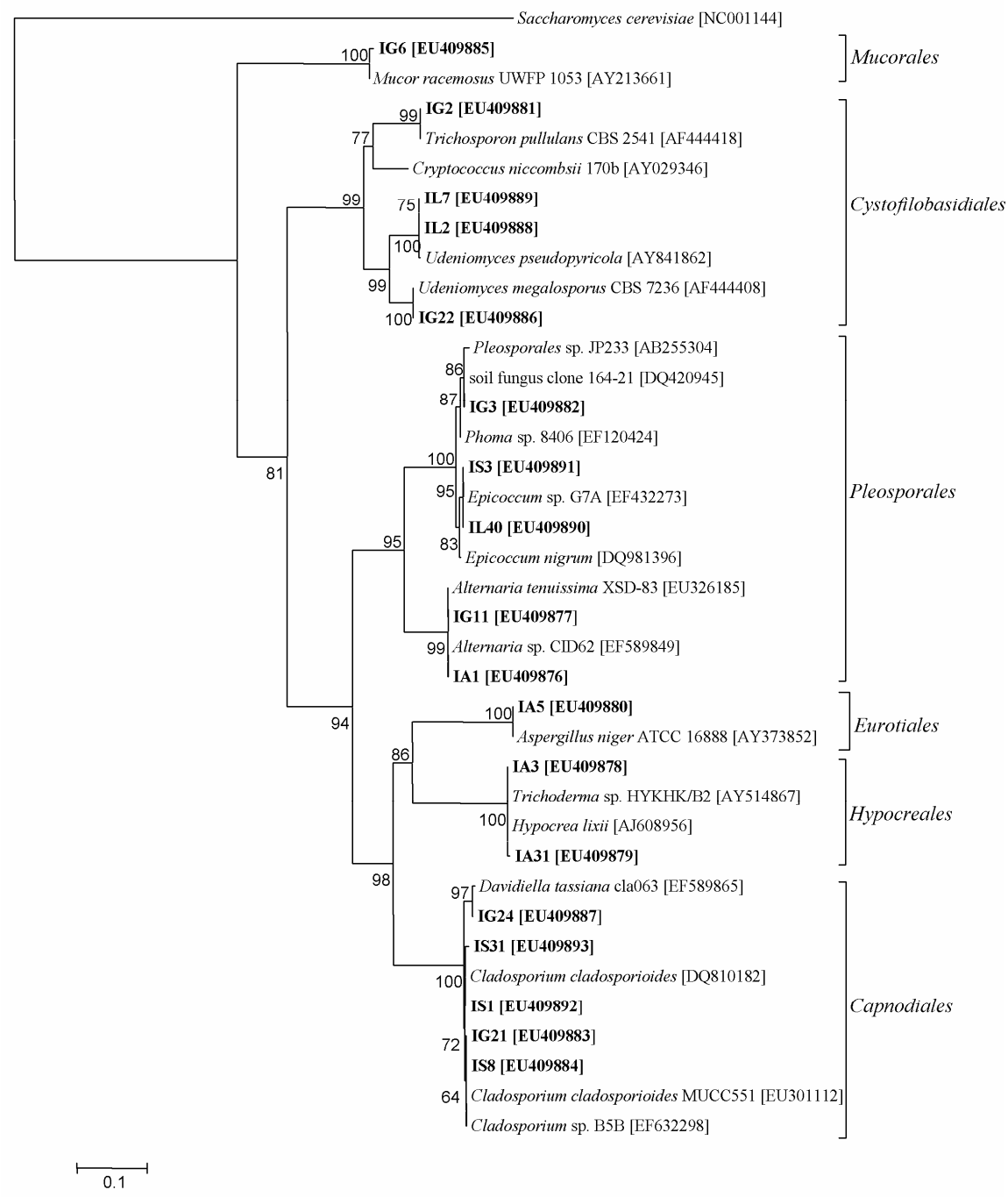

Figure 4.8. Phylogenetic analysis of ITS region of fungal rRNA gene clone sequences, as determined by distance Jukes-Cantor analysis, from concrete surfaces in Georgia, USA (in boldface), to selected cultured isolates and uncultured clones. Sequences derived from the ITS region of rRNA gene templates are denoted by I, and study site is denoted by A, Atlanta; G, Gainesville; L, LaGrange; S, Savannah. Genbank accession numbers are in brackets. Bootstrap values represent 1000 replicates and only values greater than 50% are reported. The scale bar represents 0.1 substitutions per nucleotide position.

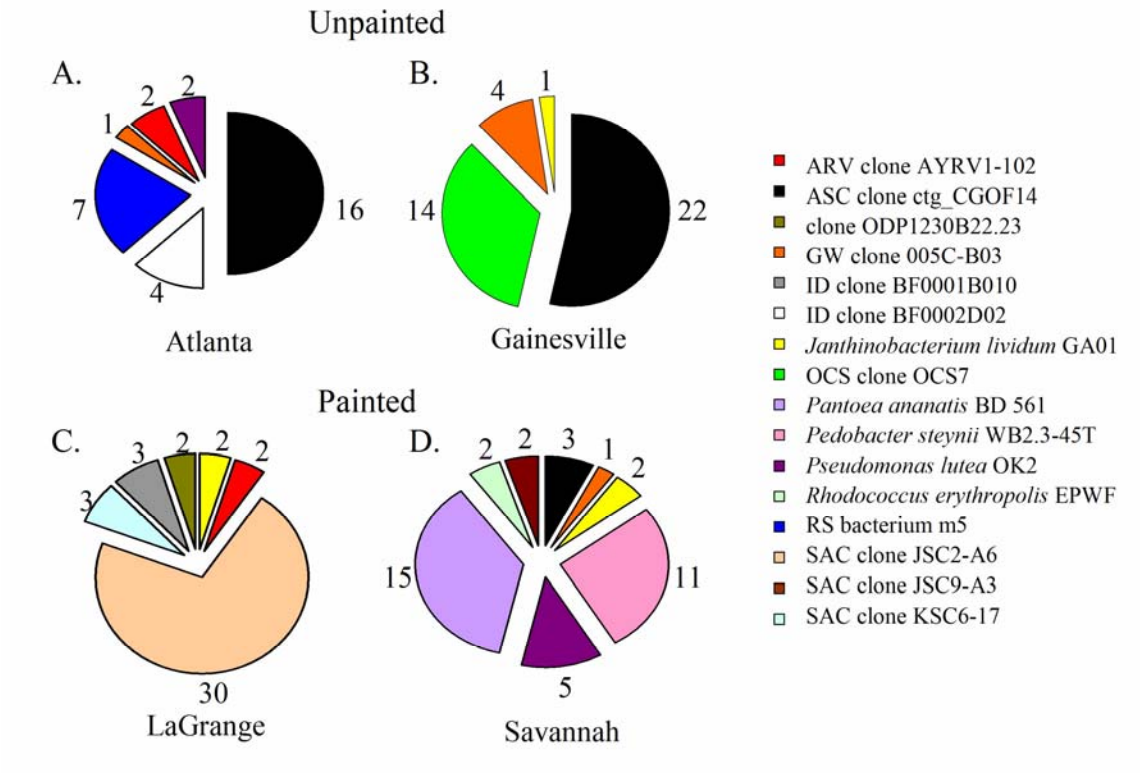

Figure 4.9. Phylotypes detected in ITS rRNA gene clone libraries derived from (A) Atlanta (B) Gainesville (C) LaGrange and (D) Savannah sites. Numbers of clones associated with each phylotype from which a representative clone had been sequenced are shown.

Phylogenetic analysis of the 165 18S rRNA gene clones from RFLP groups containing three or more members revealed low fungal community diversity at all of the biofouled sites (Table 4.2, Figure 4.10). Specifically, the Atlanta site was overwhelmingly dominated by the phylotype *Trichoderma viride* [AF525230] (99% similar) (Table 4.2, Figure 4.10), while the majority of Gainesville, LaGrange, and Savannah clones were most closely related to either the phylotype *Phoma* sp. sh1 [AB252869] (98% similar), *Cladosporium cladosporoides* AFTOL 1289 [DQ678004] (99% similar), or an uncultured ascomycete r20-12 [AJ515162] (99% similar) (Table 4.2, Figure 4.10). Also, the phylotype *Fusarium oxysporum* [AB110910] (99% similar) was

identified at the Atlanta, Gainesville, and Savannah sites (Table 4.2, Figure 4.10). However, further analysis of these clones revealed that multiple genera were represented within the same RFLP groups (Table 4.2). This redundancy was found to be due to the high sequence conservation within the 18S rRNA gene and nearly identical locations of restriction sites for clones that classified into different fungal genera. Ultimately, this skewed rarefaction and phylogenetic analysis of 18S rRNA gene clones. Thus, analysis of the ITS region of rRNA genes was used to determine the composition of fungal communities at the samples sites.

Table 4.2. Summary of representative sequences from 18S rRNA gene clone libraries.

	Representative sequence	No. related clones	Site acquired	Nearest relative	Phylogenetic group	Similarity (%)
18S	18A1	35	A	*Trichoderma viride* [AF525230]	*Ascomycota*	99
	18A5	4	A	*Fusarium oxysporum* [AB110910]	*Ascomycota*	96
	18G1	70	G, L, S	*Cladosporium cladosporioides* AFTOL 1289 [DQ678004]	*Ascomycota*	99
	18G7	10	A, G, S	*Alternaria raphani* AR6 [U05199]	*Ascomycota*	99
	18L3	70	G, L, S	*Phoma* sp. sh1 [AB252869]	*Ascomycota*	98
	18L4	46	G, L, S	soil fungus clone r20-12 [AJ515162]	*Ascomycota*	99
	18S1	46	G, L, S	*Phoma* sp. sh1 [AB252869]	*Ascomycota*	98

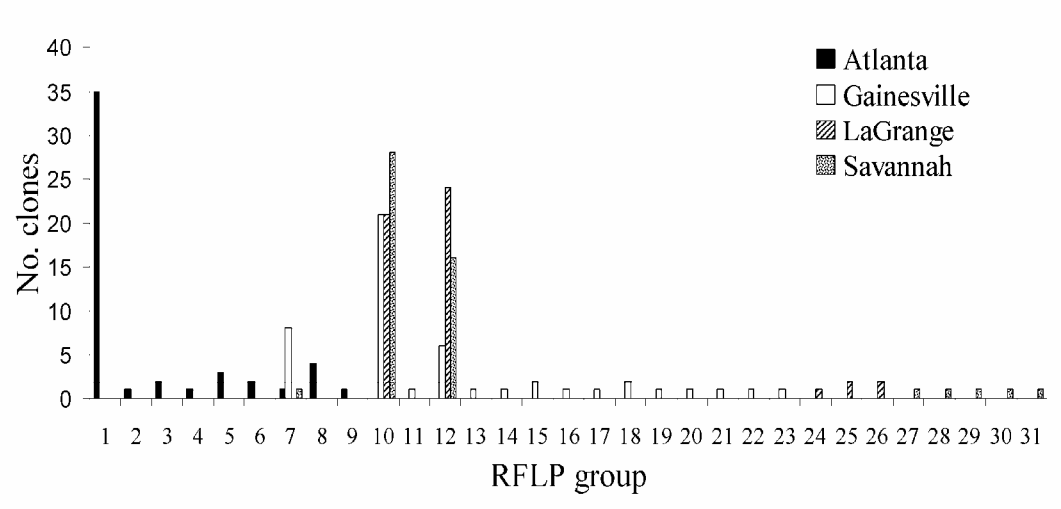

Figure 4.10. Frequency of fungal 18S RFLP groups obtained from each study site.

Photo-pigment Detection

The detection of chlorophyll and carotenoids would indicate the presence of active oxygenic photoautrophs on the fouled concrete surfaces. However, repeated attempts to detect chlorophyll a, b, c, and carotenoids did not reveal significant concentrations of these biomakers at any of the study sites (Table 4.3). After the absorbance readings of clean non-fouled concrete were taken into account, photo-pigment measurements for fouled concrete sites were below concentrations of accurate detection levels (i.e. < 0.193 μg/ml) as determined by photometric calibration using known concentrations of chlorophyll a standard.

Table 4.3. Photo-pigment detection at fouled sample sites (bd = below detection)

Site	Chlorophyll a (μg/ml)	Chlorophyll b (μg/ml)	Chlorophyll c (μg/ml)	Carotenoids (μg/ml)
Atlanta	0.058	0.087	0.186	bd
Gainesville	0.042	0.086	0.140	bd
LaGrange	0.079	0.008	bd	bd
Savannah	0.072	0.041	0.171	bd

Culturable Isolates Obtained

To complement our culture-independent characterizations of concrete-fouling microbial communities, a culture-based approach to obtain isolates for use in laboratory-controlled biofouling assays was conducted. The organisms detected by culture-dependent means are listed in Table 4.4; note that no bacterial isolates were obtained with the media used (plate count agar and potato dextrose agar). Many of the fungal isolates cultured corresponded to genera identified by molecular analysis, including *Alternaria*, *Cladosporium*, *Epicoccum*, *Fusarium*, *Mucor*, and *Trichoderma* (*Hypocrea*) sp. (note that *Hypocrea* and *Trichoderma* are the teleomorphic (sexual) and anamorphic (asexual) forms, respectively, of the same organism). However, two cultured isolates (*Penicillium oxalicum* and *Pestalotopsis maculans*) did not correspond to genera identified by molecular analysis; also, the site origins of the cultured isolates often did not match what was observed via the culture-independent approach (Table 4.1). This is likely because sampling for culturable isolates was performed at a later date than sampling for molecular analysis.

Table 4.4. List of isolates cultured from sample sites.

Isolate	Site acquired
Alternaria sp.	Atlanta
Cladosporium cladosporioides	Atlanta, LaGrange
Epicocum nigrum	Gainesville
Fusarium sp.	Savannah
Mucor sp.	LaGrange, Savannah
Penicillium oxalicum	Gainesville, Savannah
Pestalotiopsis maculans	Atlanta
Trichoderma asperellum	Atlanta, Gainesville, LaGrange

Concrete Biofouling by Individual Cultured Isolates

All culturable isolates separately inoculated onto standard mortar mix C tiles were able to successfully colonize tile surfaces while sprayed with 20% (v/v) potato dextrose broth liquid media. The biofouling by several isolates resembled the dark discoloration observed in the field. Specifically, the *Epicoccum nigrum* isolate formed a black crust that was strikingly similar to the crusts seen at the sample sites (Figure 4.11 A). Others, such as the *Cladosporium cladosporioides*, *Fusarium* sp., *Mucor* sp., *Penicillium oxalicum*, and *Trichoderma asperellum* isolates, exhibited robust fouling that ranged in color from green to dark grey, which was also somewhat similar to fouling observed in the field (Figure 4.11 B-F). The *Pestalotiopsis maculans* isolate exhibited light beige fouling that nearly covered the entire tile surface (Figure 4.11 G), while growth of the *Alternaria* sp. isolate was less abundant and darker in hue by comparison (Figure 4.11 H). The mortar tile incubated as a negative control exhibited no fouling (Figure 4.11 I).

ESEM images of tiles revealed abundant hyphae or spores present on the fouled surfaces (Figure 4.12 A-H). These fungal structures were similar to what was observed in ESEM images of fouled sample sites (Figure 4.1 F-I). No putative fungal structures

were present on the surfaces of non-fouled concrete tile control (Figure 4.12 I) or the sample site exhibiting no biofouling (Figure 4.1 J).

Figure 4.11. Biofouling of standard mortar tiles by individual cultured isolates; (A) *Epicoccum nigrum*; (B) *Cladosporium cladosporioides*; (C) *Fusarium* sp.; (D) *Mucor* sp.; (E) *Penicillium oxalicum*; (F) *Trichoderma asperellum*; (G) *Pestalotiopsis maculans*; (H) *Alternaria* sp.; (I) control incubation.

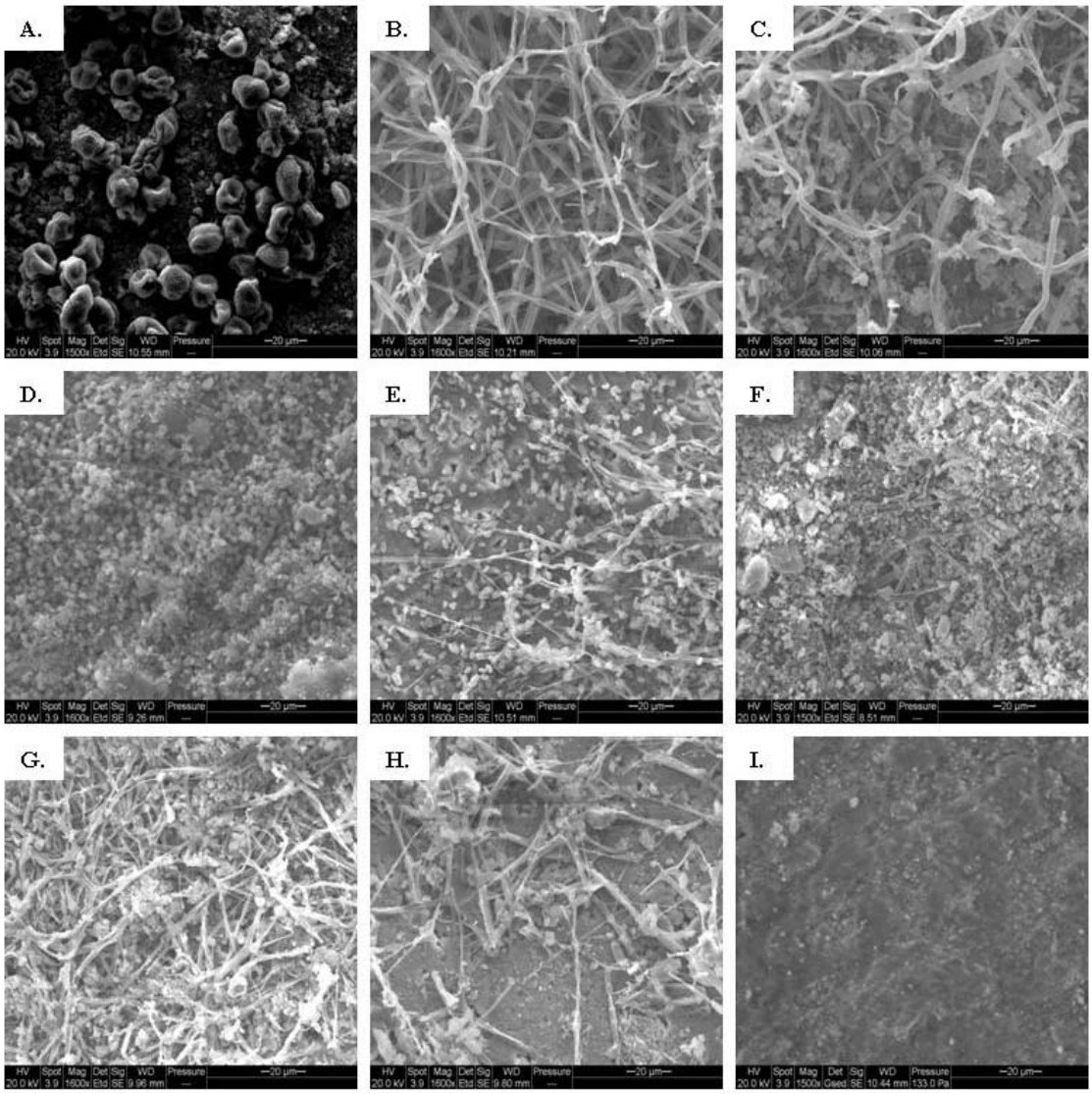

Figure 4.12. ESEM images of standard mortar tiles biofouled by individual cultured isolates; (A) *Epicoccum nigrum*; (B) *Cladosporium cladosporioides*; (C) *Fusarium* sp.; (D) *Mucor* sp.; (E) *Penicillium oxalicum*; (F) *Trichoderma asperellum*; (G) *Pestalotiopsis maculans*; (H) *Alternaria* sp.; (I) control incubation.

Effects of Concrete Composition on Biofouling

The susceptibility of different mortar tile compositions to biofouling was tested using inoculations comprised of cultured isolates pooled by sample site and incubated with 20% (v/v) potato dextrose broth. A variety of fouling occurred on the tiles, with

variations observed both between inoculation types and mortar compositions (Figures 4.13-4.17). Tiles inoculated with the pooled Atlanta-derived isolates (Figure 4.13) exhibited predominately dark growth, which ranged from areas consisting of dark green, brown, and black tints that either occurred in splotches or almost completely covered the tile. Tiles cast from mortar mixes B, E, and G exhibited cracked surfaces (Figure 4.13 B, E, & G, respectively). Tiles inoculated with Gainesville-derived isolates (Figure 4.14) also showed dark biofouling, but had a greater amount of beige and green-colored growth. The presence of grainier, black growth (Figure 4.14 A-G, J, L, M, R) as well as red fouling (Figure 4.14 B, D, F, P-R) was also observed. Mortar mixes B and E (Figure 4.14 B & E, respectively) again exhibited cracked surfaces. Tiles fouled by LaGrange-derived isolates (Figure 4.15) exhibited predominately beige/yellow and green colored-growth, though a number of tiles did still show areas covered by black biofilms (Figure 4.15 G, H, L, M, Q, R). No tiles tested with LaGrange culturables exhibited cracked surfaces. Tiles inoculated with Savannah-derived isolates (Figure 4.16) exhibited a wide variety of fouling, including beige/yellow, green, red, and black-colored growth. In addition, grey-colored fouling was present on several tiles (Figure 4.16 A-D, G, R, S). As observed with the LaGrange incubation, no tiles tested with Savannah-derived isolates had cracked surfaces. Tiles of different compositions inoculated with the *Trichoderma viride* type strain exhibited two types of morphologies: a green-colored growth that was predominately found on tiles with no SCM additions (Figure 4.17 A-G, R, T), and a tan-colored growth that was predominately found on tiles containing SCMs (Figure 4.17 H-Q). Both types of growth were cultured back to potato dextrose agar to verify the purity of the *Trichoderma viride* incubation. Uninoculated control tiles are depicted in Figure

4.18. ESEM images of select tiles of site-pooled and *Trichoderma viride* incubations revealed a variety of fungal structures on the surfaces (Figure 4.19).

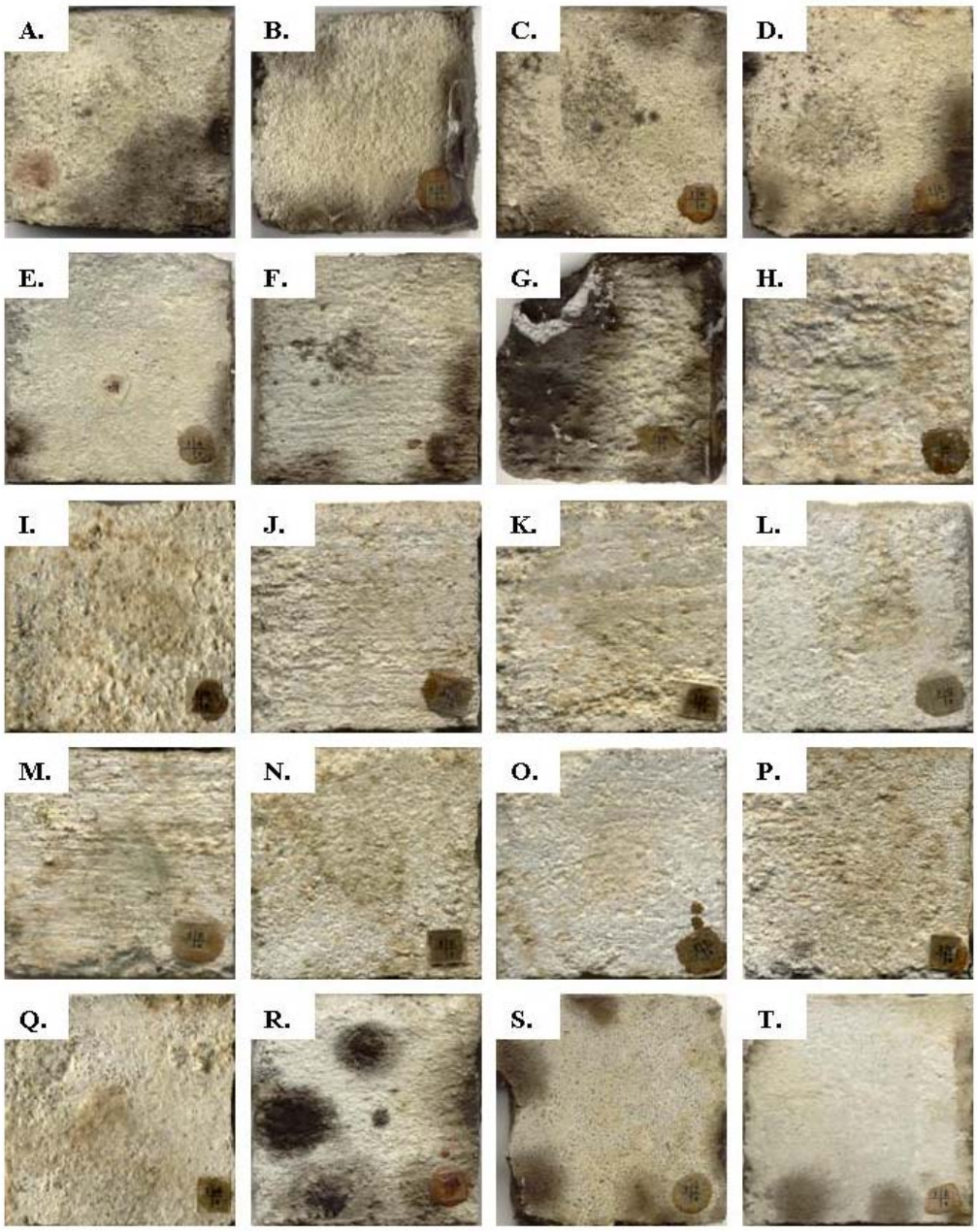

Figure 4.13. Fouling of different mortar mixes by Atlanta-pooled isolates: (A) mix A; (B) mix B; (C) mix C; (D) mix D; (E) mix E; (F) mix F; (G) mix G; (H) mix H; (I) mix I; (J) mix J; (K) mix K; (L) mix L; (M) mix M; (N) mix N; (O) mix O; (P) mix P; (Q) mix Q; (R) mix R; (S) mix S; (T) mix T.

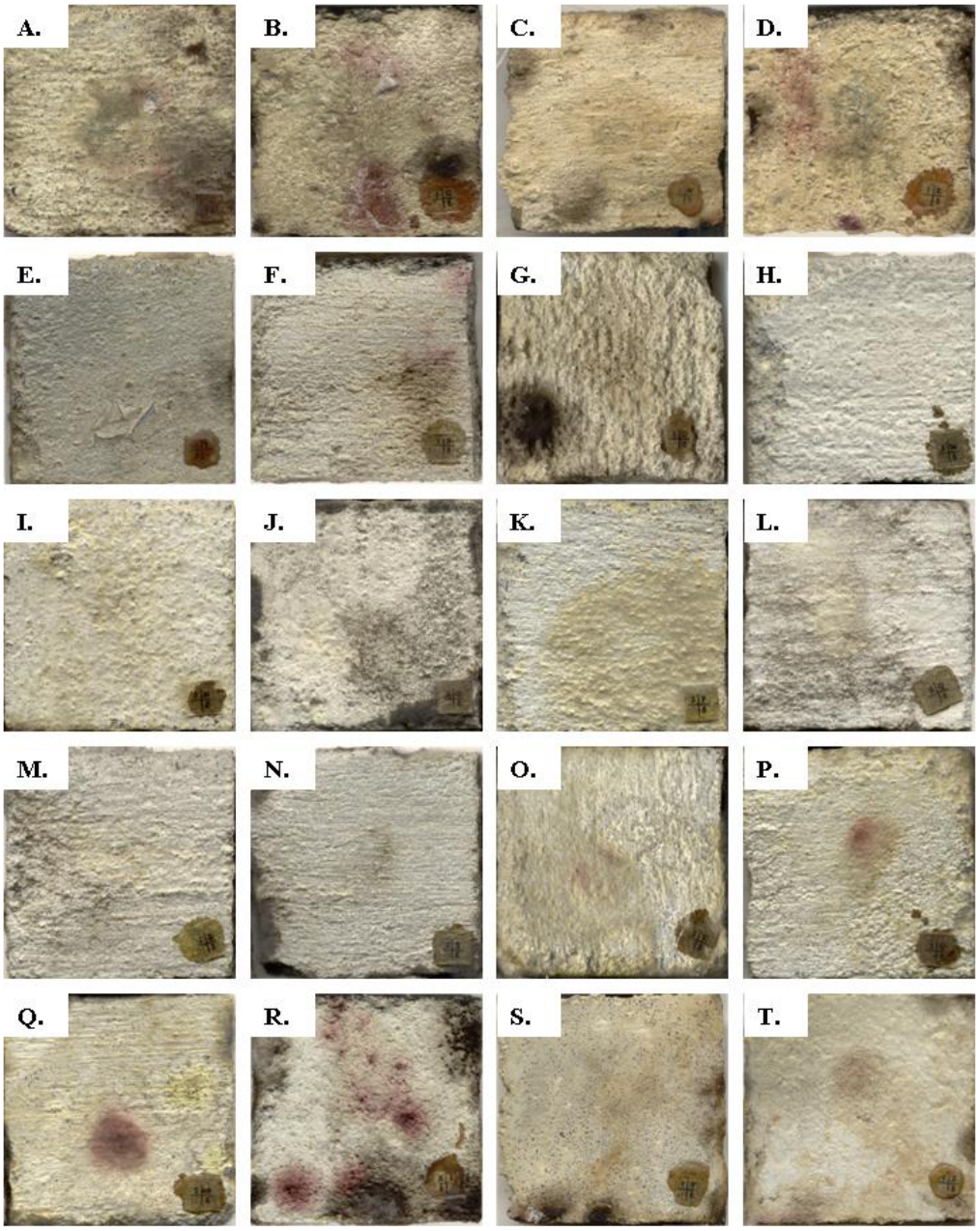

Figure 4.14. Fouling of different mortar mixes by Gainesville-pooled isolates: (A) mix A; (B) mix B; (C) mix C; (D) mix D; (E) mix E; (F) mix F; (G) mix G; (H) mix H; (I) mix I; (J) mix J; (K) mix K; (L) mix L; (M) mix M; (N) mix N; (O) mix O; (P) mix P; (Q) mix Q; (R) mix R; (S) mix S; (T) mix T.

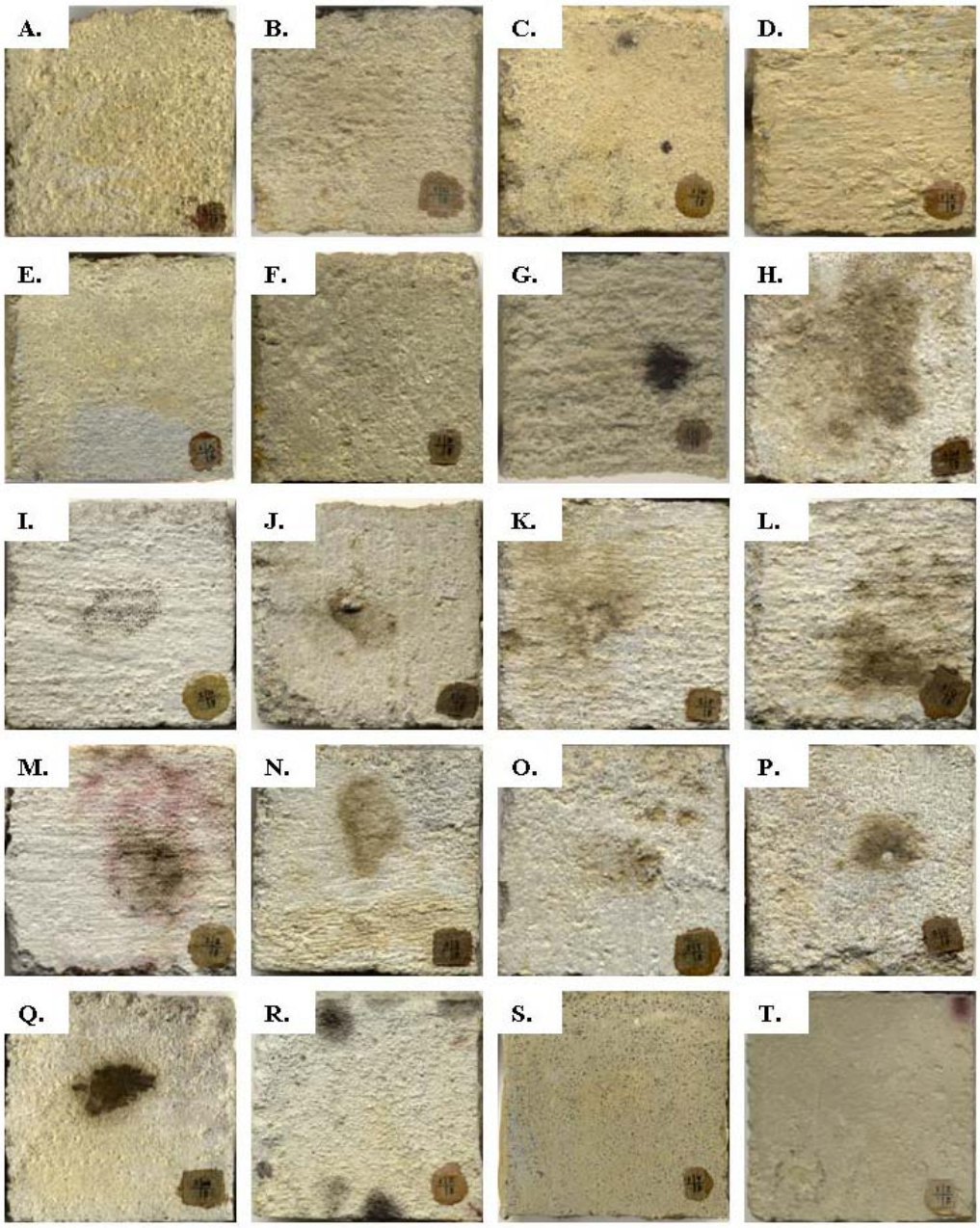

Figure 4.15. Fouling of different mortar mixes by LaGrange-pooled isolates: (A) mix A; (B) mix B; (C) mix C; (D) mix D; (E) mix E; (F) mix F; (G) mix G; (H) mix H; (I) mix I; (J) mix J; (K) mix K; (L) mix L; (M) mix M; (N) mix N; (O) mix O; (P) mix P; (Q) mix Q; (R) mix R; (S) mix S; (T) mix T.

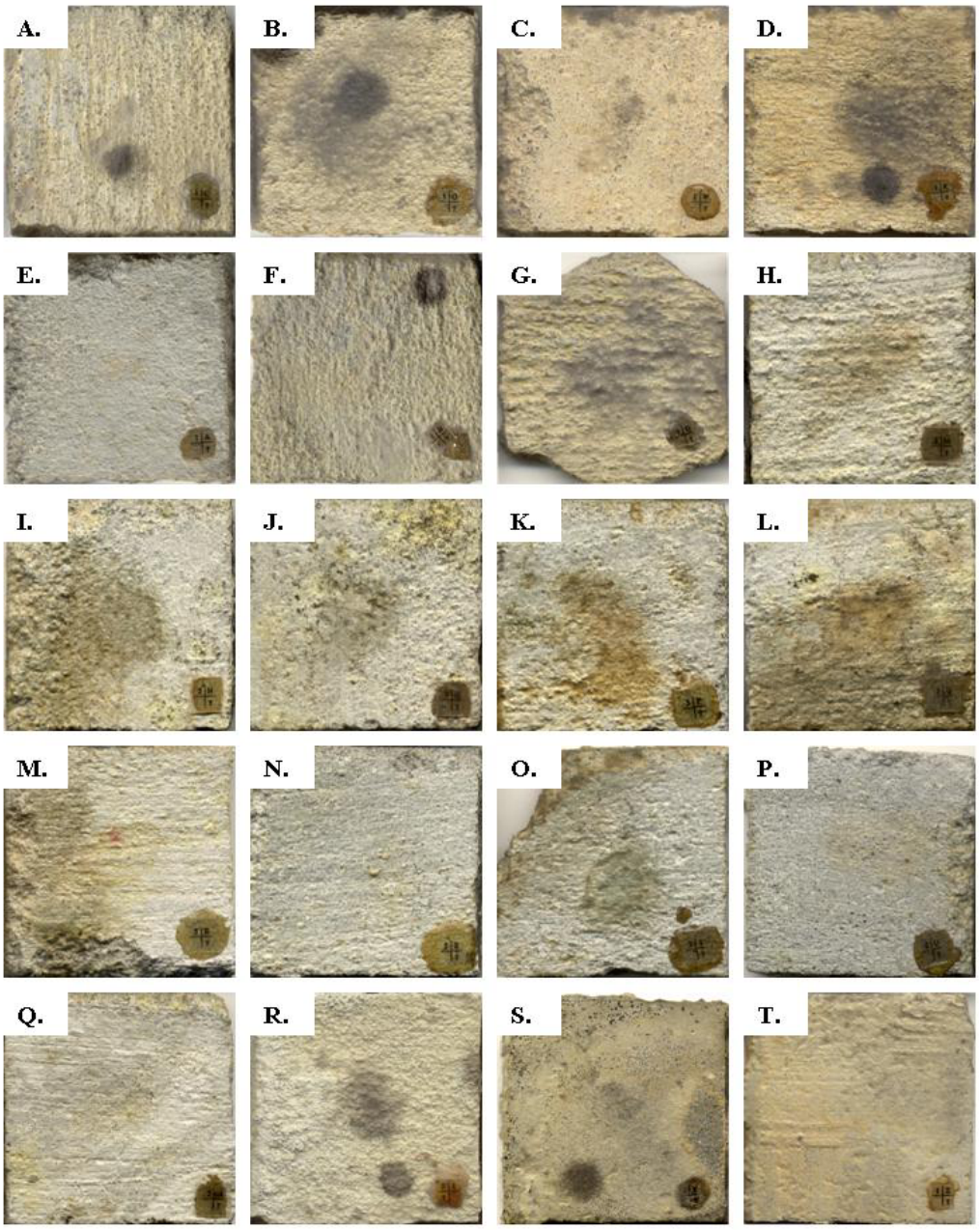

Figure 4.16. Fouling of different mortar mixes by Savannah-pooled isolates: (A) mix A; (B) mix B; (C) mix C; (D) mix D; (E) mix E; (F) mix F; (G) mix G; (H) mix H; (I) mix I; (J) mix J; (K) mix K; (L) mix L; (M) mix M; (N) mix N; (O) mix O; (P) mix P; (Q) mix Q; (R) mix R; (S) mix S; (T) mix T.

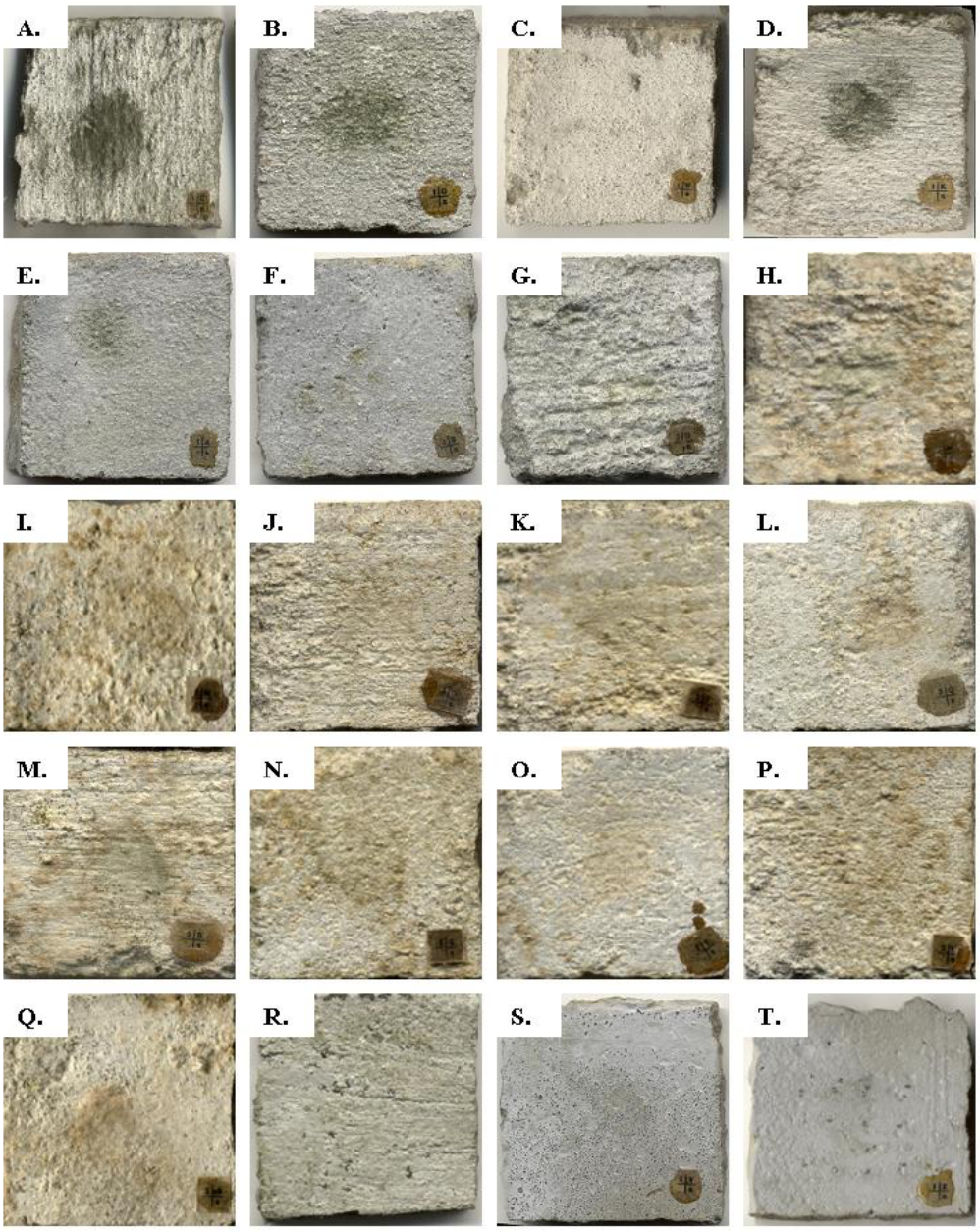

Figure 4.17. Fouling of different mortar mixes by *Trichoderma viride*: (A) mix A; (B) mix B; (C) mix C; (D) mix D; (E) mix E; (F) mix F; (G) mix G; (H) mix H; (I) mix I; (J) mix J; (K) mix K; (L) mix L; (M) mix M; (N) mix N; (O) mix O; (P) mix P; (Q) mix Q; (R) mix R; (S) mix S; (T) mix T.

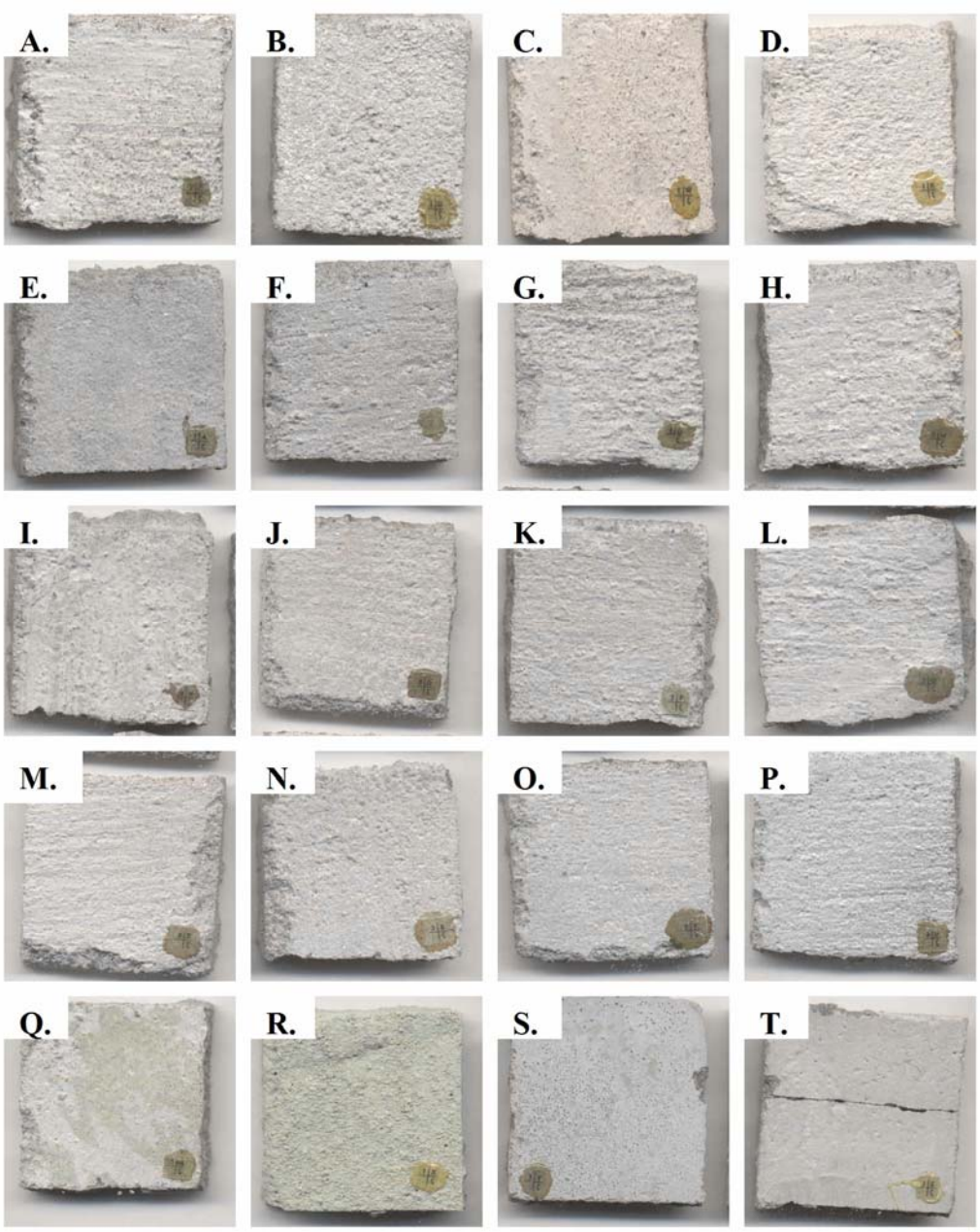

Figure 4.18. Uninoculated control tiles incubated in 20% potato dextrose broth: (A) mix A; (B) mix B; (C) mix C; (D) mix D; (E) mix E; (F) mix F; (G) mix G; (H) mix H; (I) mix I; (J) mix J; (K) mix K; (L) mix L; (M) mix M; (N) mix N; (O) mix O; (P) mix P; (Q) mix Q; (R) mix R; (S) mix S; (T) mix T.

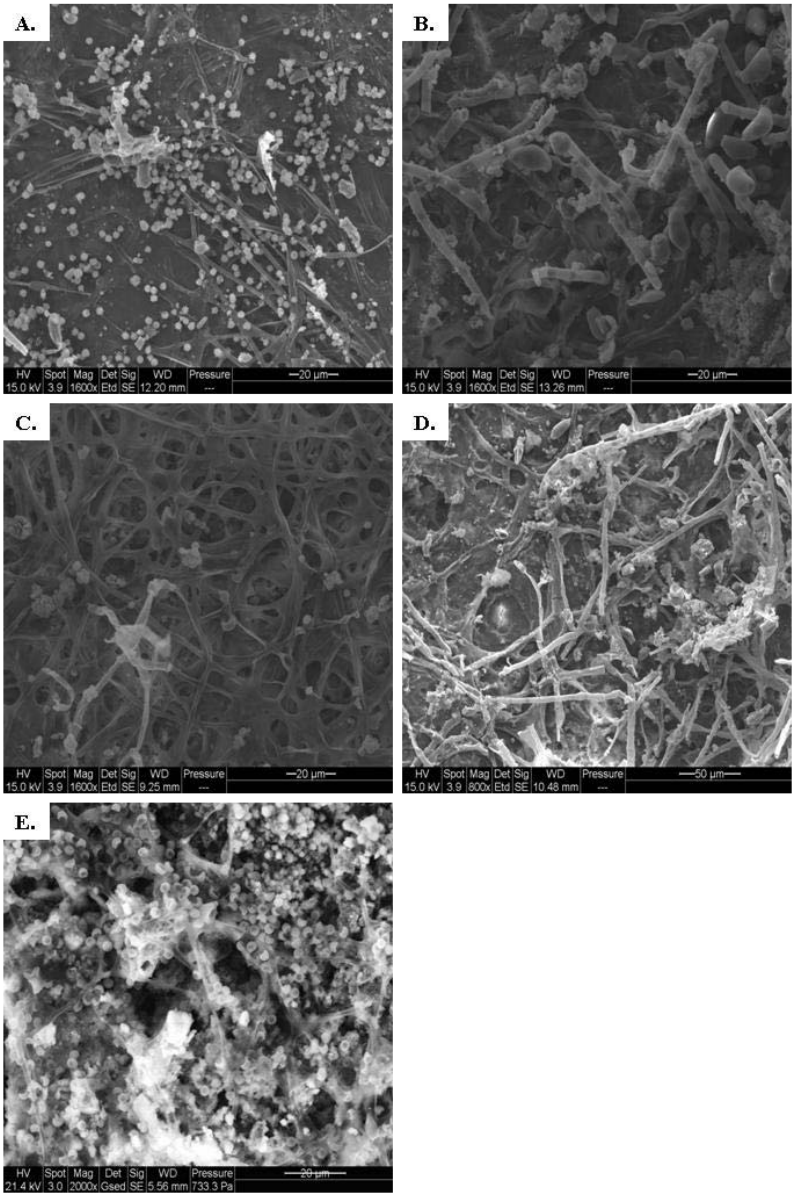

Figure 4.19. ESEM images of select tiles fouled by site-pooled isolates and *Trichoderma viride*: (A) black fouling present on tile mix D incubated with Atlanta-pooled isolates; (B) black-grey fouling observed on tile mix R incubated with Gainesville-pooled isolates; (C) tan fouling present on tile mix J incubated with LaGrange-pooled isolates; (D) grey fouling observed on tile mix B incubated with Savannah-pooled isolates; (E) Dark green fouling produced by *Trichoderma viride* on a mix A tile.

The amount of fouling observed was compared with the various cement types used to cast the mortar tiles. Fouling on each cement type by site-pooled and

Trichoderma viride incubations was compared to fouling on the standard Holcim GU Type I/II cement. Analysis revealed no significant differences when comparing standard cement to Holcim GU cement with 5% limestone ($p = 0.15$), Essroc Type I/II ($p = 0.86$), or Essroc Tx Aria ($p = 0.38$) (Table 4.5). The addition of SCMs at different replacement percentages by weight was also tested for susceptibility to biofouling. Similar to primary cement variations, the addition of fly ash ($R^2 = 0.02$), slag (R2 = 0.04), silica fume (R2 = 0.59), or metakaolin ($p = 0.45$) – at the rates examined – did not significantly affect biofouling, positively or negatively, in any of the site-pooled or *Trichoderma viride* incubations (Figure 4.20 A-C, Table 4.6). Further examination of SCM use, with a broader range of compositions and addition rates, is necessary to better understand their potential influence on biofouling.

Table 4.5. Comparison of biofouling on different primary cement types.

Cement	Coverage of biofouling (%)	Difference from Holcim GU I/II (p-value)
Holcim GU I/II	37	1.00
Holcim GU + 5% limestone	45	0.15
Essroc I/II	38	0.86
Essroc Tx Aria	41	0.38

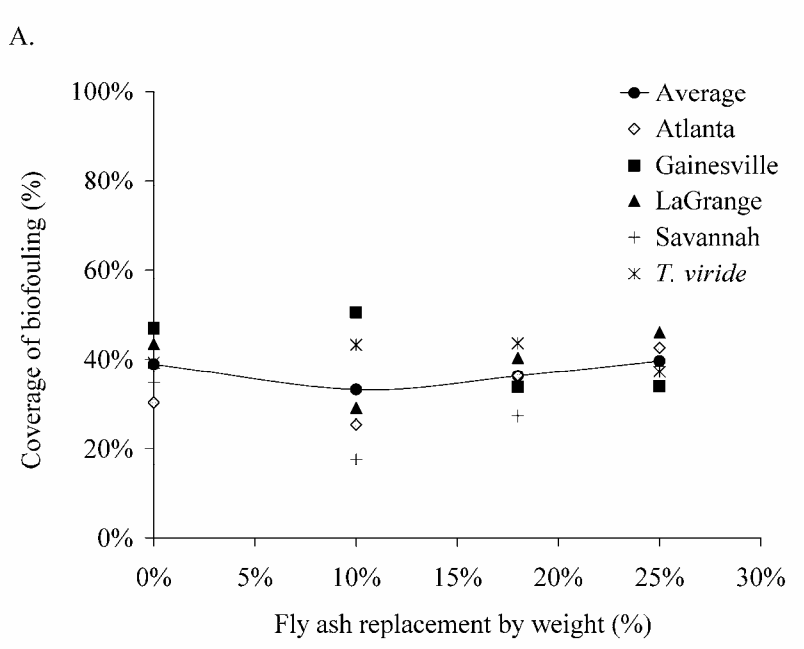

Figure 4.20.A. The effect of fly ash replacement on coverage of biofouling for site-pooled and *Trichoderma viride* incubations. No trend (R^2= 0.02) was observed through these measurements.

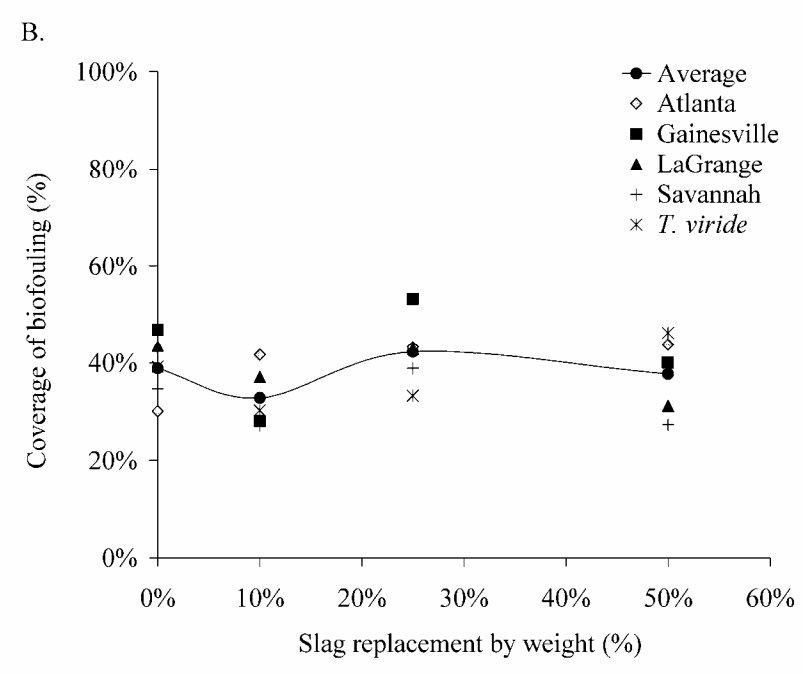

Figure 4.20.B. The effect of slag replacement on coverage of biofouling for site-pooled and *Trichoderma viride* incubations. No trend (R^2= 0.04) was observed through these measurements.

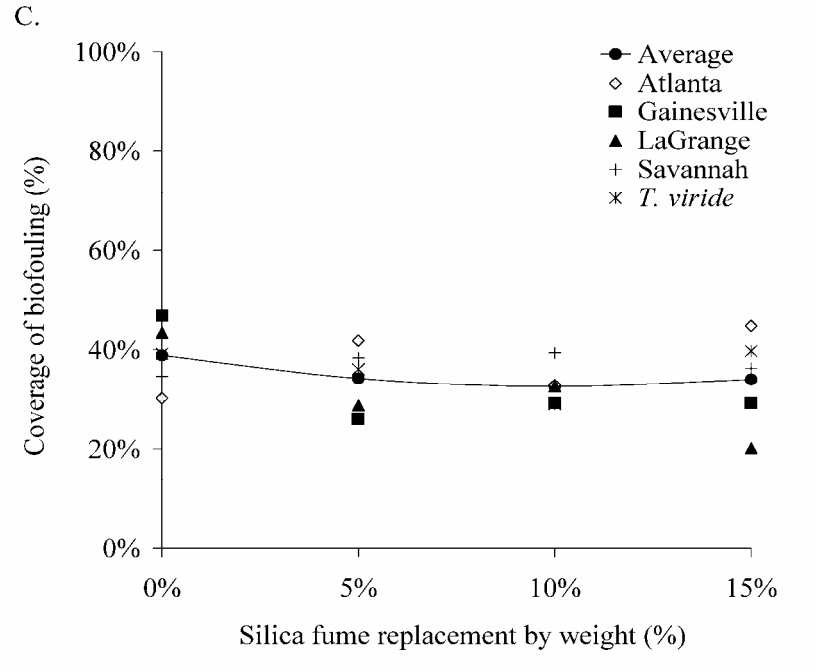

Figure 4.20.C. The effect of silica fume replacement on coverage of biofouling for site-pooled and *Trichoderma viride* incubations. No trend (R^2= 0.59) was observed through these measurements.

Table 4.6. Effects of metakaolin addition to biofouling of tiles.

Incubation	Coverage of biofouling with no metakaolin (%)	Coverage of biofouling with 8% metakaolin (%)	Significance of metakaolin addition (p-value)
Atlanta	30	41	
Gainesville	47	29	
LaGrange	43	29	
Savannah	35	32	
T.viride	39	41	
Average	39	34	0.45

The amount of fouling observed was also compared to the different water/cement ratios (0.3, 0.4, 0.5, and 0.6) used to cast tiles. A strong positive trend (R^2 = 0.98) was seen between water/cement ratio and the amount of biofouling when all incubations were incorporated into a linear regression model (Figure 4.21). Analysis of each separate

incubation showed that this positive trend was stronger in the Atlanta ($R^2 = 0.96$), Gainesville ($R^2 = 0.97$), and *Trichoderma viride* ($R^2 = 0.95$) incubations than in the LaGrange ($R^2 = 0.65$) and Savannah ($R^2 = 0.79$) isolate incubations (Figure 4.21). While tiles with lower water/cement ratios exhibited less growth on their surfaces, no tile showed complete resistance to biofouling.

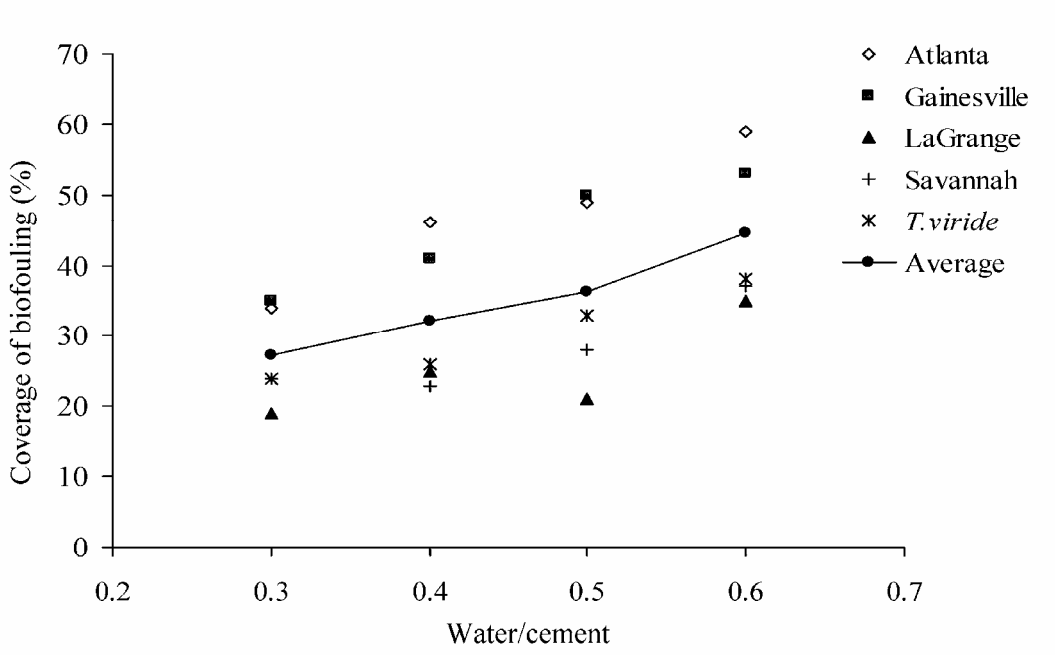

Figure 4.21. Effects of water/cement ratio on biofouling of tiles. A strong positive trend ($R^2 = 0.98$) was observed for the average of all incubations. Atlanta ($R^2 = 0.96$), Gainesville ($R^2 = 0.97$), and *T.viride* ($R^2 = 0.95$) incubations showed stronger trends than LaGrange ($R^2 = 0.65$) and Savannah ($R^2 = 0.79$) incubations.

Variations in compressive strength, as determined by crushing mortar cubes of each tile mix, were compared to the degree of biofouling. Atlanta ($R^2 < 0.01$), Gainesville ($R^2 < 0.01$), LaGrange ($R^2 = 0.31$), Savannah ($R^2 = 0.09$), and *Trichoderma viride* ($R^2 = 0.10$) incubations showed no trends that related compressive strength to biofouling (Figure 4.22 A-E). An average of all incubations also did not show any

significant trend ($R^2 = 0.22$) (Figure 4.22 F), despite the direct relationship between water/cement ratio and compressive strength.

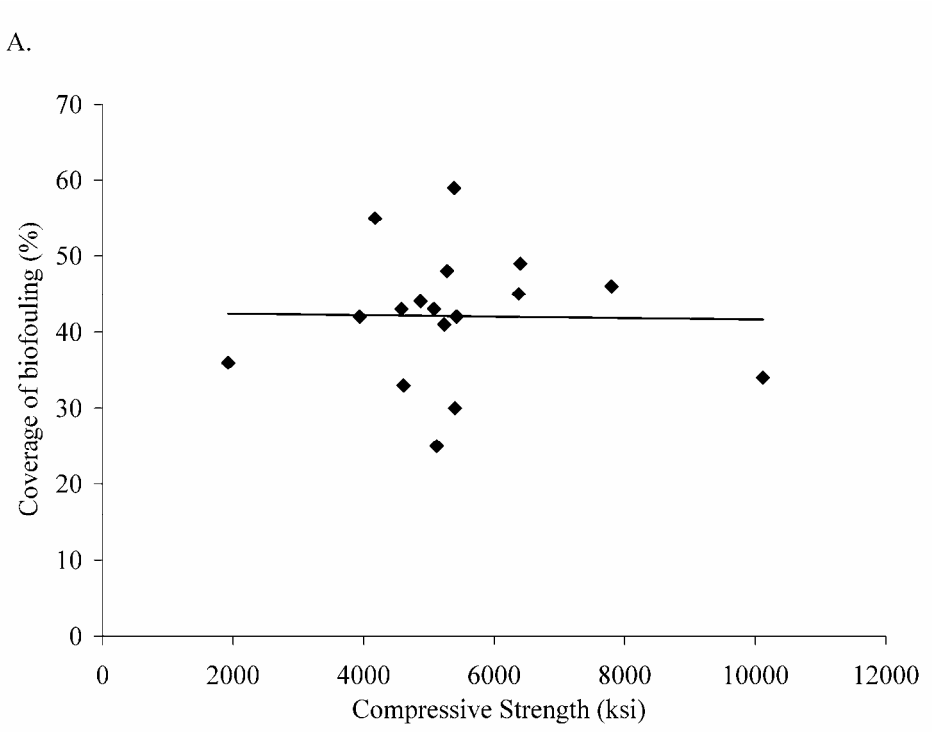

Figure 4.22.A. Effect of compressive strength on biofouling by Atlanta-pooled isolates. No apparent trend ($R^2 < 0.01$) was observed.

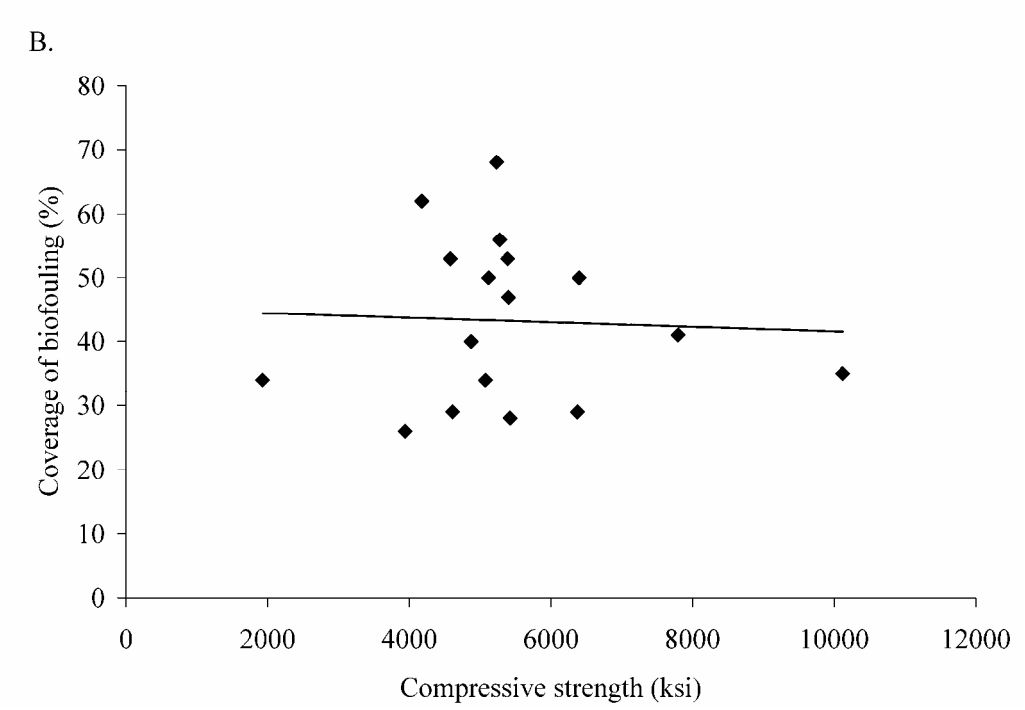

Figure 4.22.B. Effect of compressive strength on biofouling by Gainesville-pooled isolates. No apparent trend ($R^2 < 0.01$) was observed.

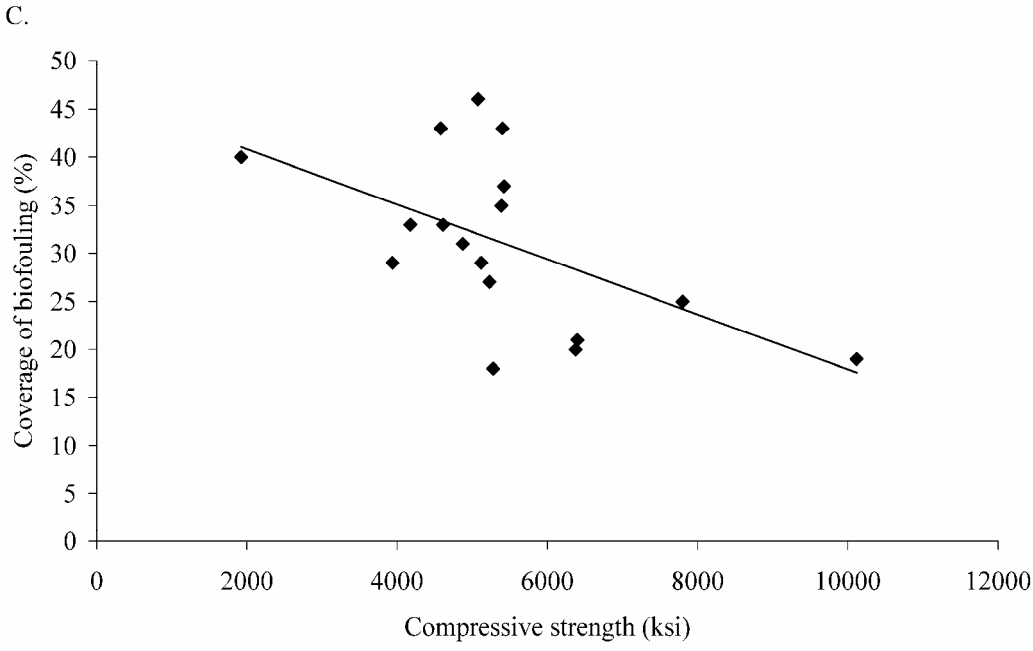

Figure 4.22.C. Effect of compressive strength on biofouling by LaGrange-pooled isolates. No apparent trend ($R^2 = 0.31$) was observed.

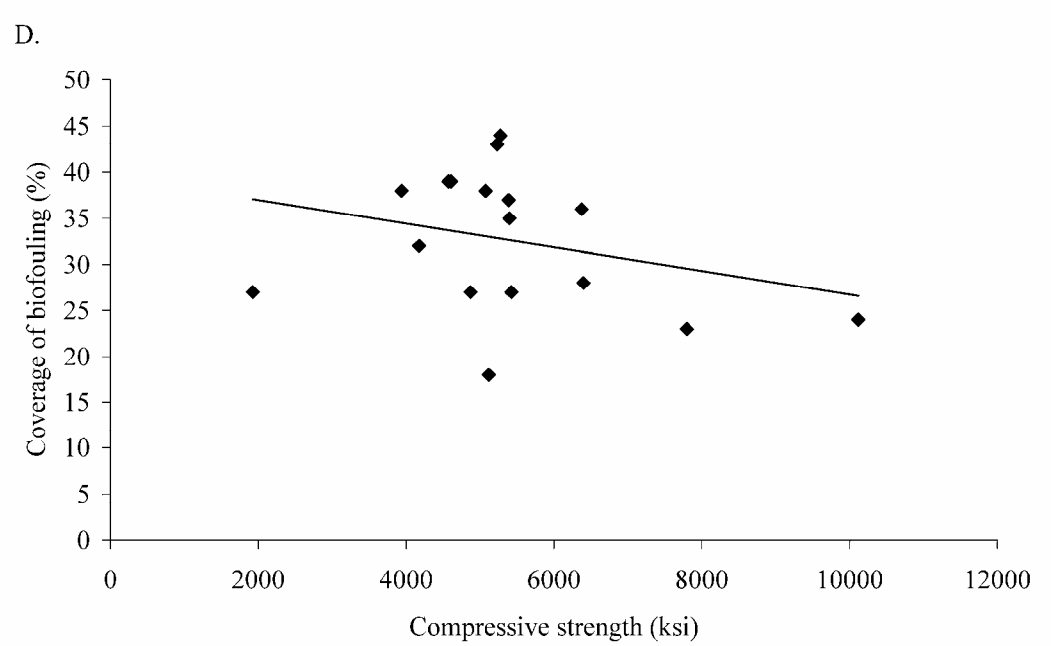

Figure 4.22.D. Effect of compressive strength on biofouling by Savannah-pooled isolates. No apparent trend ($R^2 = 0.09$) was observed.

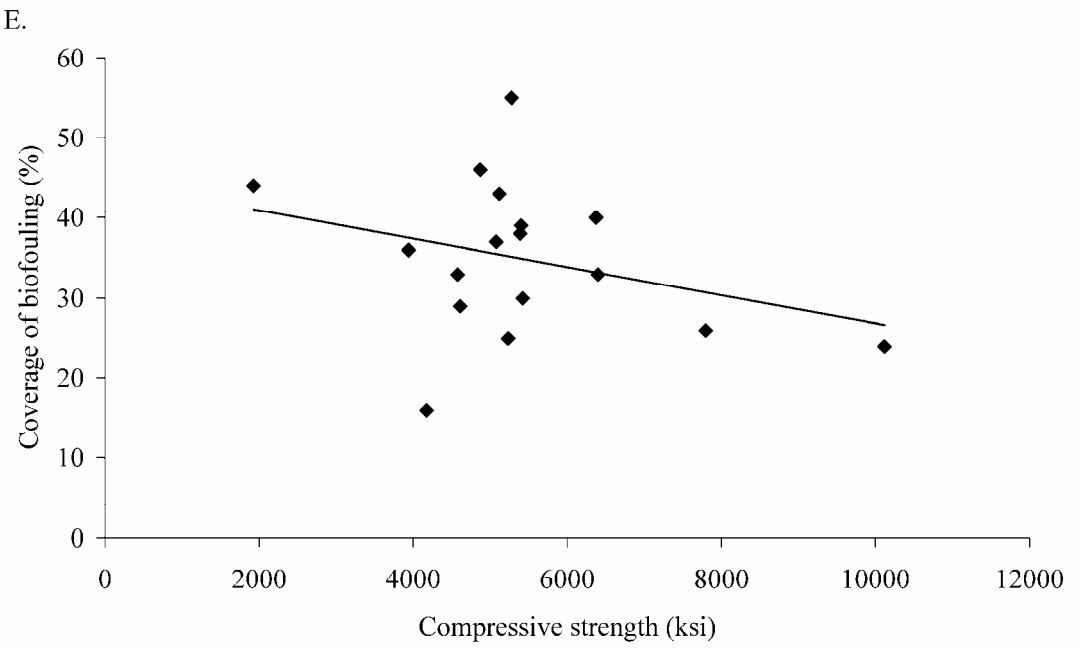

Figure 4.22.E. Effect of compressive strength on biofouling by *T.viride*. No apparent trend ($R^2 = 0.10$) was observed.

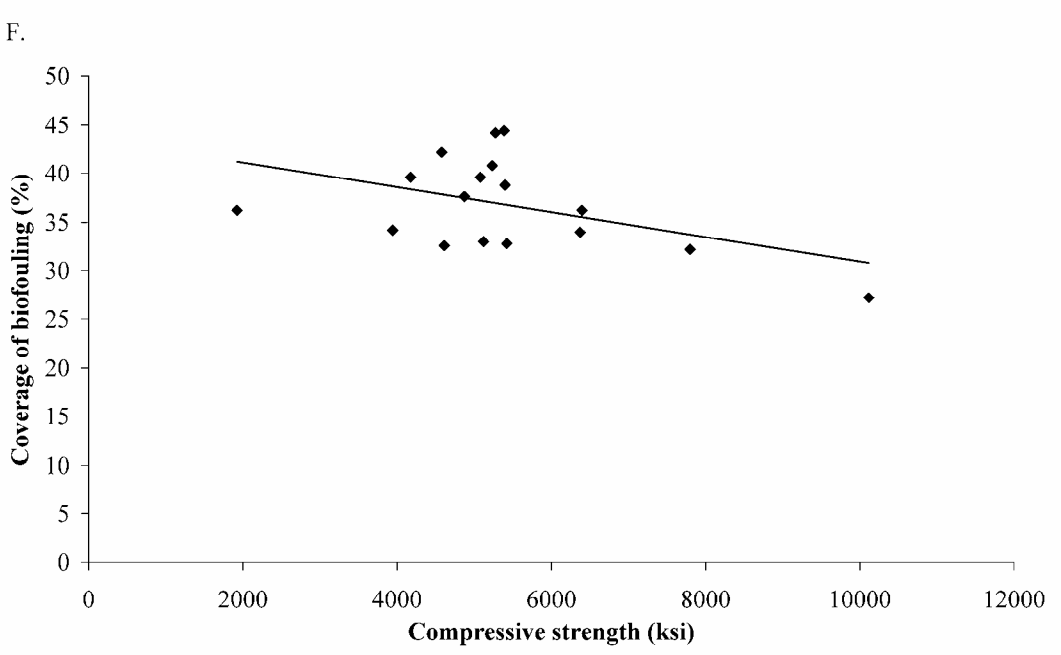

Figure 4.22.F. Effect of compressive strength on biofouling for the average of site-pooled and *T.viride* incubations. No apparent trend ($R^2 = 0.22$) was observed.

A comparison of varied surface roughness to the amount of fouling was also performed by examining various surface finishes. An average of the incubations showed a positive relationship between surface roughness and amount of biofouling ($R^2 = 1.00$). Separately analyzing site-pooled incubations revealed the Atlanta ($R^2 = 1.00$), Gainesville ($R^2 = 0.97$), and *Trichoderma viride* ($R^2 = 1.00$) runs to have a positive relationship, with smoother surfaces exhibiting a greater amount of biofouling (Figure 4.23). LaGrange and Savannah incubations, however, actually exhibited negative relationships between roughness and biofouling (Figure 4.23). In addition to surface roughness testing, another surface finish was used to examine the effect of an acrylic paint coating on biofouling. When compared to uncoated standard tiles of the same composition, the acrylic-coated tiles showed a marginally greater amount of biofouling; however, the difference was not statistically significant ($p = 0.37$).

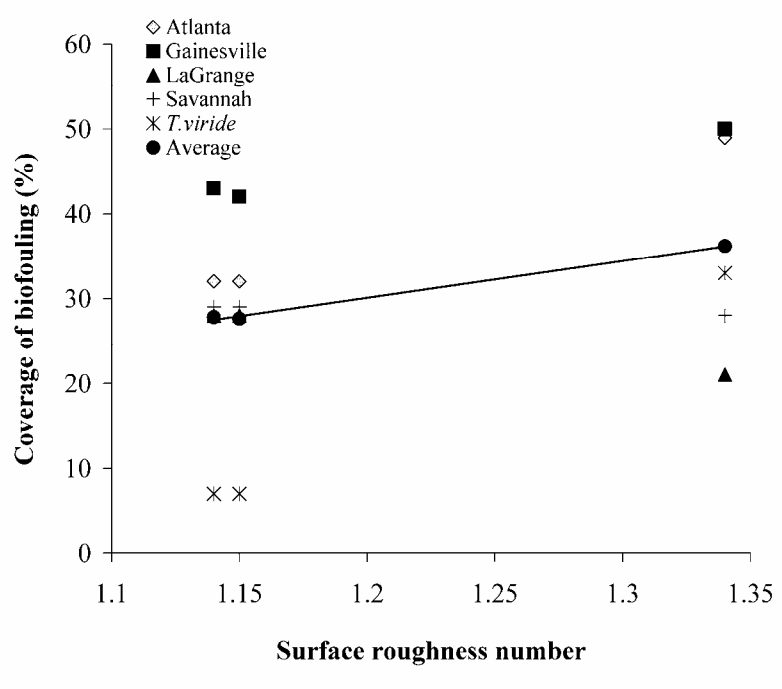

Figure 4.23. Effect of surface roughness on biofouling by site-pooled and *T.viride* incubations. An average positive trend ($R^2 = 1.00$) was observed along with positive trends for Atlanta ($R^2 = 1.00$), Gainesville ($R^2 = 0.97$), and *T.viride* ($R^2 = 1.00$) incubations. However, LaGrange ($R^2 = 1.00$) and Savannah ($R^2 = 1.00$) incubations showed slightly negative trends.

Effects of Nutrient-limited Media on Biofouling

Several biofouling incubations using a combination of all the cultured isolates were performed using nutrient-limited media designed to more closely resemble *in situ* conditions. Incubations using sterile deionized water, sterilized rainwater, and sterilized rainwater exposed to vehicular exhaust did not successfully foul any of the mortar tiles cast for this study. However, an incubation of tiles dipped in form-release oil and run with sterilized rainwater was able to produce a small amount of biofouling on a single mortar mix D tile (Figure 4.24). This fouling consisted of a dark ring on the tile surface (Figure 4.24 A), which upon closer examination was found to consist of black, spherical

structures with protruding filaments (Figure 4.24 B). ESEM imaging revealed a meshwork of hyphae along the tile's surface on the fouled area (Figure 4.24 C). While this black, crust-like fouling resembled that observed in *Epicoccum nigrum* inoculations, this could not be verified, as attempts to reculture the very small amount of fouling to solid media were unsuccessful. This suggests, however, that form-release oils may provide a potential nutrient source, aiding in colonization.

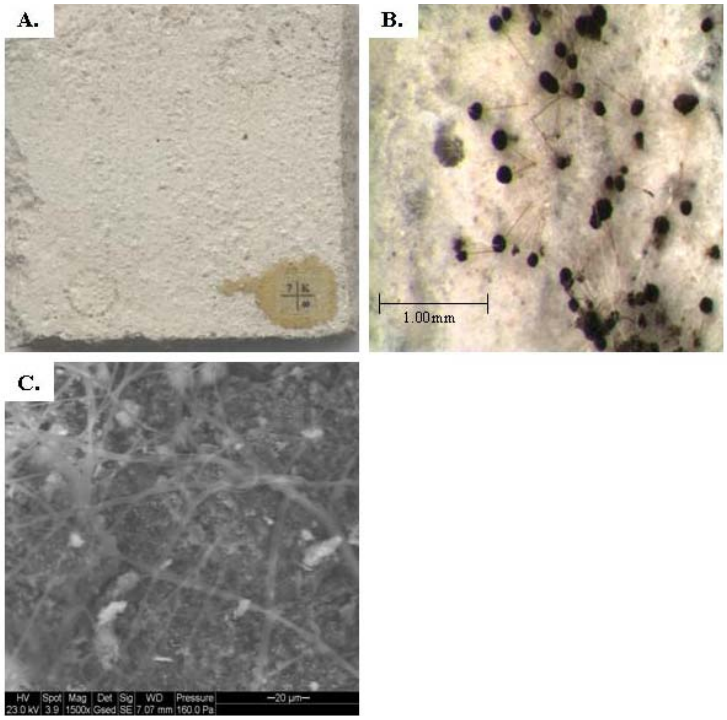

Figure 4.24. Biofouling of a tile dipped in form-release oil and incubated under sterilized rainwater: (A) image of tile exhibiting dark "rings" of fouling; (B) stereomicroscope image of the single type of fouling; (C) ESEM image of the biofouled tile.

Effects of Photocatalytically-activated Cement on Biofouling

To test the antimicrobial activity of photocatalytically-active cement, all cultured isolates were inoculated onto tiles composed of a cement containing TiO_2 and incubated

under artificial sunlight. While Essroc Type I/II non-photocatalytic cement (mortar mix C) incubated exposed to the light source exhibited a range of fouling that was black, tan, and red in color (Figure 4.25 A), Essroc Tx Aria cement containing TiO_2 (mortar mix D) exhibited only a small amount of a single type of tan-colored fouling (Figure 4.25 B-C). The reduction in biofouling was found to be statistically significant ($p = 0.05$). ESEM imaging of the fouling revealed hyphae attached to the surface of the tile (Figure 4.25 D). This tan-colored fouling was recultured onto solid media and found to be the *Trichoderma asperellum* cultured isolate, making it the only culturable observed in this study capable of fouling the Essroc Tx Aria cement under artificial sunlight.

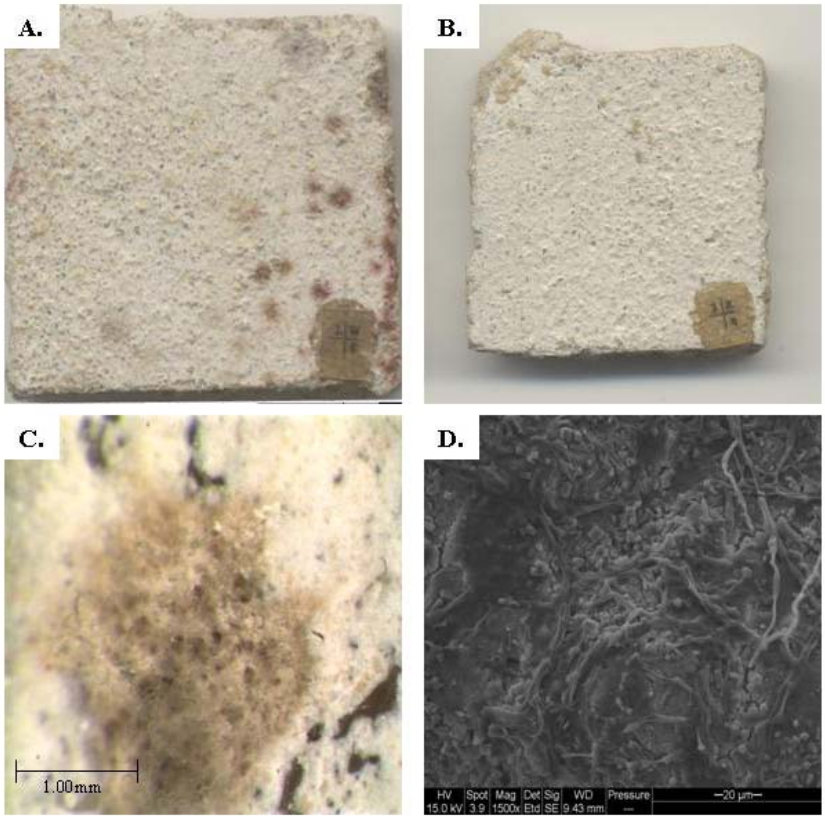

Figure 4.25. Fouling of tiles inoculated with all cultured isolates and exposed to artificial sunlight: (A) multi-colored fouling of a tile composed of Essroc Type I/II cement; (B)

fouling of tile composed of Essroc Tx Aria cement, which contains photocatalytic TiO_2; (C) stereomicroscope image of the tan-colored fouling on the TiO_2-containing tile; (D) ESEM image of the fouled tile containing TiO_2.

CHAPTER 5

DISCUSSION

The growth of microorganisms on concrete infrastructures detracts from the appearance of bridges, walls, pavements, canals and mortared joints. The discoloration of these structures by microbial biofilms may lead to public misconceptions regarding the performance and maintenance of the affected structures. Microbial activity can also significantly decrease the performance of concrete structures by the production of biogenic acids, which can result in deterioration of concrete and can accelerate corrosion of metals (Sand, 1997; Gu et al., 1998; Warscheid and Braams, 2000). The presence of microbes within the small cracks and pores of stones and rocks can cause damage via swelling due to the cellular uptake of water (Gaylarde and Morton, 1997). Similarly, fissures can be created by the penetration of fungal hyphae into concrete (Gu et al., 1998).

In this study, the compositions of microbial assemblages fouling concrete infrastructures in the state of Georgia are reported. To date, the majority of studies that have characterized microbial communities on exterior concrete and similar surfaces (e.g. indoor mortars, stone) have relied on culturing and morphological analyses (Mitchell and Gu, 2000; Dubosc et al., 2001; Shirakawa, 2003; Gaylarde and Gaylarde, 2005; Gaylarde et al., 2007). This study employed a combination of culture-independent and culture-dependent methods to identify the types of microorganisms fouling concrete in different geographical locales throughout the state. Furthermore, microorganisms isolated from this study were used to simulate biofouling of concrete surfaces under controlled

laboratory conditions. This allowed for the characterization of biofouling by individual isolates as well as the examination of the effects of concrete properties and environmental conditions on concrete surface growth.

Molecular Analysis of Sample Sites

While the phylogenetic analysis of bacterial 16S rRNA genes revealed a distinct bacterial community present at each site, the majority of the bacterial sequences present on the concrete surfaces belonged to just two phyla (i.e. *Cyanobacteria* and *Proteobacteria*), indicating low microbial diversity. This is not an unexpected finding, as one would consider concrete surfaces to be an inhospitable, extreme environment, thereby limiting the types of bacterial populations able to tolerate such conditions. Of those bacterial sequences that were most closely related (e.g., >98% similar) to previously-cultured chemoorganotrophic bacteria, we postulate that they may have originated from soils, or been associated with plants. For example, approximately 10% of the total bacterial sequences obtained were phylogenetically related to *P. ananatis*, a plant pathogen that has been recently implicated in outbreaks of center rot disease of onion, and theorized to have been transferred to Georgia via seeds produced in South Africa (Walcott et al., 2002).

The vast majority of the bacterial 16S rRNA gene sequences that were obtained, however, were only related to environmental clone sequences. Many of these sequences were isolated from extreme environments, such as deep-sea corals on Gulf of Alaska seamounts (Penn et al., 2006) and spacecraft assembly cleanrooms (Moissl et al., 2007). The most common sequences belonged to cyanobacterial, gammaproteobacterial, and betaproteobacterial lineages, which accounted for the largest fractions of each of the

communities. In addition, distinct patterns of microbial communities between sites were observed. For example, cyanobacterial sequences dominated the LaGrange site, while gammaproteobacterial sequences were only present at the Atlanta, Gainesville and Savannah sites. Oxygenic phototrophs such as *Cyanobacteria* typically serve as primary producers supporting heterotrophic (chemoorganotrophic) microbial populations (e.g., *Proteobacteria*). The absence of *Cyanobacteria* from the other study sites is intriguing and may suggest that other autotrophic metabolic capabilities could be contributing to primary productivity in these microbial communities (Warscheid and Braams, 2000; De La Torre et al., 2003), or that phototrophic colonizers have been succeeded. It is also possible that environmental pollutants associated with automobile and industrial activities serve as a source of carbon and energy for these microbial communities (Warscheid et al., 1991; Gu et al., 1998). Alternatively, chemoorganotrophic bacteria and fungi with or without the presence of photoautotrophs may collectively act as primary microbial colonizers, conditioning the surface for subsequent microbial succession (Warscheid and Braams, 2000). Finally, there may be some other aspect of concrete or construction practices that we have not considered which may be affecting microbial community composition.

The possibility of sustainable, non-phototrophic metabolism may explain the lack of photosynthetic pigments detected at the sample sites. However, the photo-pigments were expected at the LaGrange site, as *Cyanobacteria* were detected here. One possible explanation for this is that too small of a concrete sample (5 g) was used for detection. Though most LaGrange-derived 16S rRNA gene sequences were cyanobacterial, clone

library analysis is not quantitative, and the number of active phototrophs on the surface of the sample site may have been too few to detect significant levels of photo-pigments.

In contrast to the bacterial community composition, fungal sequences were most closely related to cultured isolates at an average similarity of 99%. As observed with the bacterial communities, distinct fungal communities occurred at each site. Many of the fungal genera detected in this study have been previously reported to foul concrete and stone, including *Alternaria*, *Aspergillus, Cladosporium*, *Epicoccum, Fusarium*, *Hypocrea* (*Trichoderma*), and *Mucor* (Gaylarde and Morton, 1997; Mitchell and Gu, 2000; Shirakawa et al., 2002). These fungi can have a major impact on the appearance and integrity of the concrete surfaces they inhabit, as many of these genera are capable of producing melanins and organic acids (Sterflinger, 2000).

The biodiversity patterns of bacterial and fungal communities could not be entirely explained by the presence or absence of a paint coating. Many of the clone types, including a number of frequently detected phylotypes, were present on painted and unpainted surfaces. We did observe a lower fungal diversity on coated surfaces though there were differences in fungal diversity between sites as well. In contrast, bacterial community diversity was somewhat higher on painted relative to unpainted surfaces. However, there were distinctly different bacterial communities present at each of the four sites. Thus, while paint may promote the colonization and/or growth of certain microorganisms (or inhibit others through biocidal agents it may contain), it appears that additional factors such as site location are also contributing to differences in observed microbial biodiversity patterns.

Targeting of the ITS region of fungal rRNA genes for phylogenetic analysis was valuable in revealing the fungal diversity present on the concrete surfaces. Methodology based on the sequencing of this region coupled with the characterization of RFLP banding patterns has recently been used by others for the species-level identification of fungi in different ecosystems (Gardes and Bruns, 1993; Bougoure et al., 2005; Torzilli et al., 2006; Midgley et al., 2007; Slippers et al., 2007). It is important to note that the ITS PCR primers used in this study are considered universal, as the ITS1 and ITS4 primers are not specific to fungal nuclear regions, and have been reported to co-amplify plant host rRNA genes in the case of fungal symbionts present in the *Monotropoideae* (Gardes and Bruns, 1993; Horton and Bruns, 2001). The analysis of 18S rRNA genes to characterize fungal community composition was not informative in this study. Specifically, the sequences were too conserved to group clones by RFLP patterns and did not yield the resolution obtained by ITS rRNA region analysis. This was not surprising, as the more conserved 18S rRNA gene has been previously used for broad-scale identification of organisms in diverse environments while the ITS region is used for higher resolution analysis (Hunt et al., 2004; Takano et al., 2006). Since the diversity of fungal communities at the sample sites could not be accurately described by RFLP analysis and sequencing of 18S rRNA genes, analysis of the ITS rRNA region was used in this study.

Concrete Property Analysis of Sample Sites

Analysis of concrete property measurements of the sample sites was able to yield several findings. First, the observation that biofouling did not occur appreciably beyond the exposed surfaces of the structures suggests that the nutrient and environment necessary to foster growth are not present within the material itself, but must be provided

by the environment or through interactions between the concrete and the environment. Indications of concrete surface pH and underlying concrete pH suggest that carbonation, which reduces pH to less than 9, may be required before colonization or extensive growth is possible, though the pH of the surface at the unfouled sample site was also below 9. Alternatively, it may indicate that the biofilm formation on these surfaces is relatively nascent and has not had ample time to penetrate further into the concrete. Another observation was that a greater amount of biofouling occurred on surfaces with a paint coating, suggesting that paint may provide an available carbon source to microorganisms for colonization. This could be particularly beneficial for fungal colonizers, which have been previously observed to dominate painted surfaces (Gaylarde and Gaylarde, 2005).

Thermogravimetric differential thermal analysis did not reveal surface carbonation to be greater than what was expected by atmospheric exposure alone, suggesting that biofouling at these sites is not expediting concrete carbonation, though it has been previously suggested (Gu et al., 1998). This is exemplified by the Gainesville sample site; though it was the oldest structure examined, it did not exhibit the greatest carbonation depth or the greatest amount of fouling, as expected. Also, the unfouled control site, which was the newest structure sampled, had a carbonation depth comparable to the fouled sample sites. This suggests that other factors are driving the severity of biofouling and the microbial community diversity on these particular concrete surfaces.

While no correlations could be drawn linking compressive strength, permeability, or moisture content to the amount of biofouling, the measurements taken in this study can not exclude the possibility of a relationship. The field measurements used

in this approach are not as precise as laboratory tests often performed on cores, and may not have been adequate in precision or number to reveal such relationships. More specifically, however, because these structures were designed according to narrow specifications provided by Georgia Department of Transportation Section 500 (http://tomcat2.dot.stat.ga.us/thesource/specs/index.html), their compressive strength and permeability would not be expected to vary considerably. In addition, moisture content measurements can vary over short periods of time with weather changes (e.g. rain).

Comparisons of compressive strength, moisture content, and carbonation depth to the microbial diversity at each of the sites also did not generate any significant relationships. However, a strong positive trend was observed between permeability and microbial diversity, suggesting that a greater variety of microorganisms may be able to colonize more permeable concrete. More permeable concrete (i.e. concrete containing more interconnected pores) will result in greater flow of water through the concrete as well as additional space for microbial colonizers, which may result in greater community diversity.

Analysis of Biofouling by Individual Cultured Isolates

Efforts to culture fungal isolates directly from the concrete surfaces were successful. However, bacterial isolates were not obtained, suggesting that more intensive culturing efforts might need to be undertaken to isolate bacteria from these surfaces (Connon and Giovannoni, 2002; Kaeberlein et al., 2002; Zengler et al., 2002; Bollmann et al., 2007). The inability to culture bacteria from the concrete surfaces at our sites is likely due to the fact that the majority of bacterial sequences we detected were most closely related to as yet uncultured clones, while nearly all of the fungal sequences

detected were most closely related to previously cultured isolates. We show that fungal isolates obtained from field samples colonized concrete tiles in lab-based assays when supplied with moisture and a carbon source. The appearance of fouling varied between incubations of individual isolates as well as incubations using organisms pooled by site, with site-pooled incubations often exhibiting fouling not observed for any lone isolate. This suggests that the appearance of concrete biofouling is influenced by community composition. It is also possible that the isolates can exhibit different morphologies under varying growth conditions or on different concrete surfaces. This was exemplified by *Trichoderma* spp. exhibiting green fouling predominately on tiles that did not contain SCMs and were not exposed to artificial sunlight, and tan fouling predominately on tiles containing SCMs and on all tiles exposed to artificial sunlight.

While a number of the isolates tested (e.g. *C. cladosporioides*, *Fusarium* sp.) exhibited dark-colored fouling similar to what was seen in the field, the biofouling observed on concrete tiles inoculated with the *E. nigrum* isolate most closely resembled the black staining frequently observed at our study sites. *Epicoccum* is a ubiquitous dematiaceous mold commonly isolated from air, soil and decaying plant matter, and can frequently colonize building materials (Mitchell and Gu, 2000; Shirakawa et al., 2002; Basilico et al., 2007). The staining and discoloration of the concrete surfaces are likely caused by the excretion of melanins and melanin-related pigments that provide cellular protection against UV irradiation, desiccation and temperature changes (Warscheid and Braams, 2000). As these pigments are metabolic by-products produced by some dematiaceous fungi as well as pseudomonads (Warscheid and Braams, 2000), it is

possible that both fungal and bacterial populations contribute to the discoloration process at our study sites, though only fungal populations were examined in the biofouling tests.

Analysis of Concrete Property Effects on Biofouling

A number of variables relating concrete composition to susceptibility to biofouling were examined. Of these, the strongest trend was seen with water/cement ratio variation. The positive relationship observed suggests that a higher water/cement ratio makes concrete more susceptible to biofouling. This was expected, as increasing the amount of water used in cement hydration can result in the formation of microscopic pores, which can decrease a structure's overall strength as well as increase surface roughness, porosity, and permeability, possibly giving organisms a more hospitable surface to colonize (Dubosc et al., 2001; Mehta, 2006). The numerous effects that w/cm has on concrete properties as well as its strong relationship to biofouling make it a good predictor of susceptibility.

A lack of correlation between tile compressive strength and degree of biofouling may be attributed to the difficulty of isolating this variable for testing, as compressive strength is varied by altering cement type, SCM addition, water/cement ratio, and other concrete properties (Mehta, 2006). It is possible that compressive strength does affect biofouling; however, it is also likely that it is only one of a compilation of factors, and perhaps is more of an indirect indicator compared to other biofouling susceptibility effectors, such as w/cm.

Variations in surface roughness did show positive correlations to biofouling in the Atlanta, Gainesville, and *Trichoderma viride* incubations. This agrees with previous work, which suggests that greater surface roughness (and thus likely greater porosity) is

more conducive to biofouling (Pinheiro, 2004). However, a negative trend was observed for the LaGrange, or Savannah experiments. This may be because surface roughness has a variable effect on biofouling depending on community composition. Alternatively, the trends observed in this study were generated using only three different on surface finishes; therefore, it is likely that testing a wider range of surface roughnesses could resolve these contradictory trends. While the average measurements of our results suggest that smoother surfaces may be more resistant to biofouling, it is not likely to be the most effective method of mitigating biofilm formation, as growth was still present on the smoothest surface finishes, and the trend was not seen in all incubations.

Variations in cement type and SCM additions did not seem to affect biofouling on tiles, although the range of SCM compositions in particular was quite narrow. Similar biofouling on different primary cement types is likely due to their similar Bogue potential compositions. While there are variations in the proportions of calcium silicate hydrates that the cements may form upon hydration, the hydrates all have similar chemical compositions (i.e. contain calcium, silicone, aluminum, and some iron), which would not likely result in significant variations of biofouling resistance. Furthermore, while different SCMs (and primary cements) may contain slight variations of metal oxides upon analysis, none studied have particularly large or different amounts of carbon impurities as determined by loss on ignition analysis (Kurth, 2008). Specifically, the SCMs used in this study were of relatively high quality and had low LOI values at less than 2% (ASTM allows up to 7% carbon in fly ash by mass). The effects on biofouling that the carbon impurities in our SCMs and primary cements may have caused were likely lost due to the high carbon content of the nutrient-rich 20% potato dextrose broth media. Thus, while no

strong relationships between cement type or SCM additions and biofouling were observed in this study, it is quite possible that these variables could have an effect in the field.

The photocatalytic cement under artificial sunlight exposure, however, did show near-complete resistance to biofouling when compared to the companion non-TiO_2-containing cement exposed to the same light source. These results indicate that the photocatalytic cement was capable of inhibiting biofouling when activated. These results agree with previous studies concerning the antimicrobial properties of TiO_2 (Sang, 2007; Tsuang, 2008), though this is the first evidence of the fungicidal abilities of such cements. However, it should be noted that the *Trichoderma asperellum* isolate was capable of surviving and being recultured from the photocatalytically active tile surface. This suggests that the use of TiO_2-containing cements, though effective, may not completely inhibit biofouling of concrete structures.

Analysis of Nutrient-limited Media Tests

Biofouling tests utilizing nutrient-limited media, including sterile deionized water, sterilized rainwater, sterilized rainwater exposed to vehicular exhaust, and sterilized rainwater with tiles dipped in form release oil, were performed to determine if biofouling could occur when energy sources were only available through carbon impurities and/or compounds in concrete, impurities in rainwater, compounds from vehicular exhaust/air pollution, or carbon sources remaining on concrete from construction. While incubations in potato dextrose broth were performed to quickly produce biofouling, this nutrient-rich media did not resemble *in situ* conditions, where fouling occurs much more slowly.

Unfortunately, attempts to recreate biofouling under more realistic conditions

were not as successful. This may be due to the length of time the incubations were run; it likely takes years for an appreciable amount of biofouling to manifest in the field, as opposed to our incubations, which were one month long, albeit in optimal or near-optimal conditions for growth. It is also possible that fungal isolates require *Bacteria* to be present on or initially colonize the concrete surface (especially autotrophs) if an abundant source of energy is not readily available. However, at least one culturable, likely the *Epicoccum* isolate, was able to establish itself on a tile when given sterilized rainwater and form-release oil as moisture and energy sources, suggesting that if given sufficient time, fungal isolates may be able to foul concrete in the field using exogenous nutrient sources, such as rainwater runoff, dust, form-release oil, or vehicular exhaust.

CHAPTER 6

CONCLUSIONS

This study provides insight into the microbial community diversity occupying the surfaces of outdoor concrete structures in the state of Georgia, as well as the ability of isolates cultured from these structures to foul concrete under a variety of laboratory-controlled conditions. Molecular analysis of extracted bacterial rRNA genes revealed a predominance of *Proteobacteria* at all sample sites except for one, which was dominated by *Cyanobacteria*. Analysis of the ITS region of fungal rRNA genes revealed genera previously shown to foul concrete and stone surfaces (e.g. *Cladosporium, Alternaria, Epicoccum, Hypocrea*). The fungal isolates cultured from the concrete surfaces studied were shown to be capable of fouling concrete under controlled laboratory conditions when given moisture and an ample nutrient source. Numerous concrete tile compositions were tested for their susceptibility to biofouling by these cultured isolates, revealing that water/cement ratio and surface roughness may have a positive relationship to biofouling. While cement compositions and SCM additions did not seem to affect biofouling, a cement containing TiO_2 was able to be photocatalytically activated by artificial sunlight, completely inhibiting all biofouling with the exclusion of a *Trichoderma* sp. isolated from the field. Attempts to generate biofouling using lower-nutrient media (e.g. sterile de-ionized water, sterilized rainwater, rainwater exposed to vehicular exhaust) were largely unsuccessful. However, a small amount of dark biofouling, likely produced by an *Epicoccum* sp. cultured from the field, was observed on a concrete tile coated with form-release oil and incubated under a sterile rainwater media spray. Our results indicate that

distinct bacterial and fungal communities are present on fouled concrete surfaces, and that altering the properties of concrete used in construction can change the susceptibility of a structure to biofouling, but that an ample nutrient source is necessary for widespread growth.

This study uses a combination of culture-independent and culture-dependent approaches to characterize the biofouling of concrete surfaces. While many factors, both biological and materials/construction-related, are examined, this study is far from completely encompassing either type. As more knowledge of microbial communities inhabiting a variety of concrete surfaces is attained, microbial community colonization processes, community sustainability, and the specific role concrete surface characteristics play in biofouling will be further elucidated.

REFERENCES

Anderson, I. C., Campbell, C. D., Prosser, J. I., 2003. Potential bias of fungal 18S rDNA and internal transcribed spacer polymerase chain reaction primers for estimating fungal biodiversity in soil. Environmental Microbiology 5, 36-47.

ASTM C 109 (2007) Standard test method for compressive strength of hydraulic cement mortars (using 2-in. or [50-mm] cube specimens). West Conshohocken, PA, ASTM International.

ASTM C 125 (2007) Standard terminology relating to concrete and concrete aggregates. West Conshohocken, PA, ASTM International.

ASTM C 150 (2007) Specification for portland cement. West Conshohocken, PA, ASTM International.

Bartosch, S., Mansch, R., Knotzsch, K., Bock, E., 2003. CTC staining and counting of actively respiring bacteria in natural stone using confocal laser scanning microscopy. Journal of Microbiological Methods 52, 75-84.

Basilico, M., Chiericatti, C., Aringoli, E. E., Althaus, R. L., Basilico, J. C., 2007. Influence of environmental factors on airborne fungi in houses of Santa Fe city, Argentina. Science of the Total Environment 376, 143-150.

Bhatty, J. I., Reid, K. J., Dollimore, D., Gamlen, G. A., Mangabhai, R. J., Rogers, P. F., Shah, T. H., 1988. The derivation of kinetic parameters in analysis of Portland cement for portlandite and carbonate by thermogravimetry. In: Earnest, C. M. (Eds.), Compositional Analysis by Thermogravimetry, ASTM International, West Conshohocken, PA, 204-215.

Blob, S. P., Elfenthal, L., 2007. Doped titanium dioxide as a photocatalyst for UV and visible light. In: Baglioni, P., Cassar, L. (Eds.), Proceedings of the international RILEM symposium on photocatalysis, envirnonment, and construction materials, PRO50, 31-38.

Bollmann, A., Lewis, K., Epstein, S. S., 2007. Incubation of environmental samples in a diffusion chamber increases the diversity of recovered isolates. Applied and Environmental Microbiology 73, 6386-6390.

Bougoure, J. J., Bougoure, D. S., Cairney, J. W. G., Dearnaley, J. D. W., 2005. ITS-RFLP and sequence analysis of endophytes from *Acianthus*, *Caladenia* and *Pterostylis* (Orchidaceae) in southeastern Queensland. Mycological Research 109, 452-460.

Cassar, L., Beeldens, A., Pimpinelli, N., Guerrini, G.L., 2007. Photocatalysis of cementitious materials. In: Baglioni, P., Cassar, L. (Eds.), Proceedings of the international RILEM symposium on photocatalysis, envirnonment, and construction materials, PRO50, 131-145.

Chertov, O., Gorbushina, A., Deventer, B., 2004. A model for microcolonial fungi growth on rock surfaces. Ecological Modelling 177.

Chinga, G., Johnsen, P.O., Dougherty, R., Berli, E.L., Walter, J., 2007. Quantification of the 3D microstructure of SC surfaces. Journal of Microscopy 227, 254-265.

Connon, S. A., Giovannoni, S. J., 2002. High-throughput methods for culturing microorganisms in very-low-nutrient media yield diverse new marine isolates. Applied and Environmental Microbiology 68, 3878-3885.

Cribb, G. (2006) Bridge Inspection Report 117-0022-0. Atlanta, GA, Georgia Department of Transportation.

Crispim, C. A., Gaylarde, P. M., Gaylarde, C. C., Neilan, B. A., 2006. Deteriogenic cyanobacteria, on historic buildings in Brazil detected by culture and molecular techniques. International Biodeterioration & Biodegradation 57, 239-243.

De La Torre, J. R., Christianson, L. M., Beja, O., Suzuki, M. T., Karl, D. M., Heidelberg, J., DeLong, E. F., 2003. Proteorhodopsin genes are distributed among divergent marine bacterial taxa. Proceedings of the National Academy of Sciences of the United States of America 100, 12830-12835.

De La Torre, M. A., Gomez-Alarcon, G., Vizcaino, C., Garcia, M. T., 1993. Biochemical mechanisms of stone alteration carried out by filamentous fungi living in monuments. Biogeochemistry 19, 129-147.

Dubosc, A., Escadeillas, G., Blanc, P. J., 2001. Characterization of biological stains on external concrete walls and influence of concrete as underlying material. Cement and Concrete Research 31, 1613-1617.

Ehrich, S., Helard, L., Letourneux, R., Willocq, J., Bock, Eberhard, 1999. Biogenic and chemical sulfuric acid corrosion of mortars. Journal of Materials in Civil Engineering 11, 340-344.

Gardes, M., Bruns, T. D., 1993. ITS primers with enhanced specificity for basidiomycetes - application to the identification of mycorrhizae and rusts. Molecular Ecology 2, 113-118.

Gaylarde, C. C., Gaylarde, P. M., 2005. A comparative study of the major microbial biomass of biofilms on exteriors of buildings in Europe and Latin America. International Biodeterioration & Biodegradation 55, 131-139.

Gaylarde, C. C., Morton, L. H. G., 1997. The importance of biofilms in microbial deterioration of constructional materials. Revista de Microbiologia 28, 221-229.

Gaylarde, C. C., Morton, L. H. G., 1999. Deteriogenic biofilms on buildings and their control: a review. Biofouling 14, 59-74.

Gaylarde, C. C., Ortega-Morales, B. O., Bartolo-Perez, P., 2007. Biogenic black crusts on buildings in unpolluted environments. Current Microbiology 54, 162-166.

GDOT (2001) Georgia Department of Transportation Section 500 - Concrete Structures, http://tomcat2.dot.state.ga.us/thesource/specs/index.html.

Goswami, D. Y., 2003. Decontamination of ventilation systems using photocatalytic air cleaning technology. Journal of Solar Energy Engineering 125, 359-365.

Goszczynska, T., Botha, W. J., Venter, S. N., Coutinho, T. A., 2007. Isolation and identification of the causal agent of brown stalk rot, a new disease of maize in South Africa. Plant Disease 91, 711-718.

Gu, J. D., Ford, T. E., Berke, N. S., Mitchell, R., 1998. Biodeterioration of concrete by the fungus *Fusarium*. International Biodeterioration & Biodegradation 41, 101-109.

Guillitte, O., Dreesen, R., 1995. Laboratory chamber studies of petrographical analysis as bioreceptivity assessment tools of building materials. The Science of the Total Environment 167, 365-374.

Hall, T. A., 1999. BioEdit: a user-friendly biological sequence alignment editor and analysis program for Windows 95/98/NT. Nucleic Acids Symposium Series 41, 95-98.

Hashimoto, K., 2007. TiO_2 photocatalysts towards novel building materials. In: Baglioni, P., Cassar, L. (Eds.), Proceedings of the international RILEM symposium on photocatalysis, envirnonment, and construction materials, PRO50, 3-8.

Heck, K. L., Belle, G.V., Simberloff, D., 1975. Explicit calculation of the rarefaction diversity measurement and the determination of sufficient sample size. Ecology 56, 1459-1461.

Hibbett, D. S., Binder, M., Bischoff, J. F., Blackwell, M., Cannon, P. F., Eriksson, O. E., Huhndorf, S., James, T., Kirk, P. M., Lucking, R., et al., 2007. A higher-level phylogenetic classification of the Fungi. Mycological Research 111, 509-547.

Horton, T. R., Bruns, T. D., 2001. The molecular revolution in ectomycorrhizal ecology: peeking into the black-box. Molecular Ecology 10, 1855-1871.

Hunt, J., Boddy, L., Randerson, P. F., Rogers, H. J., 2004. An evaluation of 18S rDNA approaches for the study of fungal diversity in grassland soils. Microbial Ecology 47, 385-395.

Jukes, T. H., Cantor, C. R., 1969. Evolution of protein molecules. In: Munro, H. N. (Eds.), Mammalian Protein Metabolism, Academic Press, New York, NY, 21-132.

Kaeberlein, T., Lewis, K., Epstein, S. S., 2002. Isolating "uncultivable" microorganisms in pure culture in a simulated natural environment. Science 296, 1127-1129.

Kurth, J. C., 2008. Mitigating biofilm growth through the modification of concrete design and practice, MS thesis, Georgia Institute of Technology, Atlanta, GA.

Kurtis, K. E., El-Ashkar, N.H., Collins, C.L., Naik, N.N., 2003. Examining cement-based materials by laser scanning confocal microscopy. Cement & Concrete Composites 25, 695-701.

Lagier, F., Kurtis, K.E., 2007. Influence of Portland cement composition on early age reactions with metakaolin. Cement & Concrete Composites 37, 1411-1417.

Maidak, B. L., Cole, J.R., Parker, C.T., Garrity, G.M., Larsen, N., Li, B., Lilburn, T.G., McCaughey, M.J., Olsen, G.J., Overbeek, R., Pramanik, S., Schmidt, T.M., Tiedje, J.M., Woese, C.R., 1999. A new version of the RDP (Ribosomal Database Project). Nucleic Acids Research 27, 171-173.

Martinez, R. J., Mills, H. J., Story, S., Sobecky, P. A., 2006. Prokaryotic diversity and metabolically active microbial populations in sediments from an active mud volcano in the Gulf of Mexico. Environmental Microbiology 8, 1783-1796.

Matthews, J. W. (2006) Bridge Inspection Report 031-0089-0. Atlanta, GA, Georgia Department of Transportation.

McNamara, C. J., Perry, T. D., Bearce, K. A., Hernandez-Duque, G., Mitchell, R., 2006. Epilithic and endolithic bacterial communities in limestone from a Maya archaeological site. Microbial Ecology 51, 51-64.

McPolin, D. O., Basheer, P. A. M., Long, A. E., Grattan, K. T. V., Sun, T., 2007. New test method to obtain pH profiles due to carbonation of concretes containing supplementary cementitious materials. Journal of Materials in Civil Engineering 19, 936-946.

Mehta, P. K., Monteiro, P.J.M., 2006. Concrete: Microstructure, Properties, and Materials. McGraw-Hill, New York.

Michaelsen, A., Pinzari, F., Ripka, K., Lubitz, W., Pinar, G., 2006. Application of molecular techniques for identification of fungal communities colonising paper material. International Biodeterioration & Biodegradation 58, 133-141.

Midgley, D. J., Saleeba, J. A., Stewart, M. I., Simpson, A. E., McGee, P. A., 2007. Molecular diversity of soil basidiomycete communities in northern-central New South Wales, Australia. Mycological Research 111, 370-378.

Milde, K., Sand, W., Wolff, W., Bock, E., 1983. *Thiobacilli* of the corroded concrete walls of the Hamburg sewer system. Journal of General Microbiology 129, 1327-1333.

Mills, H. J., Hodges, C., Wilson, K., MacDonald, I. R., Sobecky, P. A., 2003. Microbial diversity in sediments associated with surface-breaching gas hydrate mounds in the Gulf of Mexico. FEMS Microbiology Ecology 46, 39-52.

Mills, H. J., Martinez, R. J., Story, S., Sobecky, P. A., 2005. Characterization of microbial community structure in Gulf of Mexico gas hydrates: comparative analysis of DNA- and RNA-derived clone libraries. Applied and Environmental Microbiology 71, 3235-3247.

Mindness, S., Young, J.F., & Darwin, D., 2003. Concrete: 3rd Edition. Pearson Education, Inc., Upper Saddle River, NJ.

Mitchell, R., Gu, J. D., 2000. Changes in the biofilm microflora of limestone caused by atmospheric pollutants. International Biodeterioration & Biodegradation 46, 299-303.

Moissl, C., Osman, S., La Duc, M. T., Dekas, A., Brodie, E., DeSantis, T., Venkateswaran, K., 2007. Molecular bacterial community analysis of clean rooms where spacecraft are assembled. FEMS Microbiology Ecology 61, 509-521.

Nica, D., Davis, J. L., Kirby, L., Zuo, G., Roberts, D. J., 2000. Isolation and characterization of microorganisms involved in the biodeterioration of concrete in sewers. International Biodeterioration & Biodegradation 46, 61-68.

Norris, T. B., Castenholz, R. W., 2006. Endolithic photosynthetic communities within ancient and recent travertine deposits in Yellowstone National Park. FEMS Microbiology Ecology 57, 470-483.

Pang, K. L., Mitchell, J. I., 2005. Molecular approaches for assessing fungal diversity in marine substrata. Botanica Marina 48, 332-347.

Papadakis, V. G., 2000. Effect of supplementary cementing materials on concrete resistance against carbonation and chloride ingress. Cement and Concrete Research 30, 291-299.

Parker, C. D., 1945. The corrosion of concrete. 2. The funtion of *Thiobacillus concretivorus* (nov-spec) in the corrosion of concrete exposed to atmospheres containing hydrogen sulfide. Australian Journal of Experimental Biology and Medical Science 23, 91-98.

Parsons, T. R., Maita, Y., Lalli, C.M., 1984. Determination of chlorophylls and total carotenoids: spectrophotometric method. In: Parsons, T. R., Maita, Y., Lalli, C.M. (Eds.), A Manual of Chemical and Biological Methods for Seawater Analysis, Pergamon Press, New York, NY, 101-104.

Patterson, B. (2005) Bridge Inspection Report 285-0085-0. Atlanta, GA, Georgia Department of Transportation.

Penn, K., Wu, D. Y., Eisen, J. A., Ward, N., 2006. Characterization of bacterial communities associated with deep-sea corals on Gulf of Alaska seamounts. Applied and Environmental Microbiology 72, 1680-1683.

Perry, T. D. I., McNamara, C.J., Mitchell, R., 2005. Biodeterioration of stone. (Sackler NAS Colloquium) Scientific examination of art: modern techniques in conservation and analysis, National Academy of Sciences, 72-84.

Pinheiro, S. M. M., Silva, M.R. (2004) Microorganisms and aesthetic biodeterioration of concrete and mortar. IN Silva, M. R. (Ed. *Second International RILEM Workshop on Microbial Impact on Building Materials.* RILEM Publications SARL.

Sand, W., 1997. Microbial mechanisms of deterioration of inorganic substrates - a general mechanistic overview. International Biodeterioration & Biodegradation 40, 183-190.

Sand, W., Bock, E., 1991. Biodeterioration of mineral materials by microorganisms - biogenic sulfuric and nitric acid corrosion of concrete and natural stone. Geomicrobiology Journal 9, 129-138.

Sang, X., Phan, T.G., Sugihara, S., Yagyu, F., Okitsu, S., Maneekarn, N., Muller, W.E.G., Ushijima, H., 2007. Photocatalytic inactivation of diarrheal viruses by visible-light-catalytic titanium dioxide. Clin. Lab. 53, 413-421.

Shirakawa, M. A., Beech, I.B., Tapper, R., Cincotto, M.A., Gambale, W., 2003. The development of a method to evaluate bioreceptivity of indoor mortar plastering to fungal growth. International Biodeterioration & Biodegradation 51, 83-92.

Shirakawa, M. A., Gaylarde, C. C., Gaylarde, P. M., John, V., Gambale, W., 2002. Fungal colonization and succession on newly painted buildings and the effect of biocide. FEMS Microbiology Ecology 39, 165-173.

Shirakawa, M. A., Selmo, S.M., Cincotto, M.A., Gaylarde, C.C., Brazolin, S., Gambale, W., 2002. Susceptibility of phosphogypsum to fungal growth and the effect of various biocides. International Biodeterioration & Biodegradation 49, 293-298.

Simmons, D. (2005) Bridge Inspection Report 121-0207-0. Atlanta, GA, Georgia Department of Transportation.

Slippers, B., Smit, W. A., Crous, P. W., Coutinho, T. A., Wingfield, B. D., Wingfield, M. J., 2007. Taxonomy, phylogeny and identification of Botryosphaeriaceae associated with pome and stone fruit trees in South Africa and other regions of the world. Plant Pathology 56, 128-139.

Smit, E., Leeflang, P., Glandorf, B., van Elsas, J. D., Wernars, K., 1999. Analysis of fungal diversity in the wheat rhizosphere by sequencing of cloned PCR-amplified genes encoding 18S rRNA and temperature gradient gel electrophoresis. Applied and Environmental Microbiology 65, 2614-2621.

Staley, J. T., Konopka, A., 1985. Measurement of in situ activities of nonphotosynthetic microorganisms in aquatic and terrestrial habitats. Annual Review of Microbiology 39, 321-346.

Sterflinger, K., 2000. Fungi as geologic agents. Geomicrobiology Journal 17, 97-124.

Takano, K., Itoh, Y., Ogino, T., Kurosawa, K., Sasaki, K., 2006. Phylogenetic analysis of manganese-oxidizing fungi isolated from manganese-rich aquatic environments in Hokkaido, Japan. Limnology 7, 219-223.

Tamura, K., Dudley, J., Nei, M., Kumar, S., 2007. MEGA4: Molecular Evolutionary Genetics Analysis (MEGA) software version 4.0. Mol. Biol. & Evol. 24, 1596-1599.

Tanizaki, T., Murakami, Y., Hanada, Y., Ishikawa, S., Suzuki, M., Shinohara, R., 2007. Titanium dioxide (TiO_2)-assisted photocatalytic degradation of volatile organic compounds at ppb level. Journal of Health Science 53, 514-519.

Torzilli, A. P., Sikaroodi, M., Chalkley, D., Gillevet, P. M., 2006. A comparison of fungal communities from four salt marsh plants using automated ribosomal intergenic spacer analysis (ARISA). Mycologia 98, 690-698.

Tsuang, Y., Sun, J., Huang, Y., Lu, C., Chang, W.H., Wang, C., 2008. Studies of photokilling of Bacteria using titanium dioxide nanoparticles. Artificial Organs 32, 167-174.

Tun, C. C., Ikenaga, M., Asakawa, S., Kimura, M., 2002. Community structure of Bacteria and Fungi responsible for rice straw decomposition in a paddy field estimated by PCR-RFLP analysis. Plant Nutr. 48, 805-813.

Walcott, R. R., Gitaitis, R. D., Castro, A. C., Sanders, F. H., Diaz-Perez, J. C., 2002. Natural infestation of onion seed by *Pantoea ananatis*, causal agent of center rot. Plant Disease 86, 106-111.

Walker, J. J., Pace, N. R., 2007. Phylogenetic composition of Rocky Mountain endolithic microbial ecosystems. Applied and Environmental Microbiology 73, 3497-3504.

Warscheid, T., Braams, J., 2000. Biodeterioration of stone: a review. International Biodeterioration & Biodegradation 46, 343-368.

Warscheid, T., Oelting, M., Krumbein, W. E., 1991. Physiochemical aspects of biodeterioration processes on rocks with special regard to organic pollutants. International Biodeterioration & Biodegradation 28, 37-48.

White, T. J., Bruns, T., Lee, S., Taylor, J., 1990. Amplification and direct sequencing of fungal ribosomal RNA genes for phylogenetics. In: Innis, M. A., Gelfland, D.H., Sninsky, J.J., White, T.J. (Eds.), PCR Protocols: A Guide to Methods and Applications, Academic Press, San Diego, CA, 315-321.

Zengler, K., Toledo, G., Rappe, M., Elkins, J., Mathur, E. J., Short, J. M., Keller, M., 2002. Cultivating the uncultured. Proceedings of the National Academy of Sciences of the United States of America 99, 15681-15686.

Zherebyateva, T. V., Lebedeva, E.V., Karavaiko, G.I., 1991. Microbiological corrosion of concrete structures of hydraulic facilities. Geomicrobiology Journal 9, 119-127.

Zhou, G., Whong, W. Z., Ong, T., Chen, B., 2000. Development of a fungus-specific PCR assay for detecting low-level fungi in an indoor environment. Molecular and Cellular Probes 14, 339-348.